TECHNICAL REPORT BRL-TR-3287

BRL

BURN RATES OF LGP 1846 CONDITIONED AMBIENT, HOT, AND COLD

WILLIAM F. OBERLE
GLORIA P. WREN

OCTOBER 1991

U.S. ARMY LABORATORY COMMAND

BALLISTIC RESEARCH LABORATORY
ABERDEEN PROVING GROUND, MARYLAND

NOTICES

Destroy this report when it is no longer needed. DO NOT return it to the originator.

Additional copies of this report may be obtained from the National Technical Information Service, U.S. Department of Commerce, 5285 Port Royal Road, Springfield, VA 22161.

The findings of this report are not to be construed as an official Department of the Army position, unless so designated by other authorized documents.

The use of trade names or manufacturers' names in this report does not constitute indorsement of any commercial product.

UNCLASSIFIED

REPORT DOCUMENTATION PAGE

Form Approved
OMB No. 0704-0188

1. AGENCY USE ONLY (Leave blank)	2. REPORT DATE	3. REPORT TYPE AND DATES COVERED
	October 1991	Final, Jan 90 - Oct 90

4. TITLE AND SUBTITLE

Burn Rates of LGP 1846 Conditioned Ambient, Hot, and Cold

5. FUNDING NUMBERS

DA306709 IFYM9Y9XA450

6. AUTHOR(S)

William F. Oberle and Gloria P. Wren

7. PERFORMING ORGANIZATION NAME(S) AND ADDRESS(ES)

8. PERFORMING ORGANIZATION REPORT NUMBER

9. SPONSORING/MONITORING AGENCY NAME(S) AND ADDRESS(ES)

U.S. Army Ballistic Research Laboratory
ATTN: SLCBR-DD-T
Aberdeen Proving Ground, MD 21005-5066

10. SPONSORING/MONITORING AGENCY REPORT NUMBER

BRL-TR-3287

11. SUPPLEMENTARY NOTES

12a. DISTRIBUTION/AVAILABILITY STATEMENT

Authorized for public release; distribution is unlimited.

12b. DISTRIBUTION CODE

13. ABSTRACT *(Maximum 200 words)*

Results of closed chamber experiments using LGP 1846 are presented. The matrix of firings includes variations in igniter pressure, propellant loading density, and temperature conditioning of the propellant, ranging from approximately -25° C to +60° C. Derived burning rate laws, in the form $r = bP^n$, result in exponents of approximately 2.0 for pressures in excess of 100 MPa. However, comparison of burn rates with strand burner data at corresponding pressures indicate good agreement. The measured burn rates, although much higher than previous experiments have indicated, do not significantly alter previous results and previously chosen empirical parameters in a lumped parameter, liquid propellant gun, interior ballistic model which has been extensively validated against gun data.

14. SUBJECT TERMS	15. NUMBER OF PAGES
Closed chamber, liquid gun propellant, burning rate	101
	16. PRICE CODE

17. SECURITY CLASSIFICATION OF REPORT	18. SECURITY CLASSIFICATION OF THIS PAGE	19. SECURITY CLASSIFICATION OF ABSTRACT	20. LIMITATION OF ABSTRACT
UNCLASSIFIED	UNCLASSIFIED	UNCLASSIFIED	SAR

INTENTIONALLY LEFT BLANK.

TABLE OF CONTENTS

A-1

INTENTIONALLY LEFT BLANK.

LIST OF FIGURES

LIST OF TABLES

INTENTIONALLY LEFT BLANK.

ACKNOWLEDGMENTS

The authors would like to thank Charles Leveritt, Terence Coffee, Nathan Klein, Arpad Juhasz, William Aungst, and Joyce Newberry of the U.S. Army Ballistic Research Laboratory for their advice and assistance with this work.

The authors would also like to thank Charles Leveritt for his encouragement of this project.

INTENTIONALLY LEFT BLANK.

1. INTRODUCTION

Measurement of the apparent laminar regression or burning rate for liquid propellants has been investigated extensively over the past forty years as documented in McBratney, Bensinger, and Arford (1976); McBratney (1981); Vosen (1989); and Lee, Tseng, and Faeth (1989). For these studies, the burning rates were deduced from strand burner or atomized spray experiments for pressures up to 100 MPa, with the majority of experiments performed at pressures below 50 MPa (McBratney, Bensinger, and Arford 1976; Vosen 1989; Lee, Tseng, and Faeth 1989). In addition, in order to moderate surface turbulence, several of the experiments were performed with "gelled" propellants, in which the neat liquid propellant was modified with additives to increase viscosity. Unfortunately, the effect of the gelling agents on the combustion chemistry and burning rate of liquid propellants is not known (Vosen 1989).

Of current interest is the liquid gun propellant LGP 1846, which is being utilized by the U.S. Army in the development of a regenerative liquid propellant gun (RLPG) for use with the next generation artillery howitzer. Klein (1990) has provided a summary of the combustion process. He explains that the HAN-based liquid propellants contain water, hydroxylammonium nitrate, NH_3OHNO_3 (HAN), and the nitrate salt of an aliphatic amine (AAN). The AAN salt used in LGP 1846 is triethanolammonium nitrate, $(HOCH_2CH_2)_3NHNO_3$ (TEAN). Combustion of the HAN-based propellants is sequential. When reaction is initiated, the HAN component decomposes generating heat and various gases. The AAN is not chemically changed but is converted to fine, molten salt droplets that are dispersed in the HAN decomposition gases. Ignition is observed when the AAN droplets become involved, and reaction and their rates are such that the amount of energy released is sufficient to at least sustain the reaction sequence. Combustion, the third and final phase, accounts for the majority of the energy released by the propellant.

Figure 1, from the report by Lee, Tseng, and Faeth (1989), presents the currently known information on the burning rates for LGP 1846 and LGP 1845, a mixture containing 2% less water. Vosen (1989) attributes the increased burning rates obtained in his study to surface instabilities. Although the burning rates recorded by Lee, Tseng, Faeth, and McBratney (2% gel) are consistent, the pressure range is limited, 0.7–7 MPa for Lee et al. and

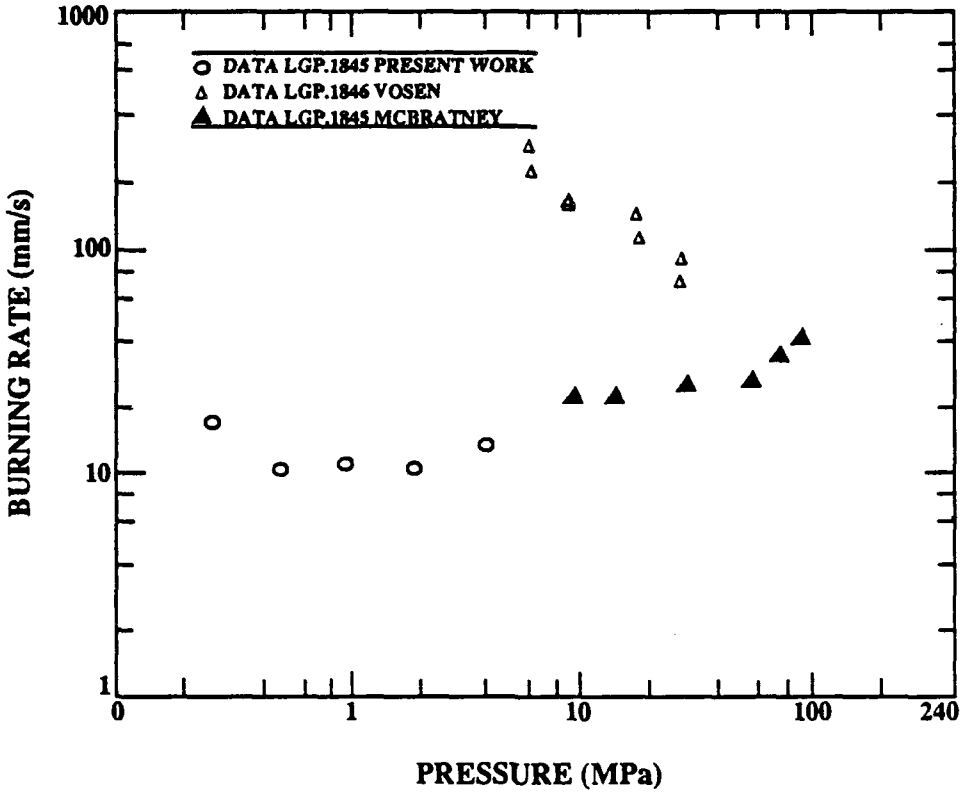

Figure 1. Apparent Burning Rates for LGP 1845 and LGP 1846 (Lee and Faeth 1989).

10–60 MPa for McBratney. Above 60 MPa, the burn rates by McBratney show a substantial increase.

The objectives of the present work are as follows: Without the addition of a "gelling" agent to the propellant (1) determine apparent laminar regression or burn rate for LGP 1846 at gun pressures, particularly in the range of 50–200 MPa; (2) determine the effect on burn rate resulting from conditioning the propellant to 60° C and -25° C; (3) determine if the sharp break in burn rate measured by McBratney at approximately 60–100 MPa for LGP 1845 is present for LGP 1846; and (4) determine the effect of using the measured burn rates in interior ballistic performance codes.

2. EXPERIMENTAL FIXTURE AND BURN RATE ANALYSIS

In order to obtain burn rate information for LGP 1846 at elevated pressures, a series of closed chamber experiments was performed. A schematic of the closed chamber is shown in Figure 2. Total chamber volume is 73 cm^3, and the sample holder volume is 24.4 cm^3. To prevent contamination of the liquid propellant, the sample holder is coated with silicon. The igniter is DuPont IMR 4350 packaged in cellophane with ignition initiated by an electric match. Pressure-time data are recorded on a model 2092 Nicolet oscilloscope which is connected to the closed chamber via a Kistler model 504E charge amplifier and Kistler model 607C4 pressure transducer.

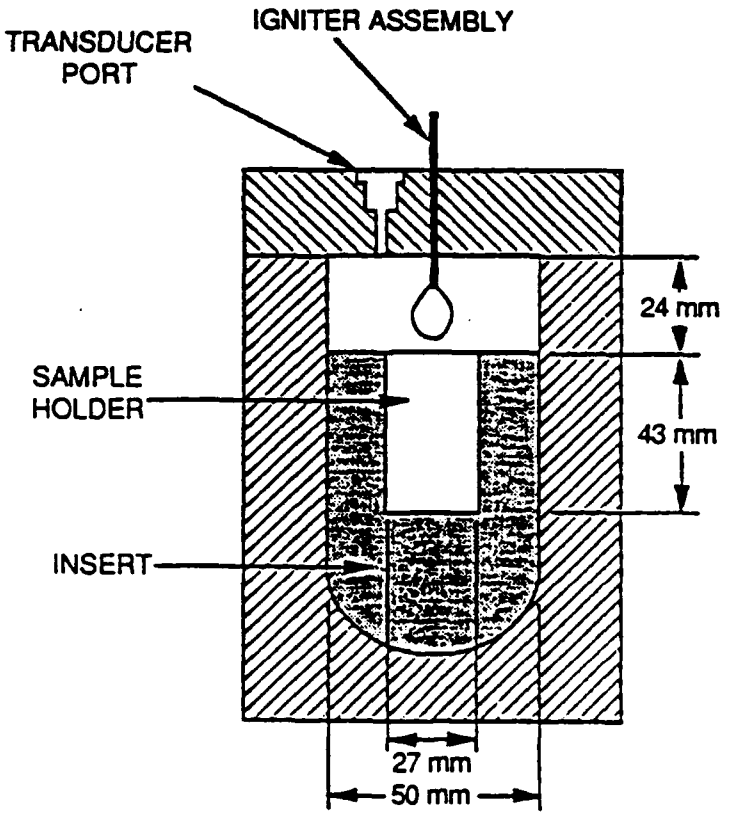

Figure 2. Closed Chamber Schematic.

The experimental closed chamber data are reduced to apparent burn rates using the BRLCB (Oberle and Kooker 1989) closed chamber data analysis program. The analysis is based upon a Nobel-Abel covolume equation-of-state,*

$$P\left(V - \eta m - \frac{(C-m)}{\rho}\right) = \frac{R\,T_a}{M}\,m\,, \tag{1}$$

where P is pressure, V the free volume of the closed chamber, η the propellant covolume, m the mass of propellant burned, C the total propellant mass, ρ the propellant density, R the Universal Gas constant, M the propellant molecular weight, and T_a the average gas temperature. Using a thermochemical code such as BLAKE (Freedman 1982), η and M are calculated based upon the chemical composition of the propellant. Density, ρ, is a measurable time-independent quantity which is dependent on the propellant composition. Finally, the volume, V, and total charge mass, C, are measurable parameters for each experimental firing. Hence, Equation 1 has three undetermined quantities, P, T_a, and m. However, conservation of energy,*

$$m e_s - Q_w\,(P) = T_a\,m\,c_v\,, \tag{2}$$

where e_s is the specific internal energy of the propellant, $Q_w(P)$ a heat-loss function dependent on pressure, and C_v the specific heat at constant volume, provides a second coupled equation to Equation 1. Thus, using the measured pressure at each time step, Equations 1 and 2 can be solved simultaneously for m and T_a.

Utilizing a numerical differentiation scheme, the time rate of change of the mass propellant, dm/dt, is computed for each time step. The burn rate at each time step is then computed using,

$$r = \frac{dm/dt}{\rho A}\,, \tag{3}$$

where r is the apparent burn rate and A the instanteous reacting surface area which is based upon the propellant geometry. However, since a liquid has no fixed geometry, for the data reduction it is assumed that propellant burning will proceed in a cigarette fashion down the

*For simplicity, igniter material and air in the chamber are not included.

sample holder, Figure 2. Thus, the reacting surface area, A, for these calculation is constant and is the cross-sectional area of the sample holder.

Computed burn rates are traditionally plotted on a log-log scale as a function of pressure. A typical plot from this study is shown in Figure 3. Three distinct burn rate regions are evident—(1) a linear region up to about 100 MPa, (2) a second linear region from approximately 100 to 150 MPa, and (3) a region of sharp rise and fall in the burn rate (from point A forward). This last region is not thought to represent the actual burn rate but is a result of a "mismatch" in the amount of propellant surface area which is actually reacting vs. that which is used to compute the burn rate, Equation 3. This type of behavior in computed burn rates has been observed before in solid propellants which deconsolidate or have "in-depth" burning (Leveritt 1981).

One final comment on the burn rate calculation. As mentioned previously, the reacting surface area is assumed to be flat and equal to the cross-sectional area of the sample holder, Figure 4a. However, it is generally accepted (McBratney 1976; Vosen 1989; Leveritt 1990; and Klein 1990) that the regressing propellant surface will not be flat but undulating or turbulant as depicted in Figure 4b. If this is the case, then the actual reating surface area will be greater than the surface area assumed in the burn rate computation, Equation 3. Therefore, since the burn rate is inversely proportional to the value of the reacting propellant surface area, the computed burn rates could be higher than the true LGP 1846 burn rates. *In this study, the computed burn rates can be higher than the actual burn rates, but not lower.*

3. FIRING MATRIX

A total of 29 firings were used for the study. The firings were divided into four categories with the following objectives: (1) igniter study, to determine the effect that initial pressure will have on liquid propellant burn rate; (2) loading density study, to determine if the burn rate is dependent on initial loading density (loading density is the ratio of propellant mass to chamber volume); (3) conditioned cold, to determine the effect on burn rate of liquid propellant conditioned to -25° C; and (4) conditioned hot, to determine the effect on burn rate of liquid propellant conditioned to 60° C. Table 1 summarizes the firing matrix.

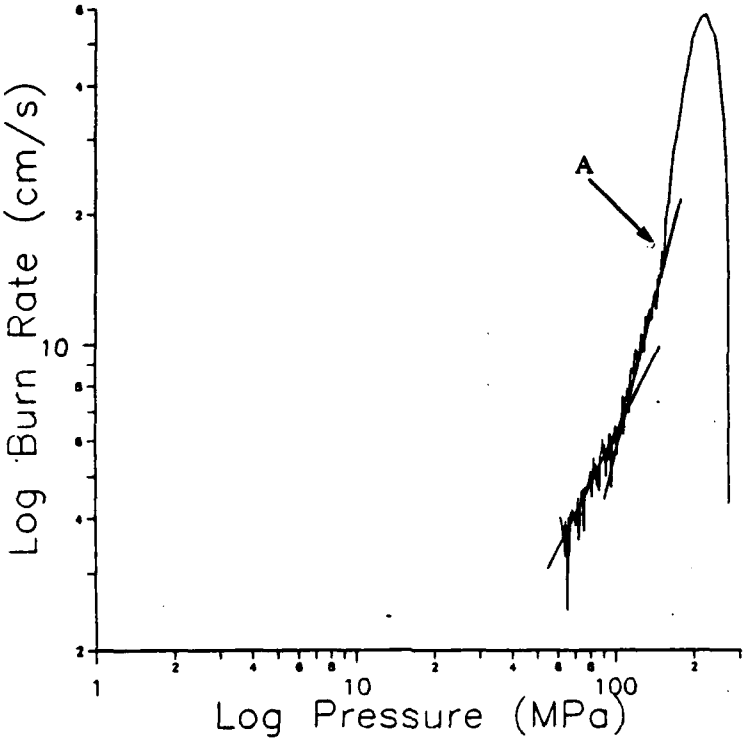

Figure 3. Typical Burn Rate vs. Pressure Plot.

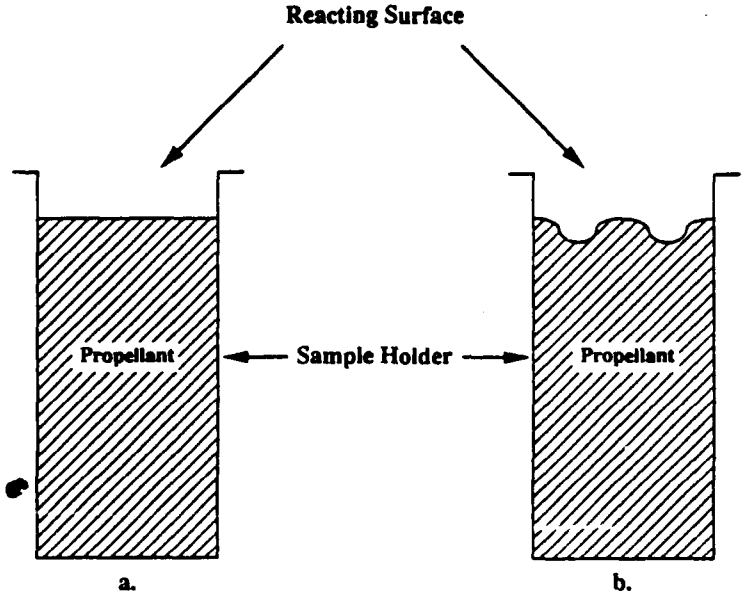

Figure 4. Schematic of Possible Propellant Reacting Surface.

Table 1. Firing Matrix

Shot No.	Igniter Mass (g)	Igniter Press (MPa)	LGP Mass (g)	Loading Density (g/cm^3)
Igniter Study:				
1	4.7	70	16.6	0.23
2	6.8	105	14.1	0.19
3	8.7	138	11.7	0.16
4	10.6	172	9.4	0.13
5	12.4	207	7.3	0.10
Loading Density Study:				
6–9	2.8	26	11.0	0.15
10–12	2.8	30	14.6	0.20
13–15	2.8	35	18.3	0.25
16–18	2.8	40	21.9	0.30
Conditioned Cold (-25° C):				
19–24	2.8	40	21.9	0.30
Conditioned Hot (60° C):				
25–29	2.8	40	21.9	0.30

4. RESULTS

Figure 5 is the pressure-time data recorded for shot number 7 and is typical, in shape, for all firings (1–12) with a loading density for the liquid propellant of up to about 0.25 g/cm^3. The curve has the following three distinct regions: (1) -0.04 s to -.006 s, where the pressure rises to about 30 MPa which is approximately the pressure due to the igniter; (2) -0.006 s to 0.04 s with a pressure rise from 30 MPa to approximately 52 MPa; and (3) 0.04 s to 0.08 s with a pressure rise from 52 MPa to 132 MPa. It is interesting to note that the time duration for the second region is slightly longer than that of region three, .046 s to .04 s, yet has a pressure rise of only 22 MPa compared to the 80 MPa for region three. Region two may be indicative of the time associated with accumulation which has been noted in modeling liquid propellant combustion (Coffee, Wren, and Morrison 1989, 1990; Coffee, Baer, Morrison, and Wren 1989). Analyses of pressure histories in liquid propellant gun firings

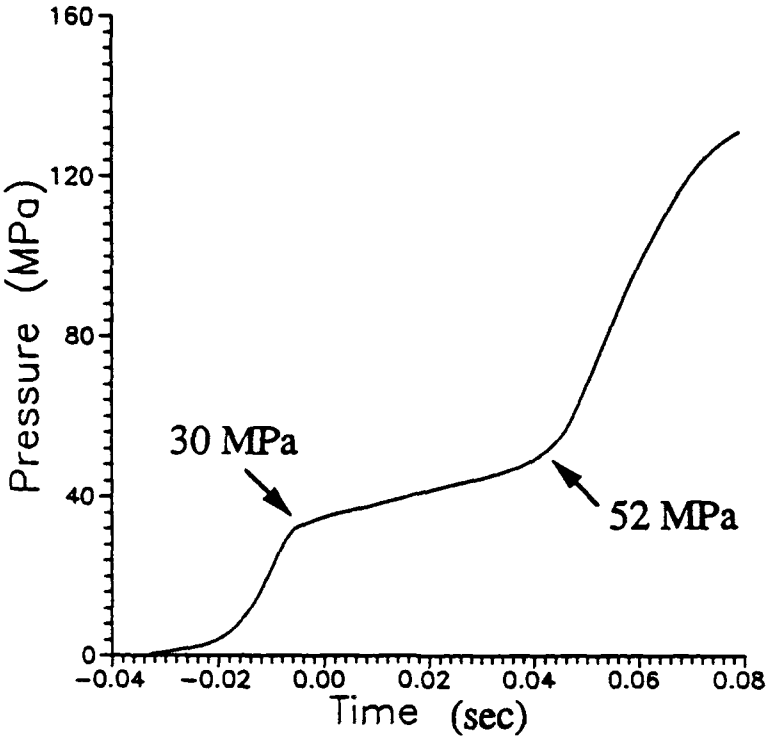

Figure 5. Pressure-Time Data, Shot No. 7.

have indicated that LGP 1846 releases only a portion of its energy during the initial pressure and temperature rise in the combustion chamber (Coffee 1986). The time associated with the transition to rapid and complete combustion has been termed the accumulation phase and is generally associated with the pressure rise to approximately 50 MPa.

Figure 6 is the calculated burn rate associated with the pressure-time curve of Figure 5. The portion of the curve between points A and B corresponds to the pressure region from approximately 52 MPa to 132 MPa. The near vertical rise in the computed burn rate between A and B is probably not indicative of the actual burn rate of LGP 1846 but indicates that a significately larger surface area of the propellant was reacting than used in Equation 3 for the burn rate computation. This result is consistent with experimental observation for combustion of LGP 1846 at low loading densities. Klein (1991) has proposed that the sensitivity of burn rate to loading density is related to the decomposition process of the liquid propellant. A higher loading density provides a higher gas concentration from the initial HAN decomposition. The subsequent gas/liquid (AAN droplets) reaction is a function of the amount and concentration of gases in the gas phase. As mentioned previously, the pressure-time histories

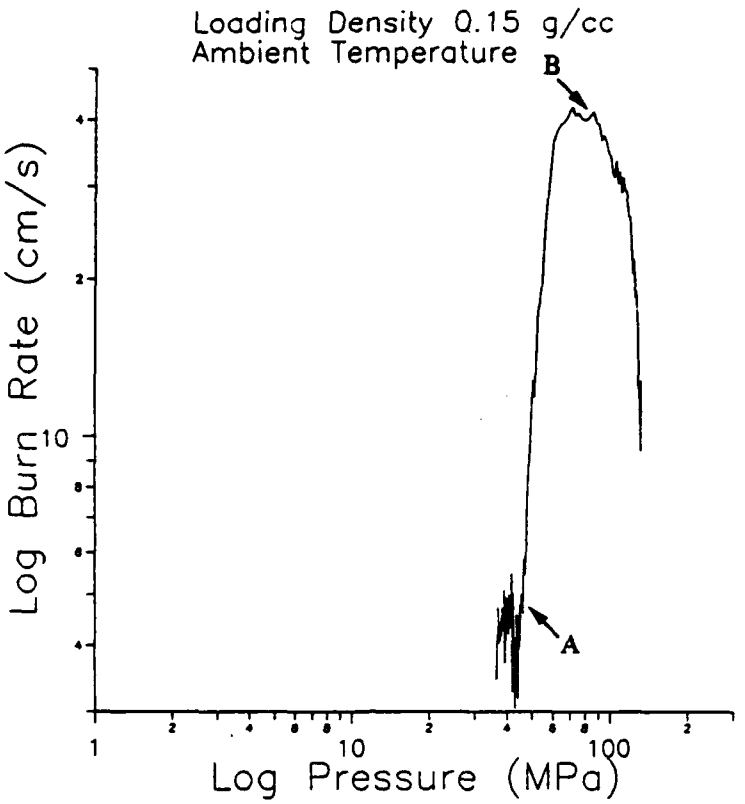

Figure 6. Apparent Burn Rate, Shot No. 7.

and, hence, the burn rate curves for firings 1 through 12 are similar in shape to Figures 5 and 6, although they do differ in timing. Thus, for this study it is felt that no meaningful information concerning the burn rate for LGP 1846 can be obtained from firings 1–12.

However, Figures 7 and 8 present the corresponding information for shot number 24, which is typical for firings (13–29) with liquid propellant loading density 0.25 g/cm^3 and above. The curve consists of two regions—(1) -0.10 s to -0.05 s with a pressure rise to about 35 MPa, approximately the igniter pressure and (2) -0.05 s to 0.30 s with a typical closed chamber pressure curve to about 260 MPa. The pressure-time profile of Figure 7 produces the apparent burn rate information shown in Figure 8, which appears to provide meaningful results up to about 180 MPa.

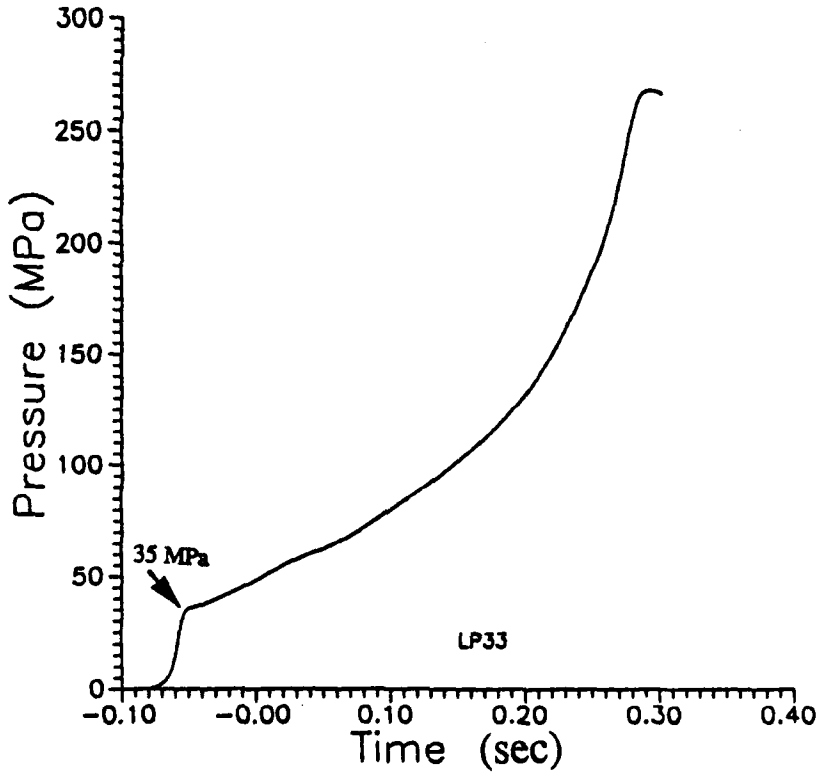

Figure 7. Pressure-Time Data, Shot No. 24.

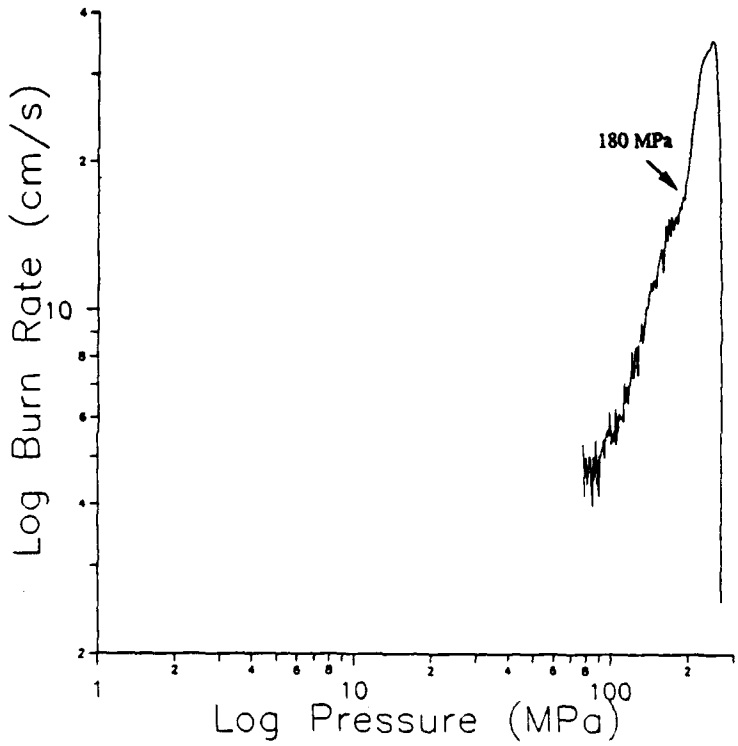

Figure 8. Apparent Burn Rate, Shot No. 24.

5. BURN RATE CALCULATIONS (AMBIENT TEMPERATURE) AND COMPARISONS WITH EARLIER WORK

Based upon the discussion of the previous section, for the calculation of a burn rate at ambient temperature, the results from the 0.3 g/cm^3 loading density, firings 16–18, will be utilized. The "meaningful" portion of the computed burn rate curves for firings 16–18 are shown in Figure 9. As can be observed, two of the three firings produce "similar" curves. The burn rate at ambient temperature for LGP 1846 will be based upon these two curves. One additional observation, Figure 10, is a log-log graph of pressure vs. burn rate for shot number 16. As observed in the McBratney, Bensinger, and Arford (1976) results for NOS propellant, there appears to be a change in slope for the burn rate at about 100 MPa, as indicated by the straight lines on the burn rate curve. Similar slope changes are present in all the firings—ambient, conditioned hot, and conditioned cold— performed at the 0.3 g/cm^3 loading density and for several firings at lower loading densities.

Table 2 presents the combined computed burn rate law for the data from shots number 16 and 17, the two lower curves in Figure 9. The burn rate law is given in $r = bP^n$ form, with r having units in centimeters per second. Table 3 provides the burn rate information for the LGP 1845 McBratney (1981) strand burner data and combined burn rate information provided by Vosen (1989) for the McBratney, Vosen, and Lee data (McBratney, Bensinger, and Arford 1976; Vosen 1989; Lee, Tseng, and Faeth 1989).

Table 2. Burn Rates for LGP 1846 at a 0.3-g/cm^3 Loading Density in the Form $r = bP^n$

Pressure Range (MPa)	Coefficient (b) (cm/s-MPa)	Exponent (n)
75–101	0.0024	1.67
101–190	0.000548	1.99

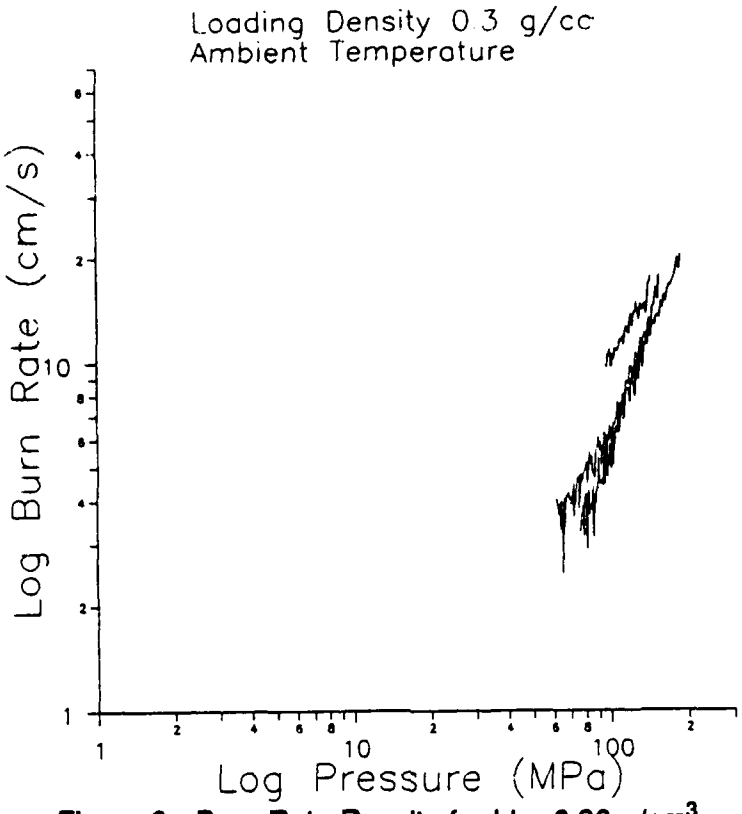

Figure 9. Burn Rate Results for ld = 0.30 g/cm^3.

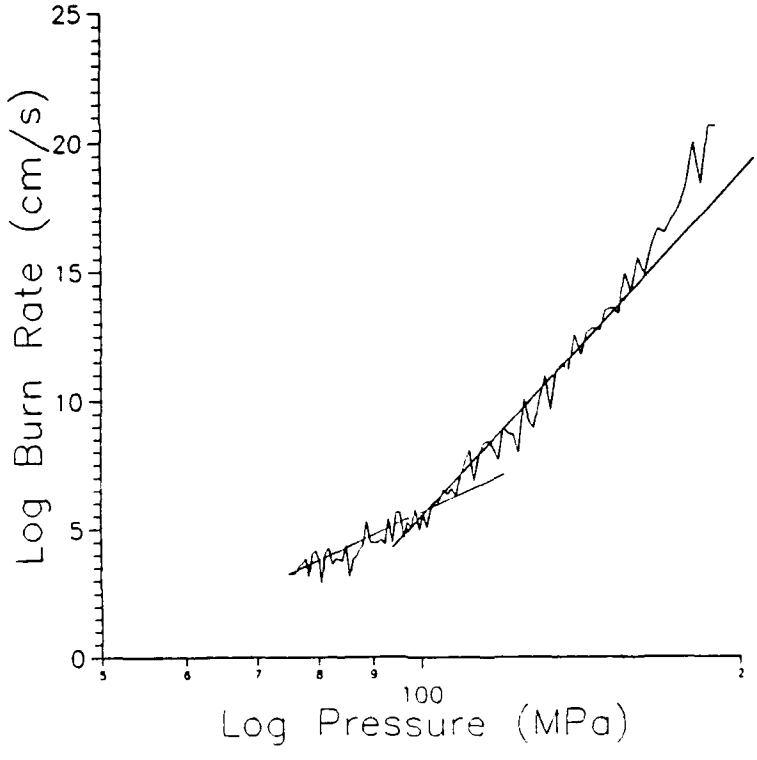

Figure 10. Burn Rate for Shot Number 16 With Slope Break.

Table 3. Burn Rate Information by McBratney and Vosen[a] in the Form $r = bP^n$

Pressure Range (MPa)	Coefficient (b) (cm/s-MPa)	Exponent (n)
McBratney:		
10–60	1.64	0.103
Vosen:		
1–100	0.945	0.237

[a] Coffee, Wren, and Morrison 1989; Vosen 1989.

The most obvious difference between the data in Tables 2 and 3 is the magnitude of pressure exponent. However, considering the different pressure regimes, a direct comparison may not be valid, except possibly in the 60–70 MPa region. The McBratney strand burner data indicates a distinct increased slope (pressure exponent) (see Figure 1) for the measurements at 80 and 95 MPa. McBratney did not include these points in his burn rate law computation. Although Vosen, in computing the burn rate law to 100 MPa, did include the two data points by McBratney at 80 and 95 MPa, this was the only burning rate data for pressures above 60 MPa and no special consideration was given to the increased slope indicated by these two data points.

A comparison of the burn rates from 60 to 70 MPa, possibly a valid regime for extrapolation for the burn rates computed in this study, indicates reasonable agreement with earlier work (see Table 4).

Table 4. Comparison of Computed Burn Rates Between 60 and 70 MPa

Pressure (MPa)	Burn Rate, Present Study (cm/s)	Burn Rate, McBratney (cm/s)	Burn Rate, Vosen (cm/s)
60	2.24	2.50	2.49
65	2.56	2.52	2.54
70	2.89	2.54	2.59

6. BURN RATE CALCULATIONS FOR TEMPERATURE-CONDITIONED PROPELLANT

Firings 19 to 24 were performed with the liquid propellant conditioned to a temperature of -25° C and firings 25 to 29 with the propellant conditioned to a temperature of +60° C. Loading density in all firings is 0.3 g/cm^3. Computed burn rates for these firings are presented in Table 5.

Table 5. Burn Rates for LGP 1846 Conditioned to -25° C and +60° C Temperatures, at a 0.3-g/cm^3 Loading Density of in the Form $r = bP^n$

Pressure Range (MPa)	Coefficient (b) (cm/s-MPa)	Exponent (n)
Conditioned -25° C:		
75–100	0.139	0.848
100–200	0.0218	1.25
Conditioned +60° C:		
65–100	0.00132	1.87
100–220	0.00018	2.3

Figure 11 shows a comparison of the burn rates for the temperature-conditioned and ambient firings. The measured burn rates for the conditioned-cold and ambient firings are similar while the rate for the conditioned-hot propellant is substantially higher.

7. INTERIOR BALLISTIC CALCULATIONS

In the regenerative liquid propellant gun, a liquid jet is introduced into the combustion chamber through an annulus where it undergoes a complex series of steps including breakup and combustion. These processes are not well understood and have not successfully been resolved into component processes. However, recent work with a lumped parameter code (Coffee, Wren, and Morrison 1989, 1990; Coffee, Baer, Morrison, and Wren 1989) has shown that a theoretical model of jet breakup into droplets in combination with a pressure-dependent burn rate for the liquid droplets provides good agreement with 30-mm, 105-mm, and 155-mm experimental data. The current burn rate used in the code is the McBratney measured burn

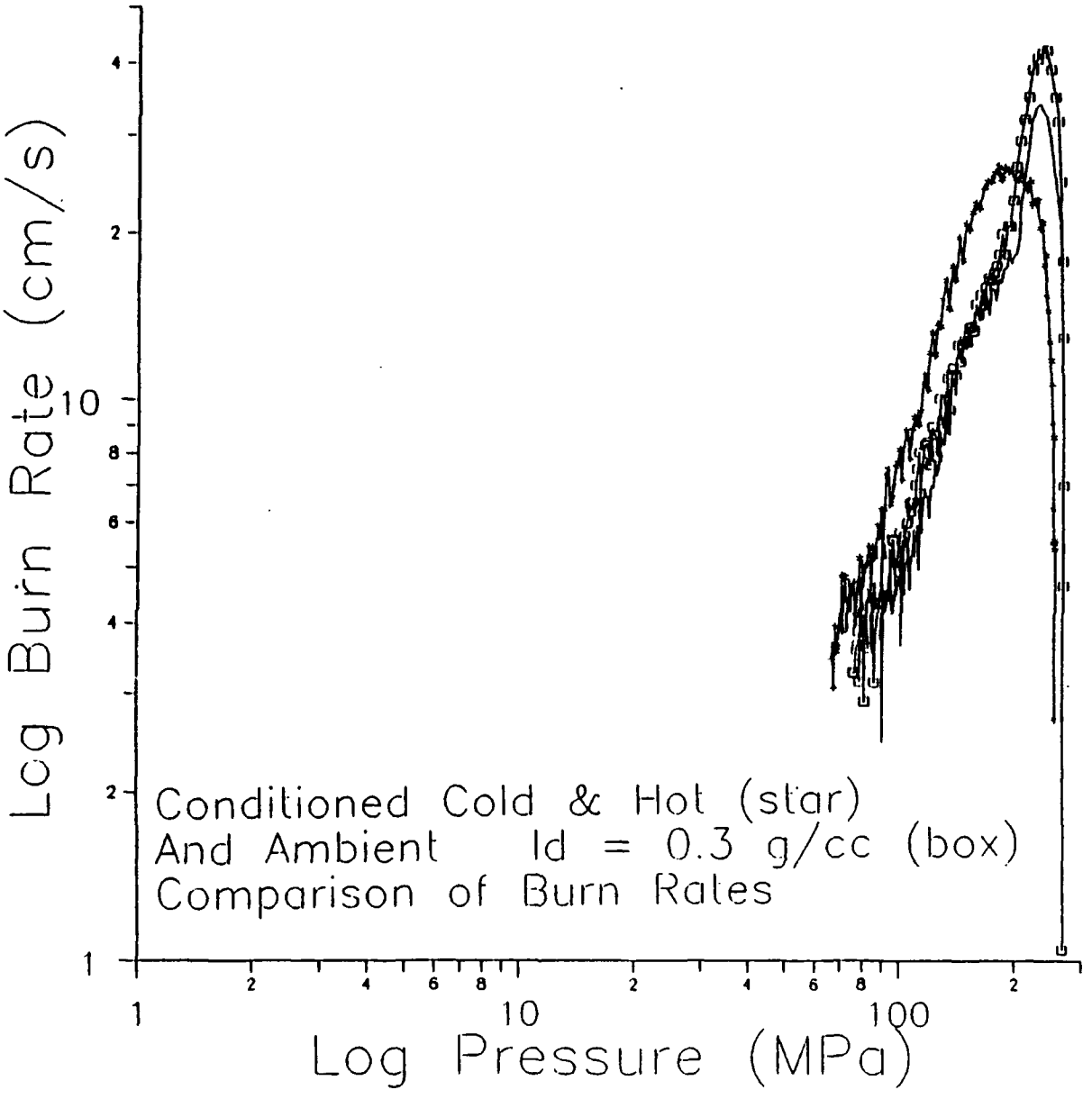

Figure 11. Burn Rate Comparison for Temperature-Conditioned and Ambient Liquid Propellant.

rate shown in Table 3. It has previously been recognized that an increase in burn rate may occur for pressures above about 80 MPa, and the influence of higher burn rates in model results is of interest.

For solid propellants, temperature conditioning has a marked effect on pressure with variations of up to 15% in maximum pressure. It is of interest to determine if the same response of the propellant is observed with liquid propellants. Thus, a two-part burn rate was added to the interior ballistic model (Coffee 1990) as shown in Table 6. The McBratney data are used for ambient, cold, and hot conditions up to 65 MPa. The burn rates determined from the current set of firings is used for pressures above 65 MPa for the respective conditions.

Table 6. Burn Rates Used in Interior Ballistic Calculations

	Pressure Range (MPa)	Coefficient (b) (cm/s-MPa)	Exponent (n)
	0–65	1.64	0.103
ambient	> 65	0.000548	1.99
cold	> 65	0.0218	1.25
hot	> 65	0.00018	2.3

A comparison of the model at ambient conditions with experimental mean chamber pressure is shown in Figure 12 for a 155-mm, 5-liter charge firing. In Figure 13, a comparison of model results using the derived ambient, cold, and hot burning rates is shown. The general observation from Figures 12 and 13 is that at pressures above 65 MPa the energy release is primarily governed mechanically by the injection rate as opposed to the burning rate. Thus, the current burn rates make little difference in model results compared to the experiment.

However, the cold and hot conditioning of the propellant may affect the discharge coefficients from the reservoir and the damper. The model will need to consider the combination of altered discharge coefficients and altered burn rates to make a meaningful statement about gun performance at temperature extremes.

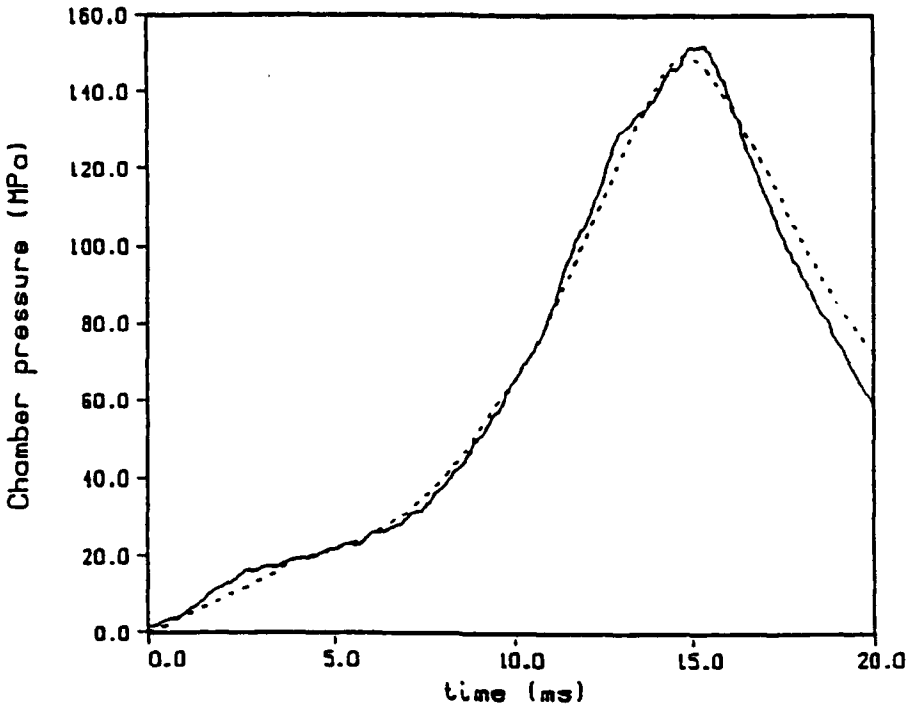

Figure 12. 155-mm, 5-liter Charge Experimental Chamber Pressure (Line); Model With Ambient Burn Rate (Dot).

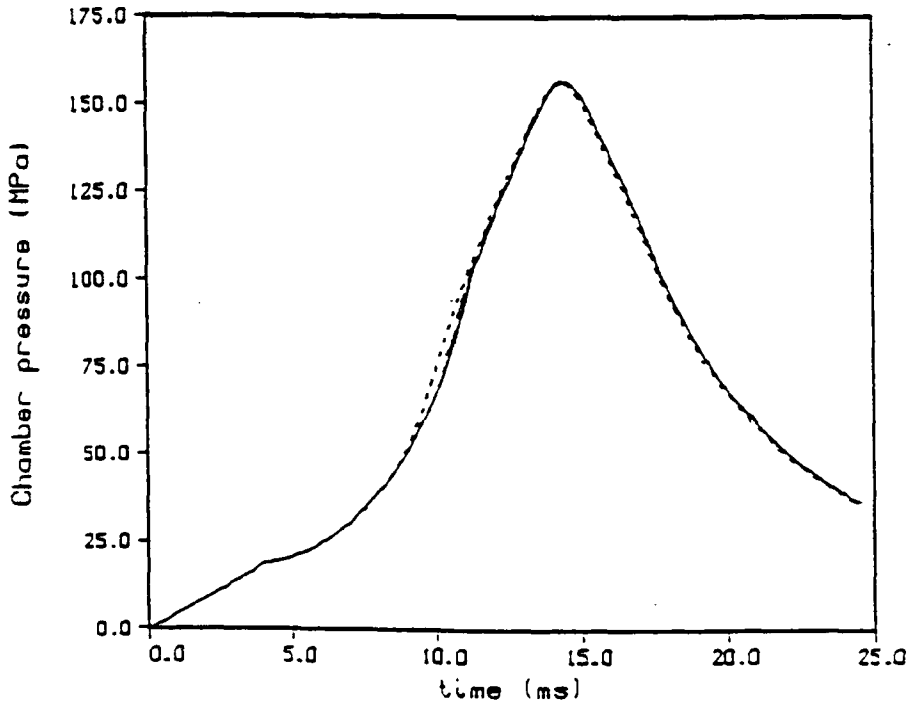

Figure 13. Model With Ambient (Line), Cold (Dot), and Hot (Dash) Burning Rates.

8. CONCLUSIONS

In this study, samples of LGP 1846, without gelling, were fired in a closed chamber to pressures up to 200 MPa. The firings were performed under various loading densities, igniter pressures, and temperature conditioning. Computed burn rate laws, $r = bP^n$, resulted in higher than expected exponents, approximately 2.0. It is possible that the large exponent is a result of the assumption concerning the reacting propellant surface area, which is underestimated if the reacting surface is undulating or turbulent. However, in a limited pressure range (60–70 MPa) where extrapolation of the results from this work and previous studies may be valid, reasonable agreement in burning rates is obtained. The burn rate results for the temperature-conditioned propellant indicate that when conditioned "hot" the burn rate is substantially higher than the computed burn rate of the propellant at ambient temperature. If conditioned "cold," the computed burn rate is slightly lower than the burn rate at ambient. Finally, interior ballistic calculations show that the interior ballistic process above 65 MPa is primarily injection controlled rather than controlled by the burning rate of the propellant.

9. FUTURE WORK

Additional work is needed to accurately measure burn rates of liquid propellant at elevated pressures (100–400 MPa). Visualization at these pressures would allow more accurate determination of reacting surface area. In addition, interior ballistic codes of the regenerative liquid propellant gun process should consider the effect of temperature on the discharge coefficient.

10. REFERENCES

Coffee, T. "The Analysis of Experimental Measurements on Liquid Regenerative Guns." BRL-TR-2731, U.S. Army Ballistic Research Laboratory, Aberdeen Proving Ground, MD, May 1986.

Coffee, T. Private communication. U.S. Army Ballistic Research Laboratory, Aberdeen Proving Ground, MD, 1990.

Coffee, T. P., P. G. Baer, W. F. Morrison, and G. P. Wren. "Jet Breakup and Combustion Modeling for the Regenerative Liquid Propellant Gun." Proceedings of the 26th JANNAF, Combustion Meeting, Johns Hopkins University, Baltimore, MD, October 1989.

Coffee, T. P., G. P. Wren, and W. F. Morrison. "A Comparison Between Experiment and Simulation for Concept VIC Regenerative Liquid Propellant Guns: I. 30 mm." BRL-TR-3072, U.S. Army Ballistic Research Laboratory, Aberdeen Proving Ground, MD, December 1989.

Coffee, T. P., G. P. Wren, and W. F. Morrison. "A Comparison Between Experiment and Simulation for Concept VIC Regenerative Liquid Propellant Guns: I. 105 mm." BRL-TR-3093, U.S. Army Ballistic Research Laboratory, Aberdeen Proving Ground, MD, March 1990.

Freedman, E. "BLAKE - A Thermodynamics Code Based on TIGER: User's Guide and Manual." BRL-TR-02411, U.S. Army Ballistic Research Laboratory, Aberdeen Proving Ground, MD, July 1982.

Klein. "Ignition and Combustion of the HAN-Based Liquid Propellants." Proceedings of the 27th JANNAF Combustion Meeting, Cheyenne, WY, October 1990.

Klein, N. Private communication. U.S. Army Ballistic Research Laboratory, Aberdeen Proving Ground, MD, 1991.

Lee, T., L. Tseng, and G. Faeth. "Separated Flow Considerations for Pressure Atomized Combustion Monopropellant Sprays." AIAA Report 89-0049, Proceedings of 27th Aerospace Sciences Meeting, Reno, NV, January 1989.

Leveritt, C. "Ultra High Burning Rate Propellants for Traveling Charge Gun." BRL-CR-00447, U.S. Army Ballistic Research Laboratory, Aberdeen Proving Ground, MD, 1981.

Leveritt, C. Private communication. U.S. Army Ballistic Research Laboratory, Aberdeen Proving Ground, MD, 1990.

McBratney, W. F., B. D. Bensinger, and W. B. Arford. "Strand Combustion Rates for Some Liquid Monopropellants at Gun Functioning Pressures." BRL-MR-2658, U.S. Army Ballistic Research Laboratory, Aberdeen Proving Ground, MD, August 1976.

McBratney, W. F. "Burning Rate Data, LGP 1845." BRL-MR-03128, U.S. Army Ballistic Research Laboratory, Aberdeen Proving Ground, MD, August 1981.

Oberle, W. F., and D. E. Kooker. "BRLCB: A Closed Chamber Data Analysis Program With Provisions for Deterred and Layered Propellants." Proceeding of the 26th JANNAF Combustion Meeting, Johns Hopkins University, Baltimore, MD, October 1989.

Vosen, S. R. "Hydroxylammonium Nitrate-Based Liquid Propellant Combustion - Interpretation of Strand Burner Data and the Laminar Burning Velocity." Sandia National Laboratories, Livermore, CA, August 1989.

Wren, G. P., T. P. Coffee, and W. F. Morrison. "A Comparison Between Experiment and Simulation for Concept VIC Regenerative Liquid Propellant Guns: I. 155 mm." U.S. Army Ballistic Research Laboratory, Aberdeen Proving Ground, MD, to be published.

APPENDIX A:

PRESSURE-vs.-TIME PLOTS

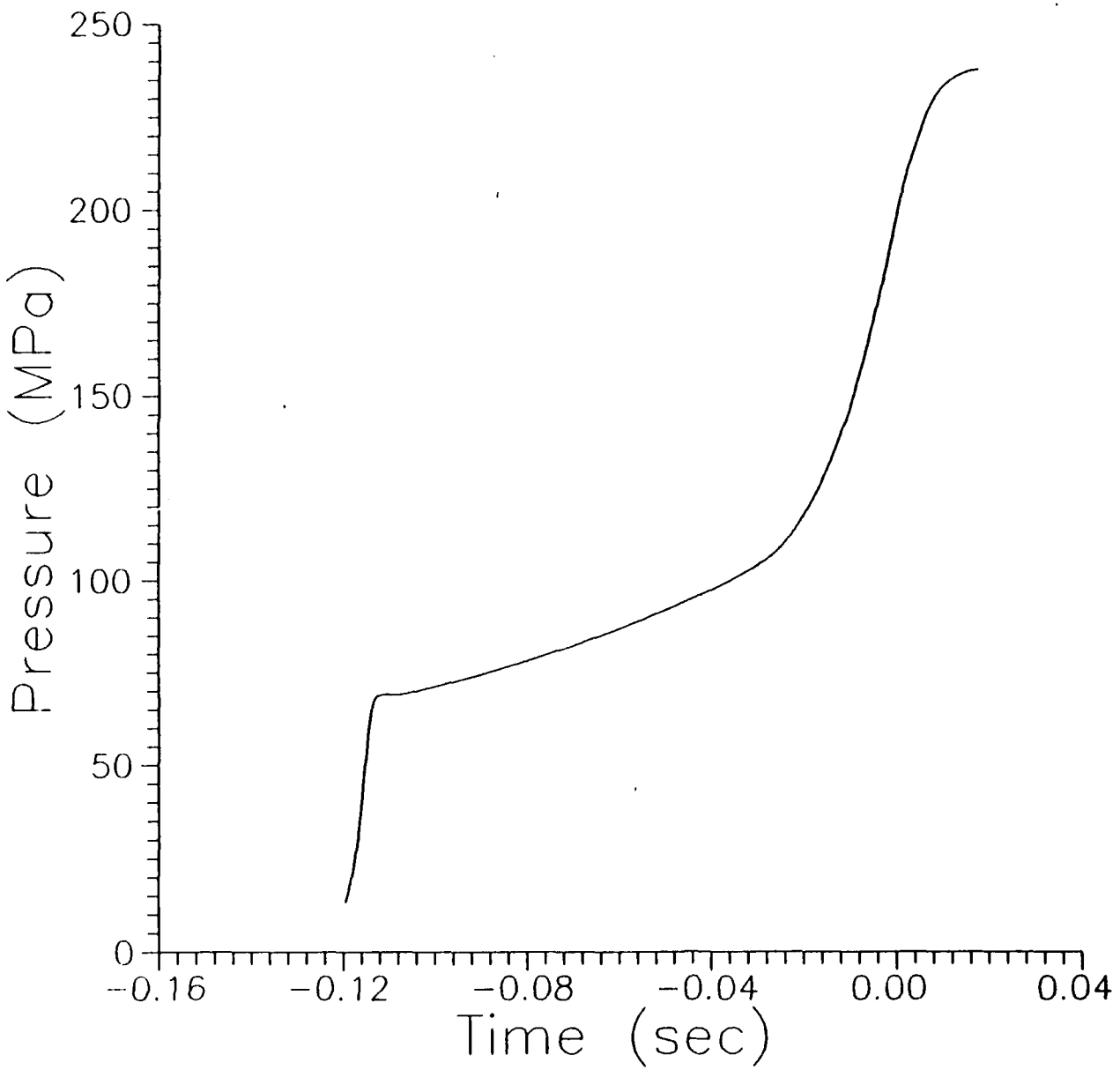

Figure A-1. Pressure vs. Time, Shot 1.

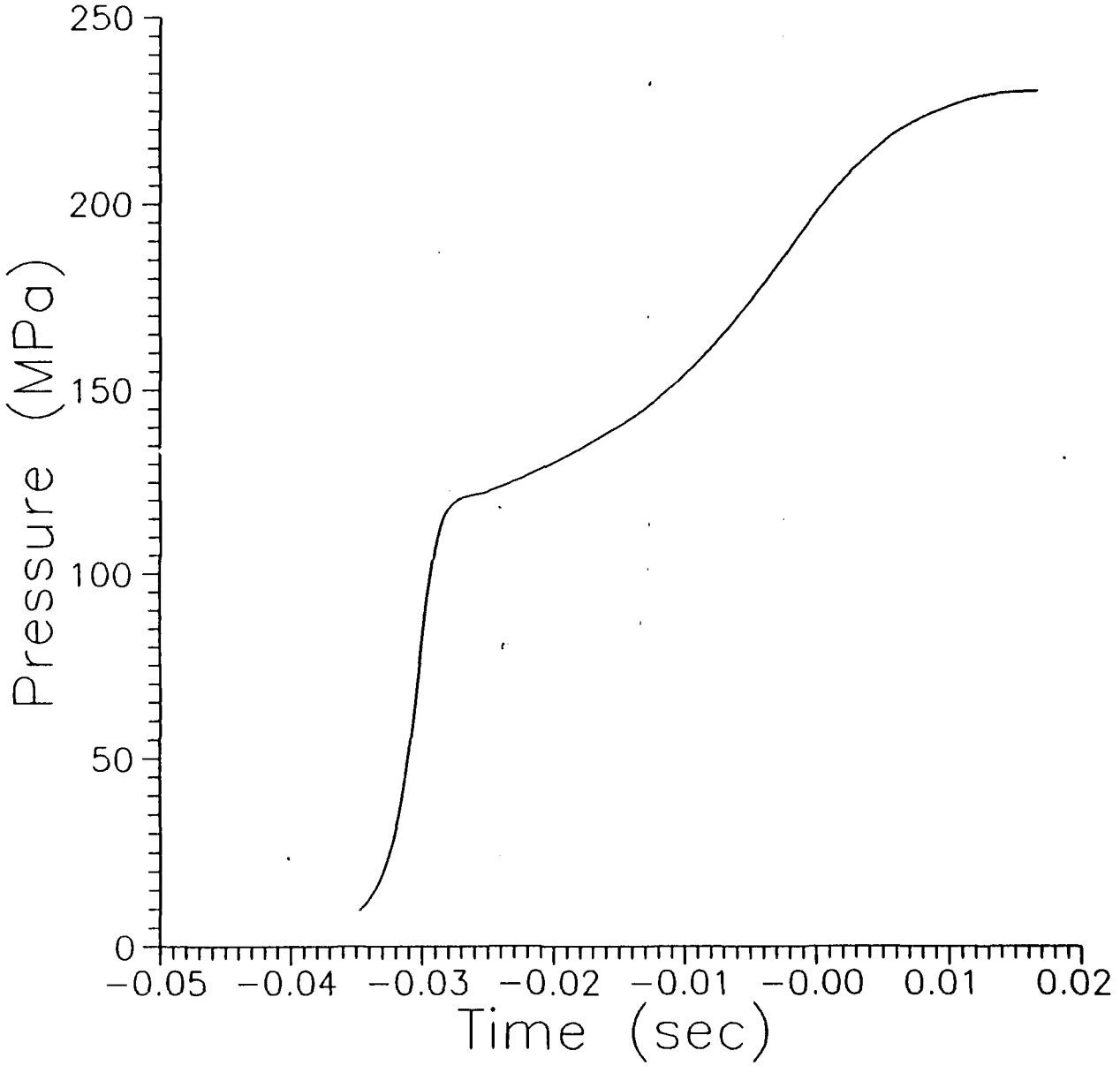

Figure A-2. Pressure vs. Time, Shot 2.

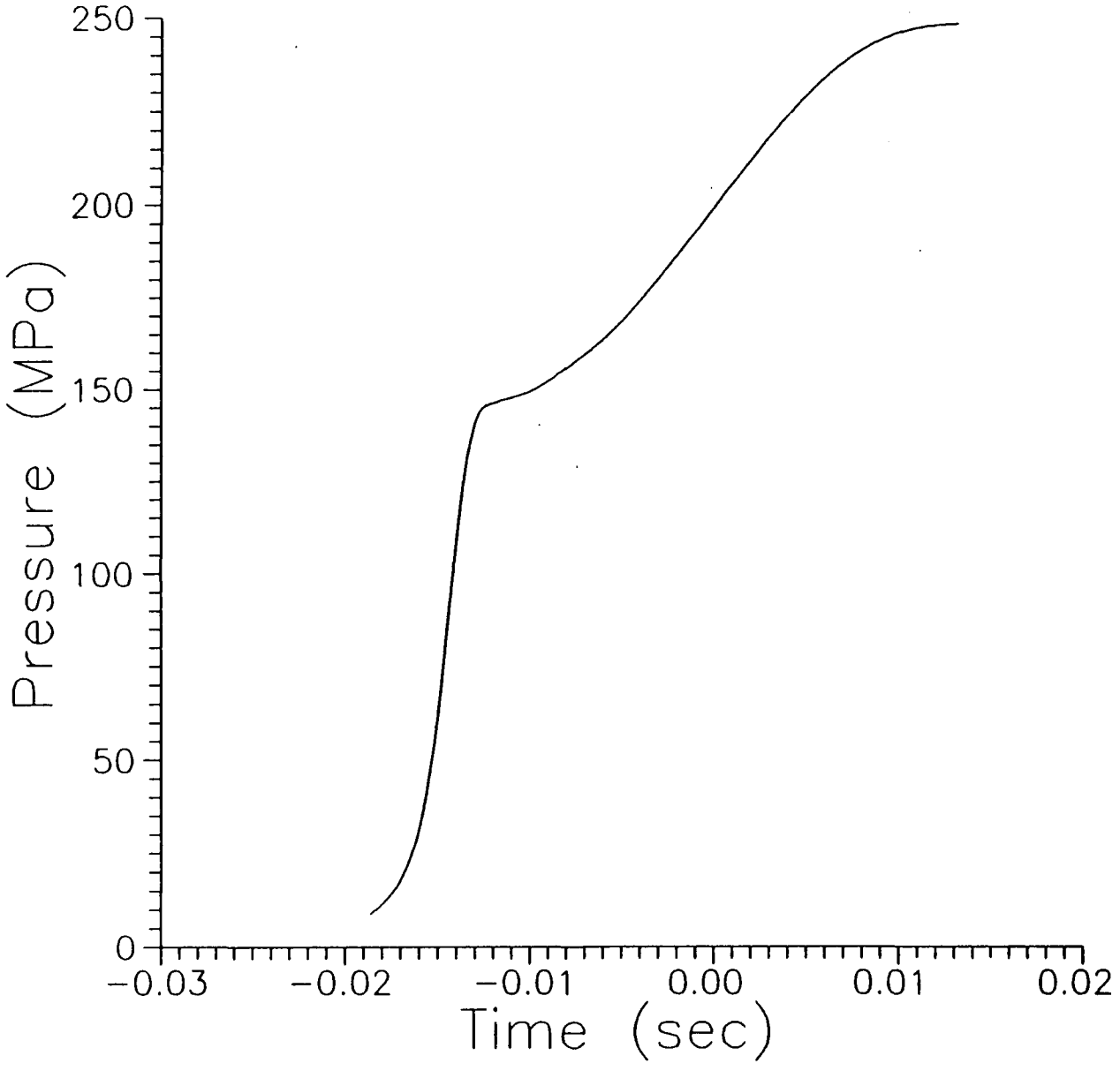

Figure A-3. Pressure vs. Time, Shot 3.

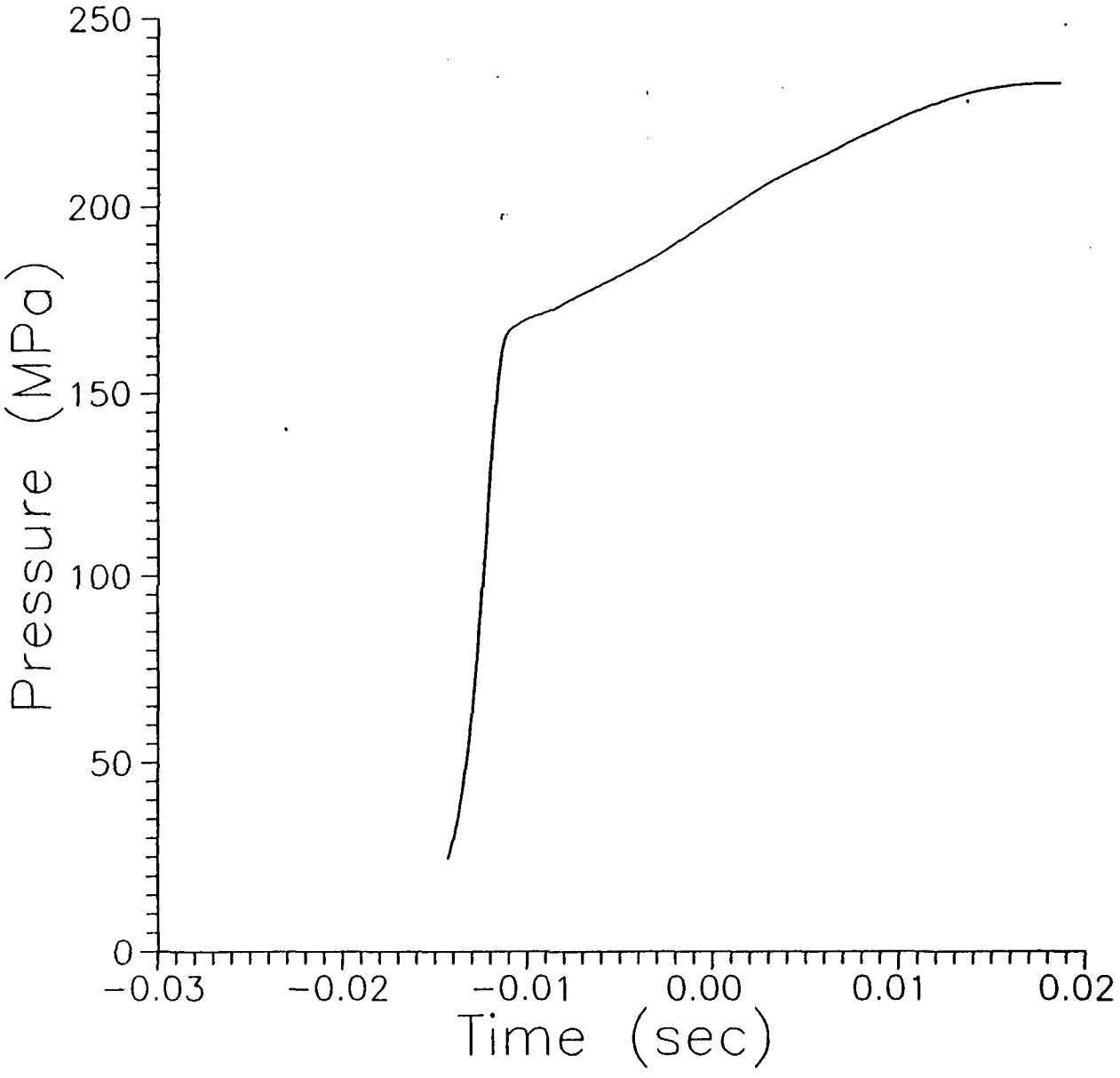

Figure A-4. Pressure vs. Time, Shot 4.

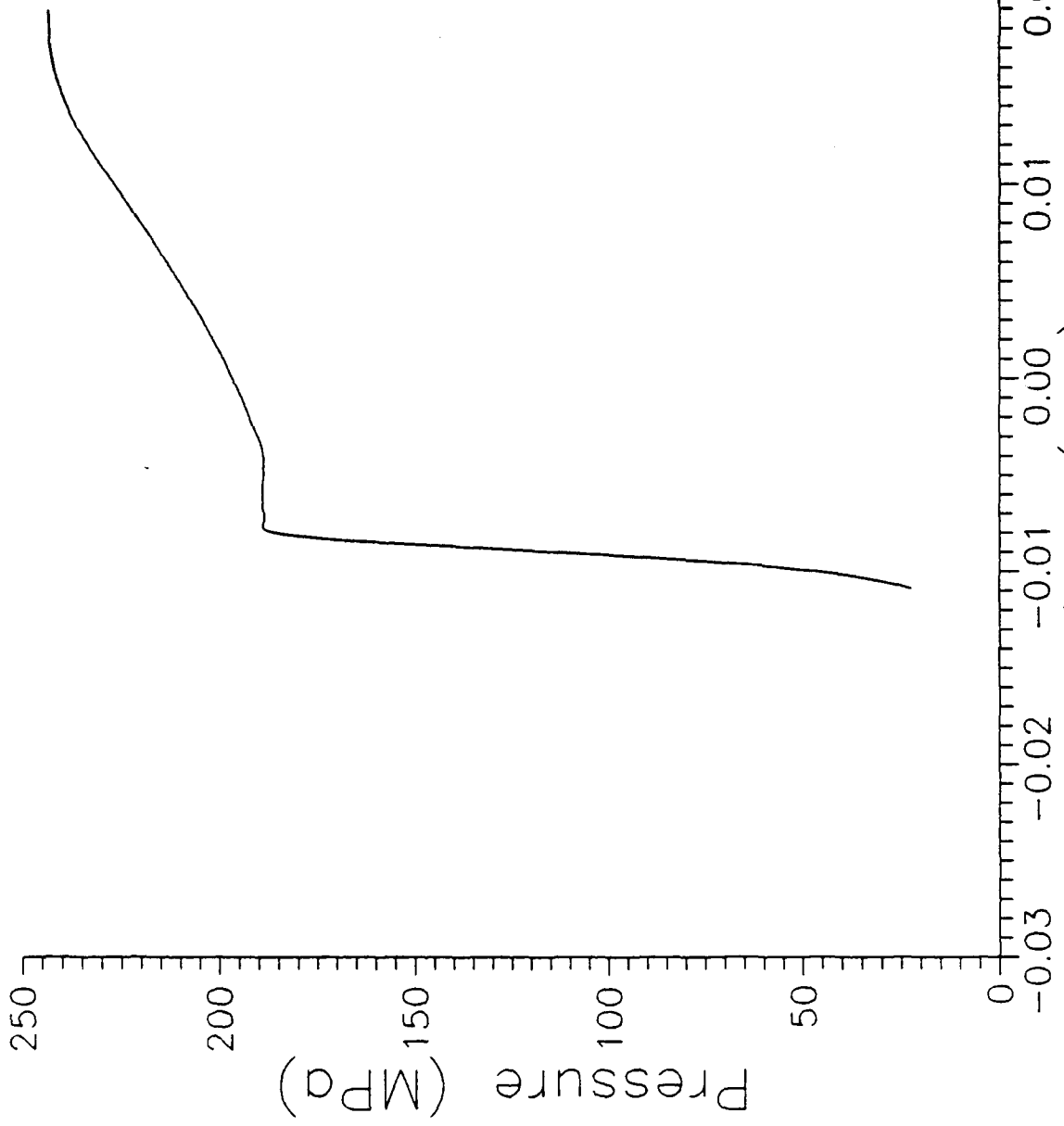

Figure A-5. Pressure vs. Time, Shot 5.

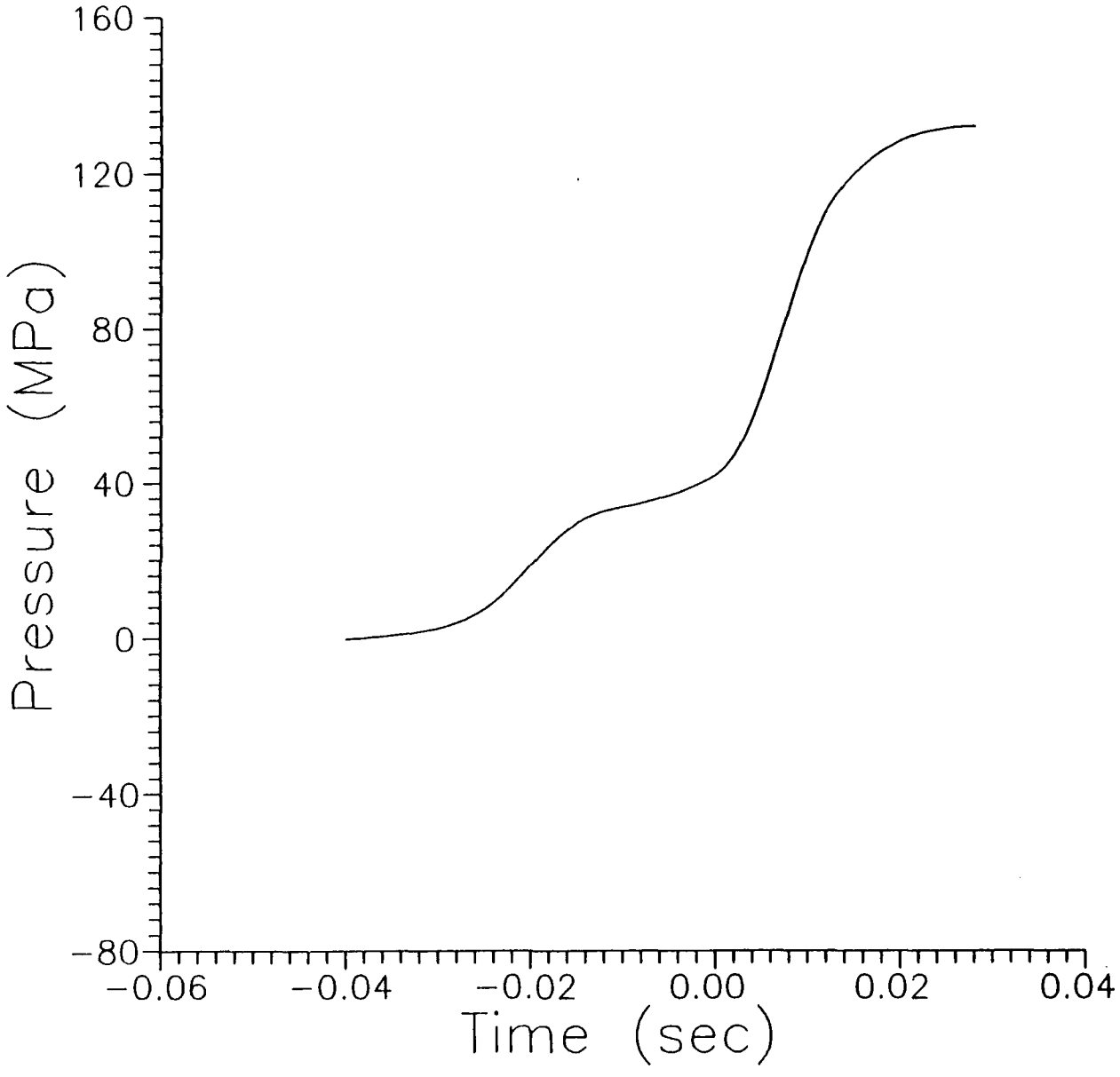

Figure A-6. Pressure vs. Time, Shot 6.

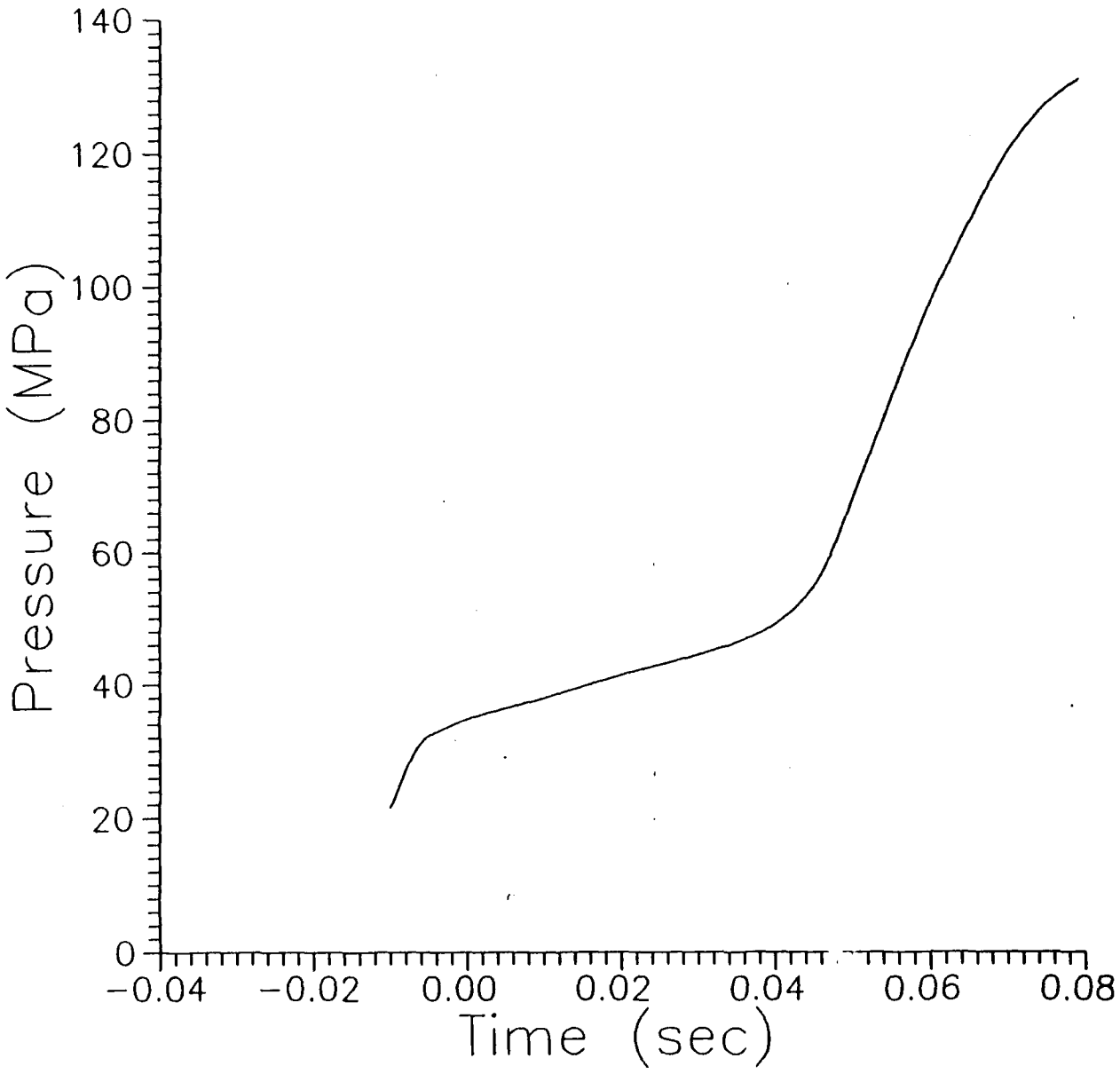

Figure A-7. Pressure vs. Time, Shot 7.

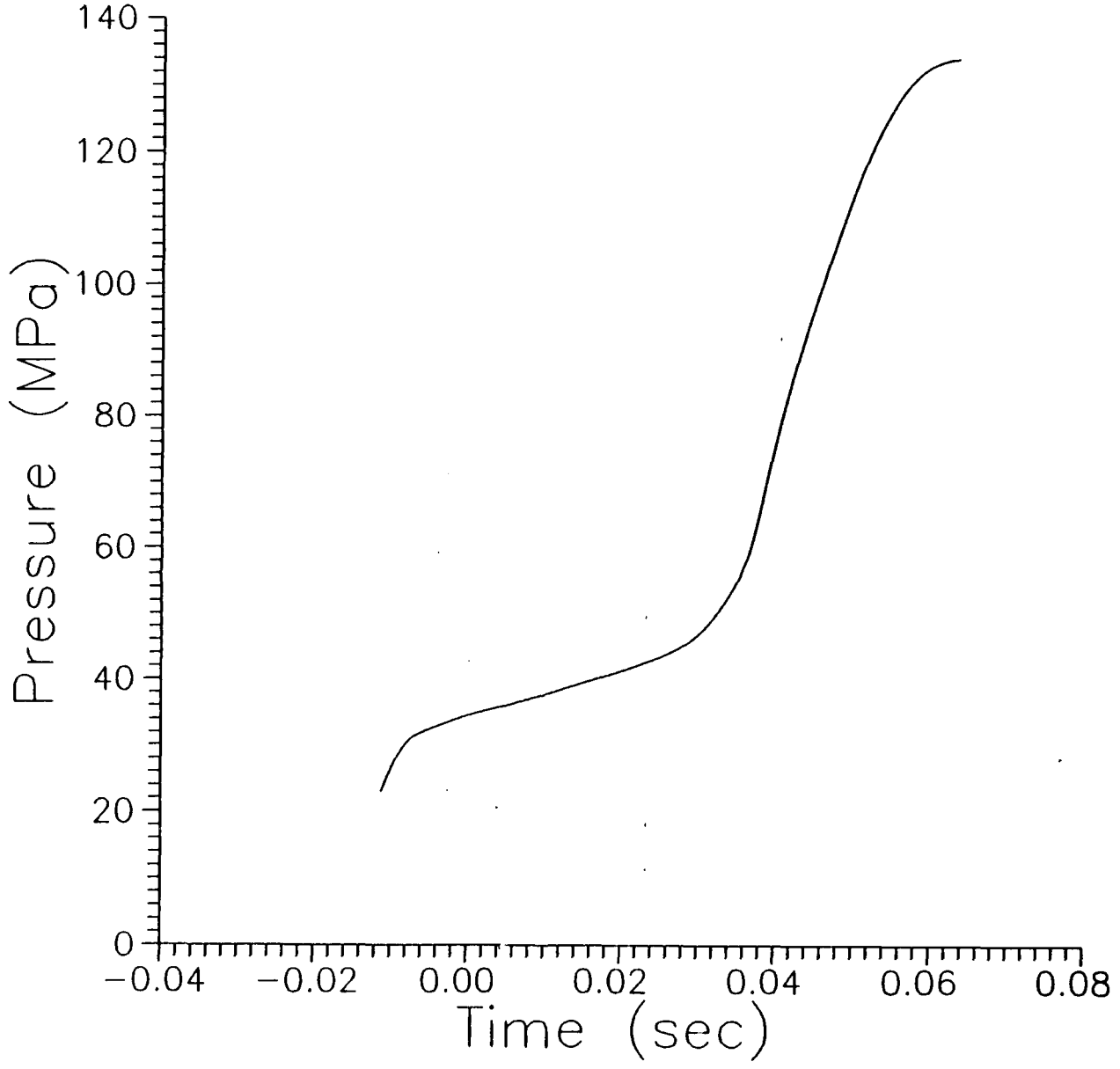

Figure A-8. Pressure vs. Time, Shot 8.

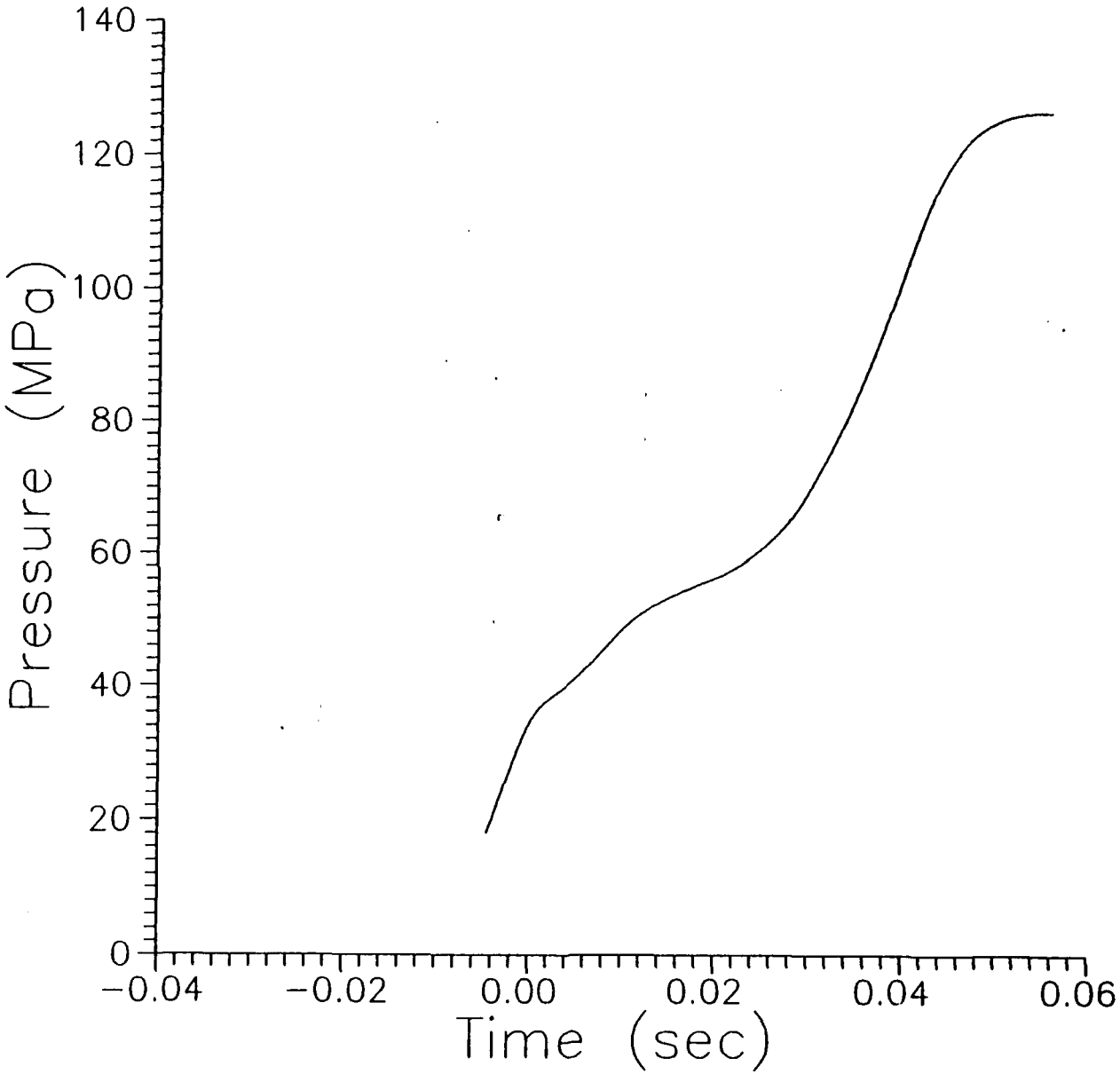

Figure A-9. Pressure vs. Time, Shot 9.

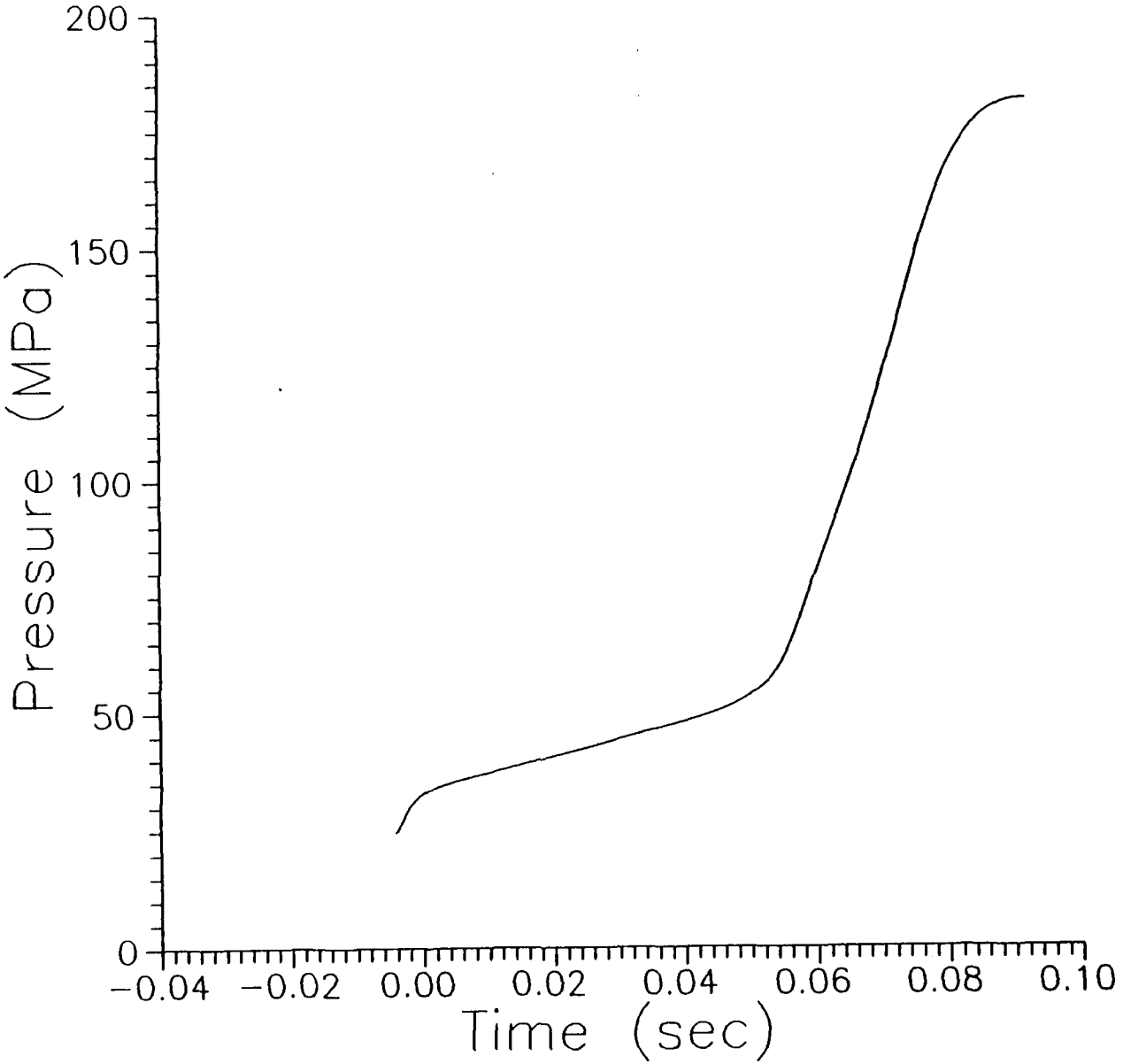

Figure A-10. Pressure vs. Time, Shot 10.

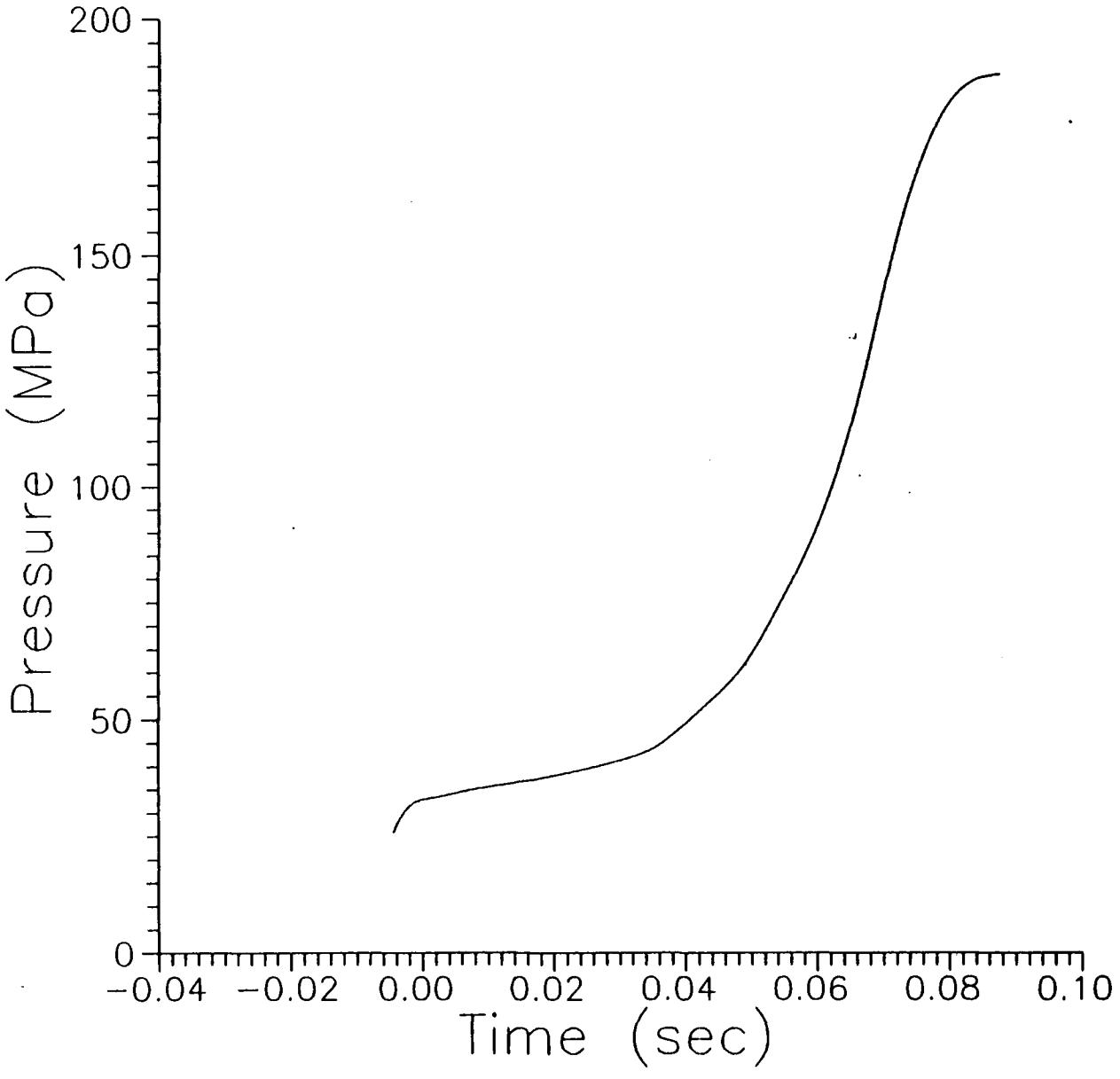

Figure A-11. Pressure vs. Time, Shot 11.

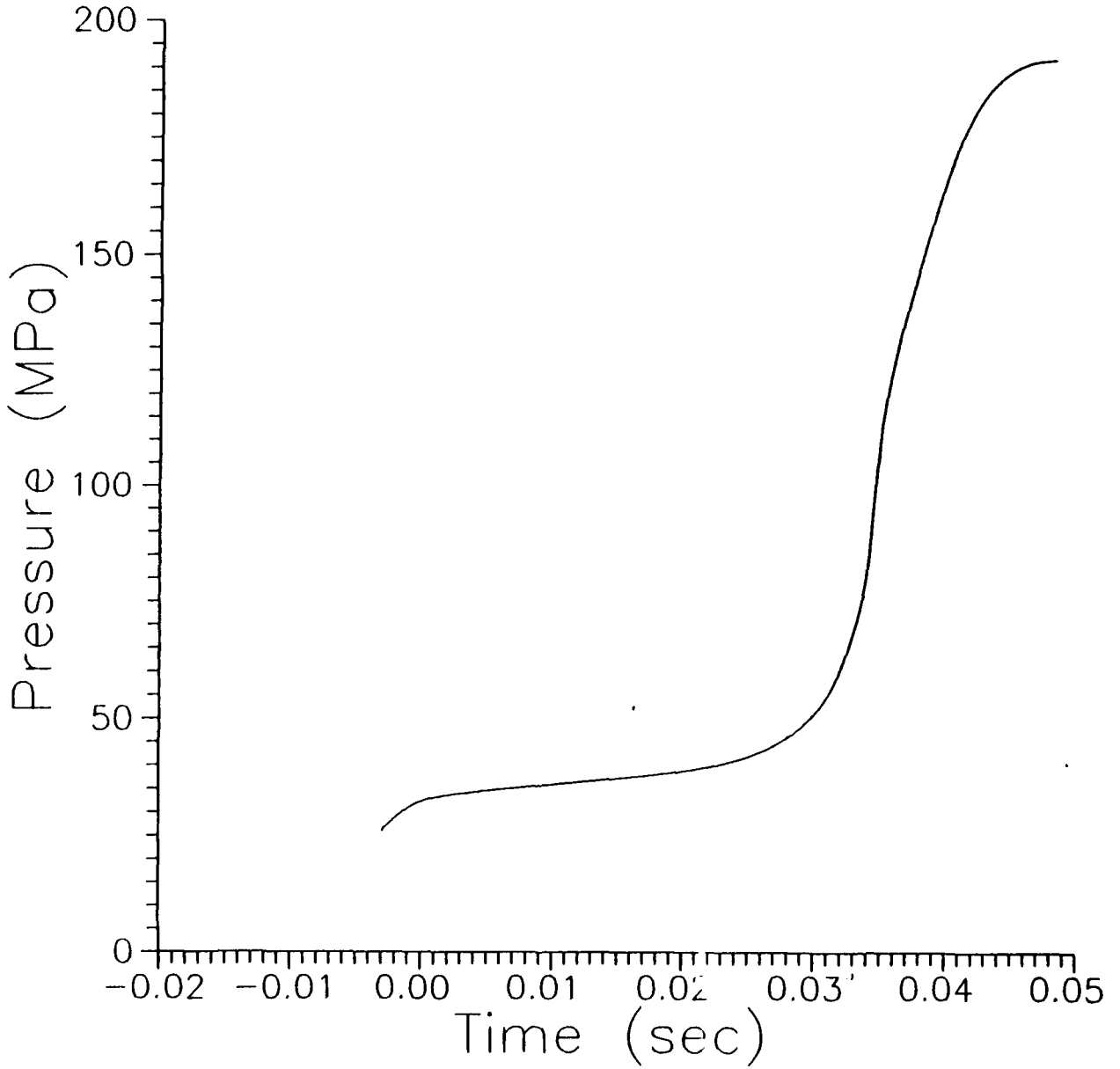

Figure A-12. Pressure vs. Time, Shot 12.

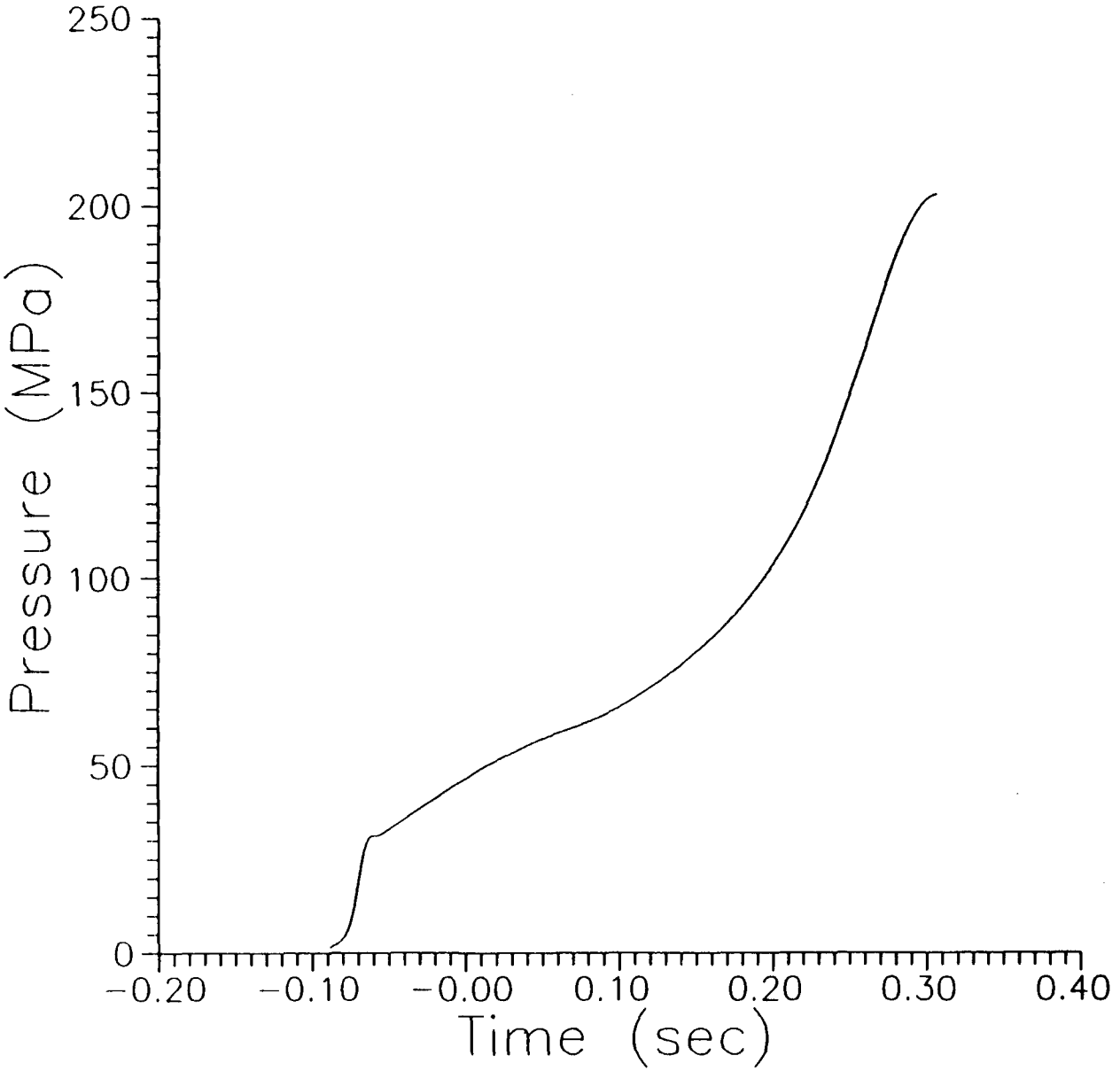

Figure A-13. Pressure vs. Time, Shot 13.

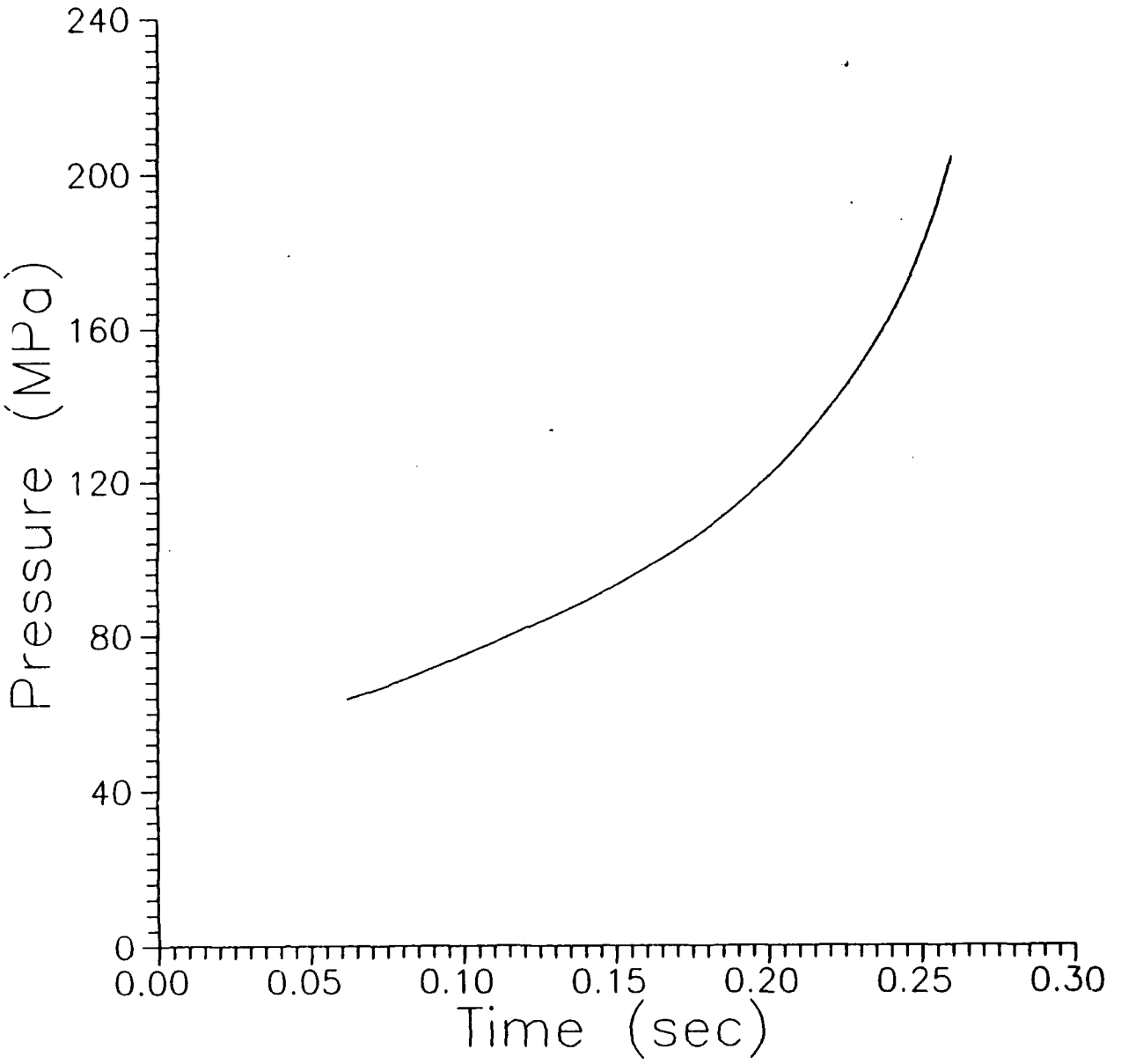

Figure A-14. Pressure vs. Time, Shot 14.

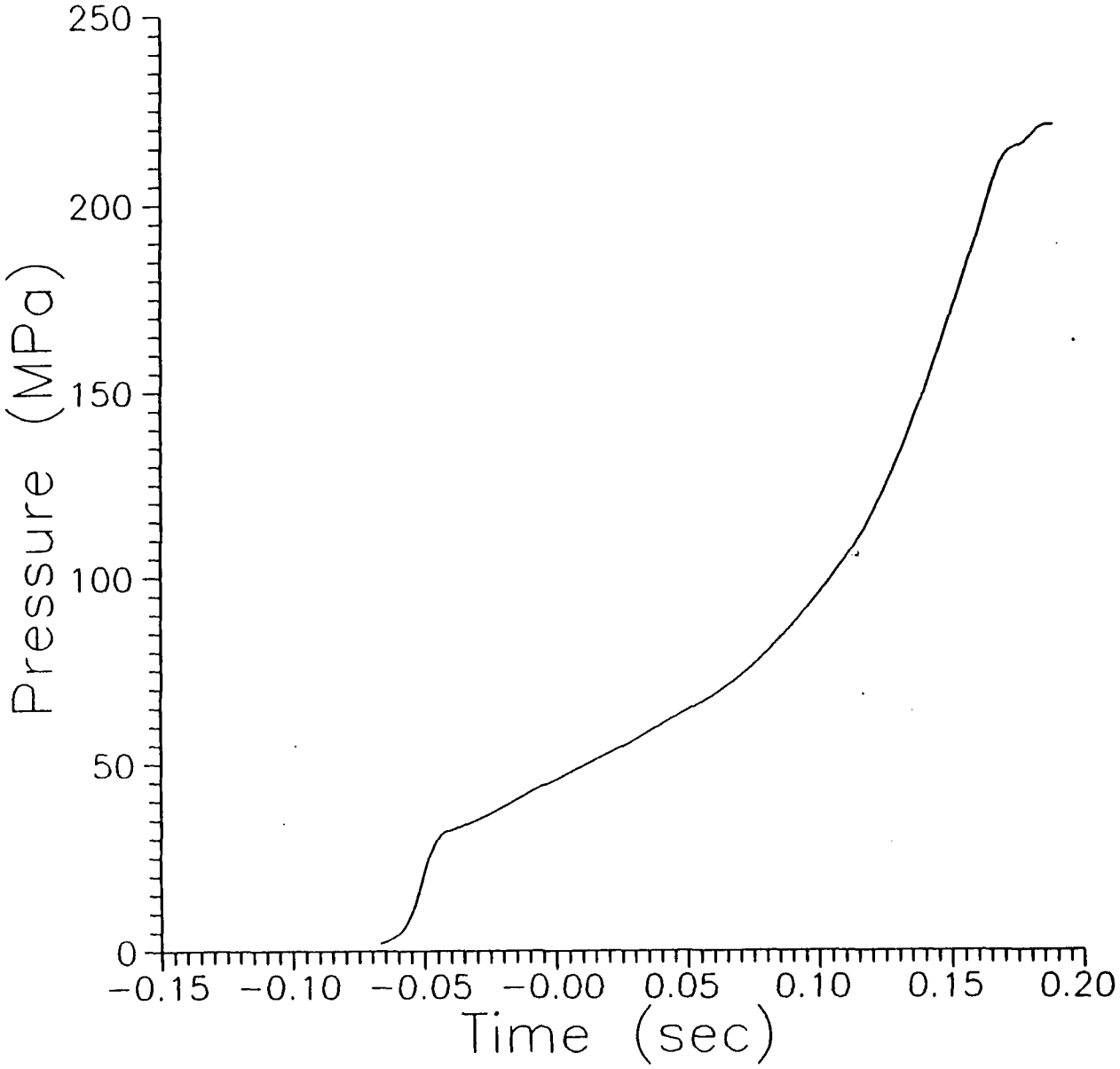

Figure A-15. Pressure vs. Time, Shot 15.

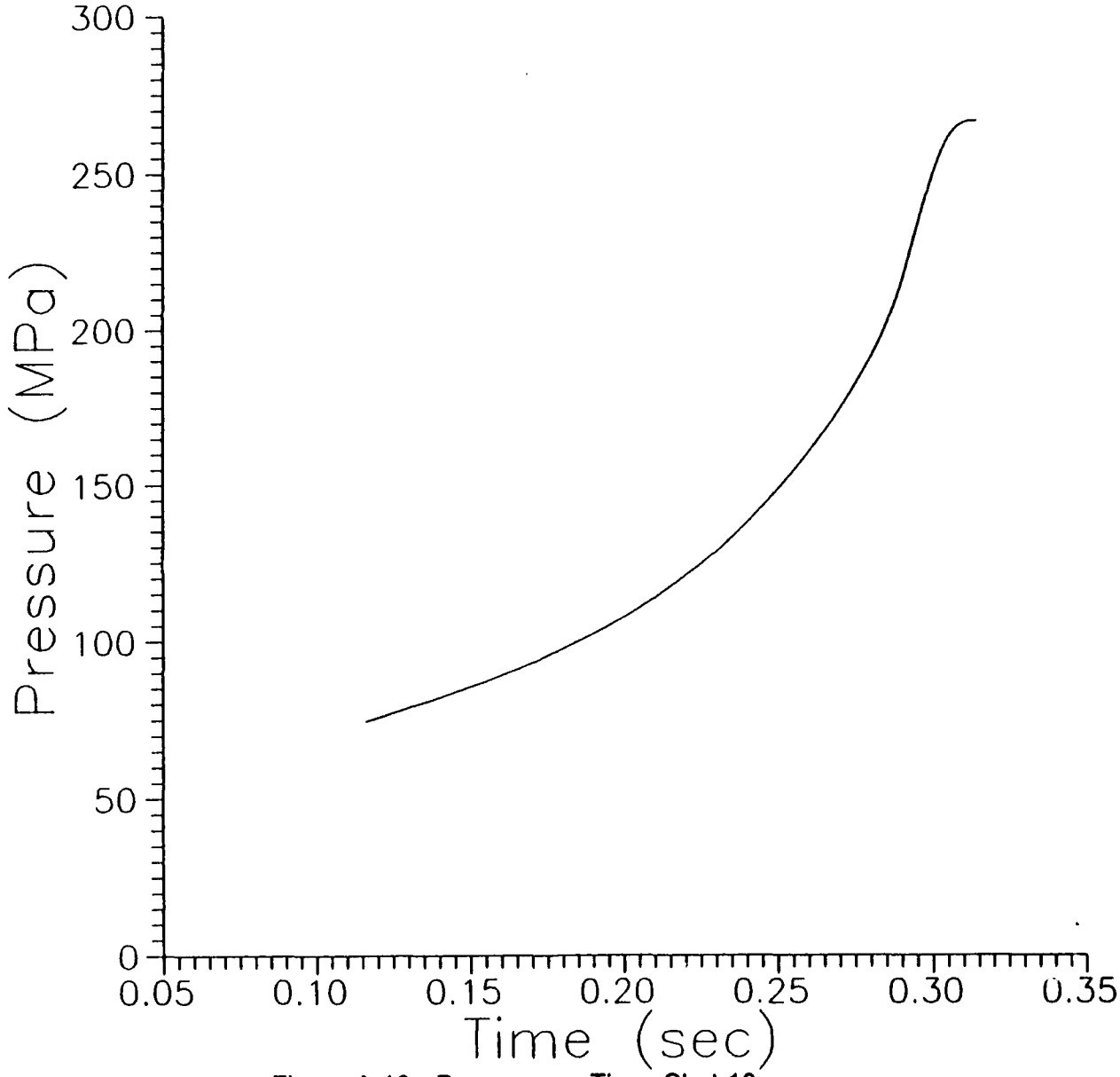

Figure A-16. Pressure vs. Time, Shot 16.

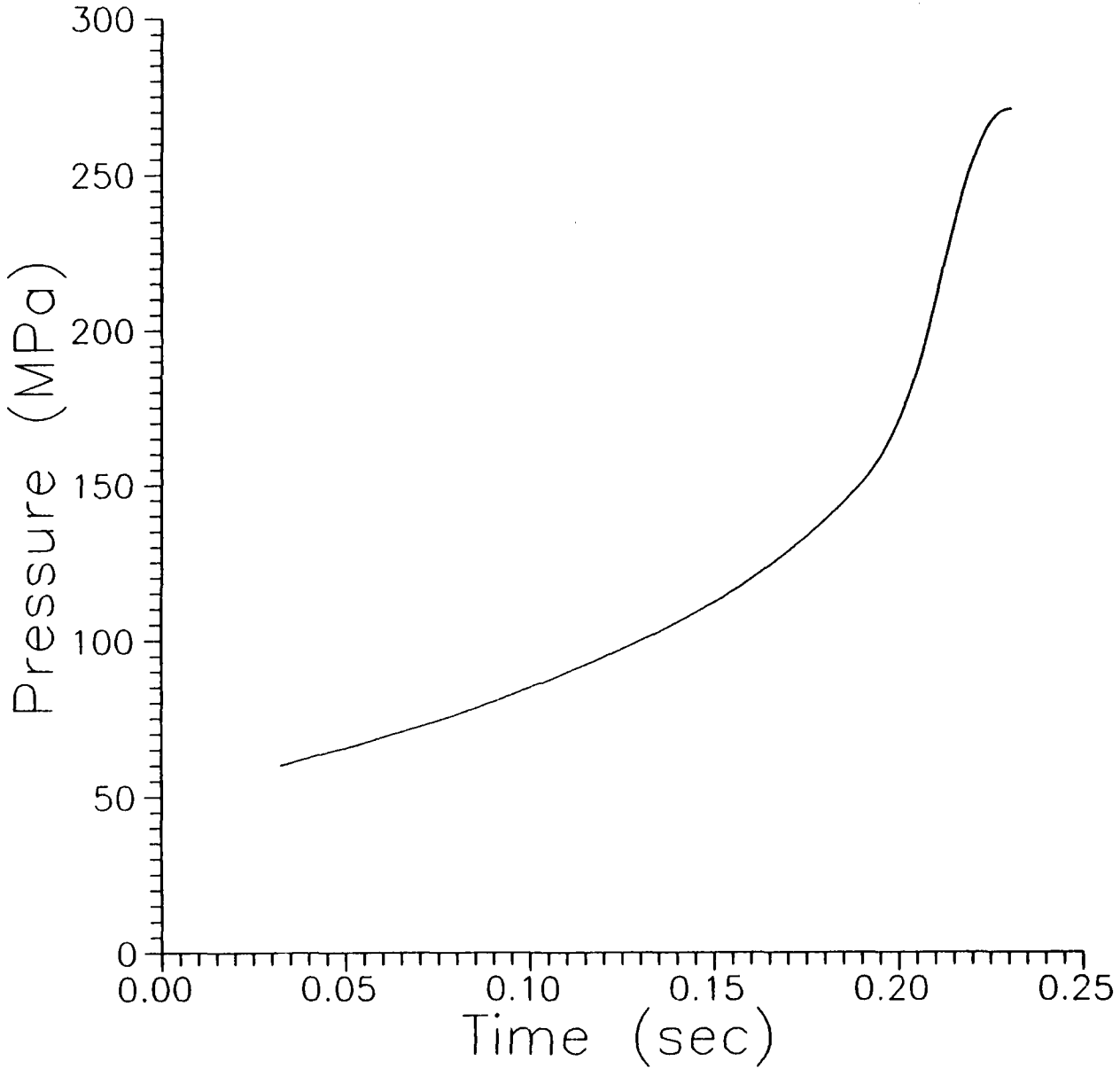

Figure A-17. Pressure vs. Time, Shot 17.

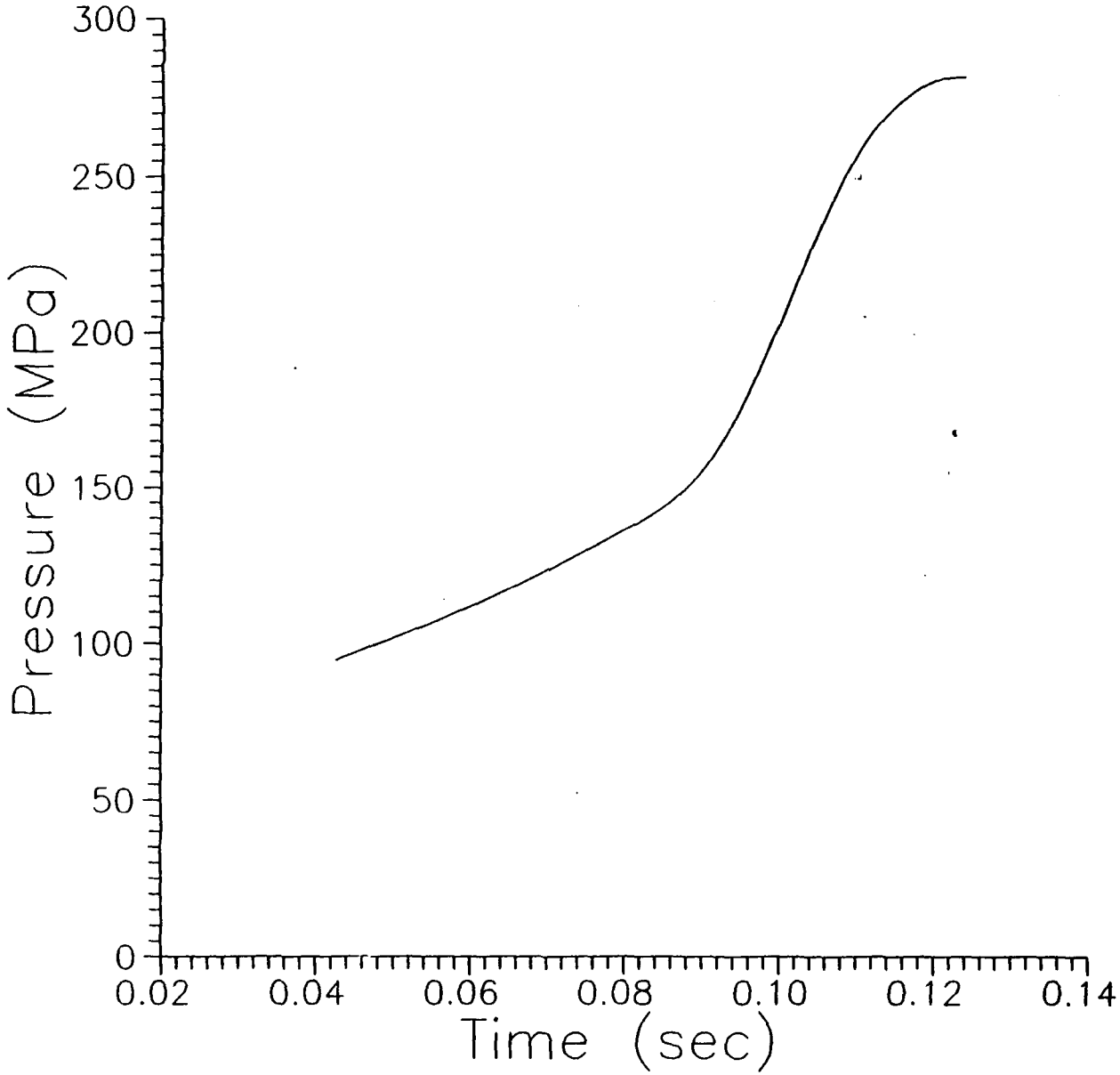

Figure A-18. Pressure vs. Time, Shot 18.

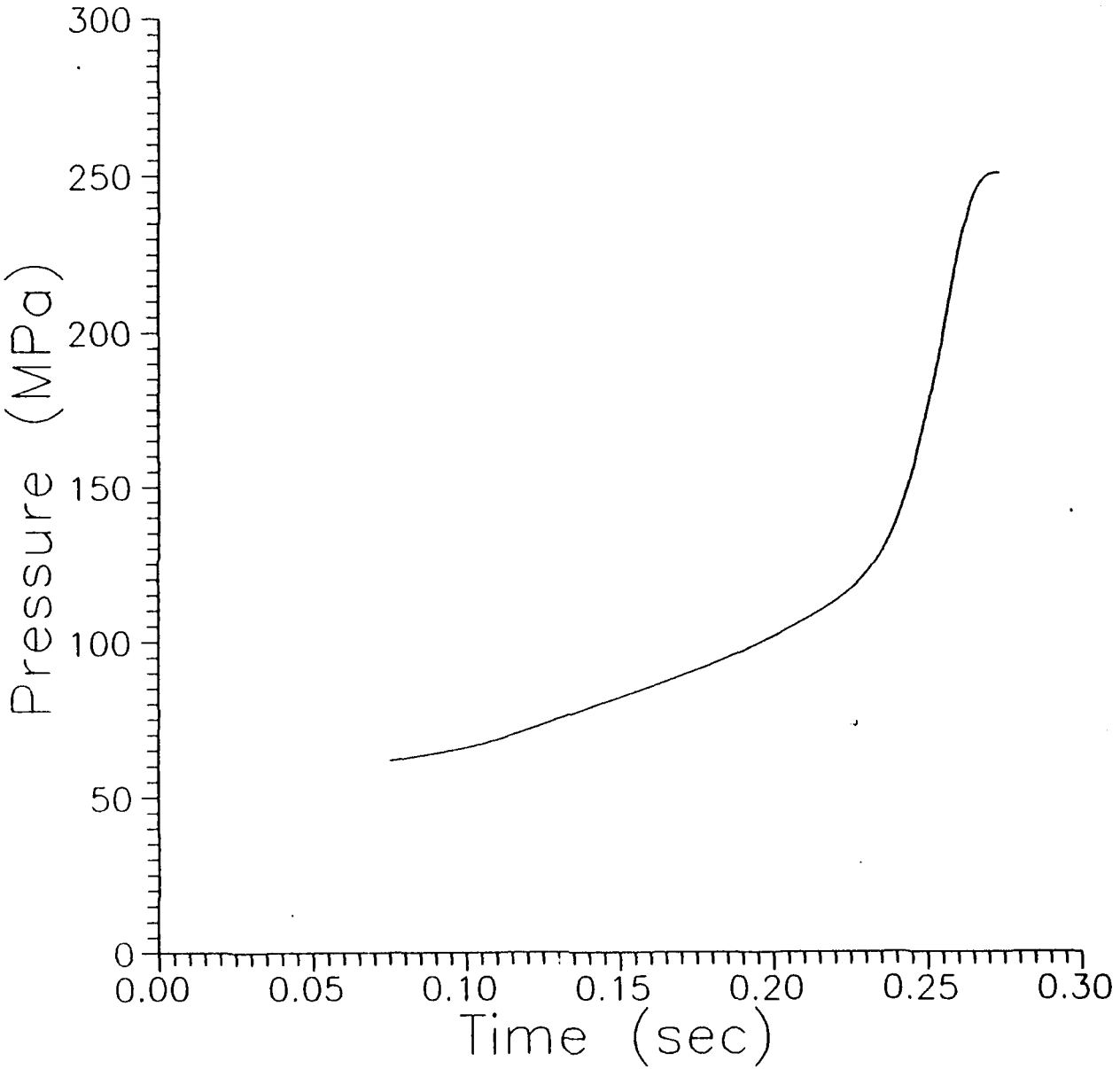

Figure A-19. Pressure vs. Time, Shot 19.

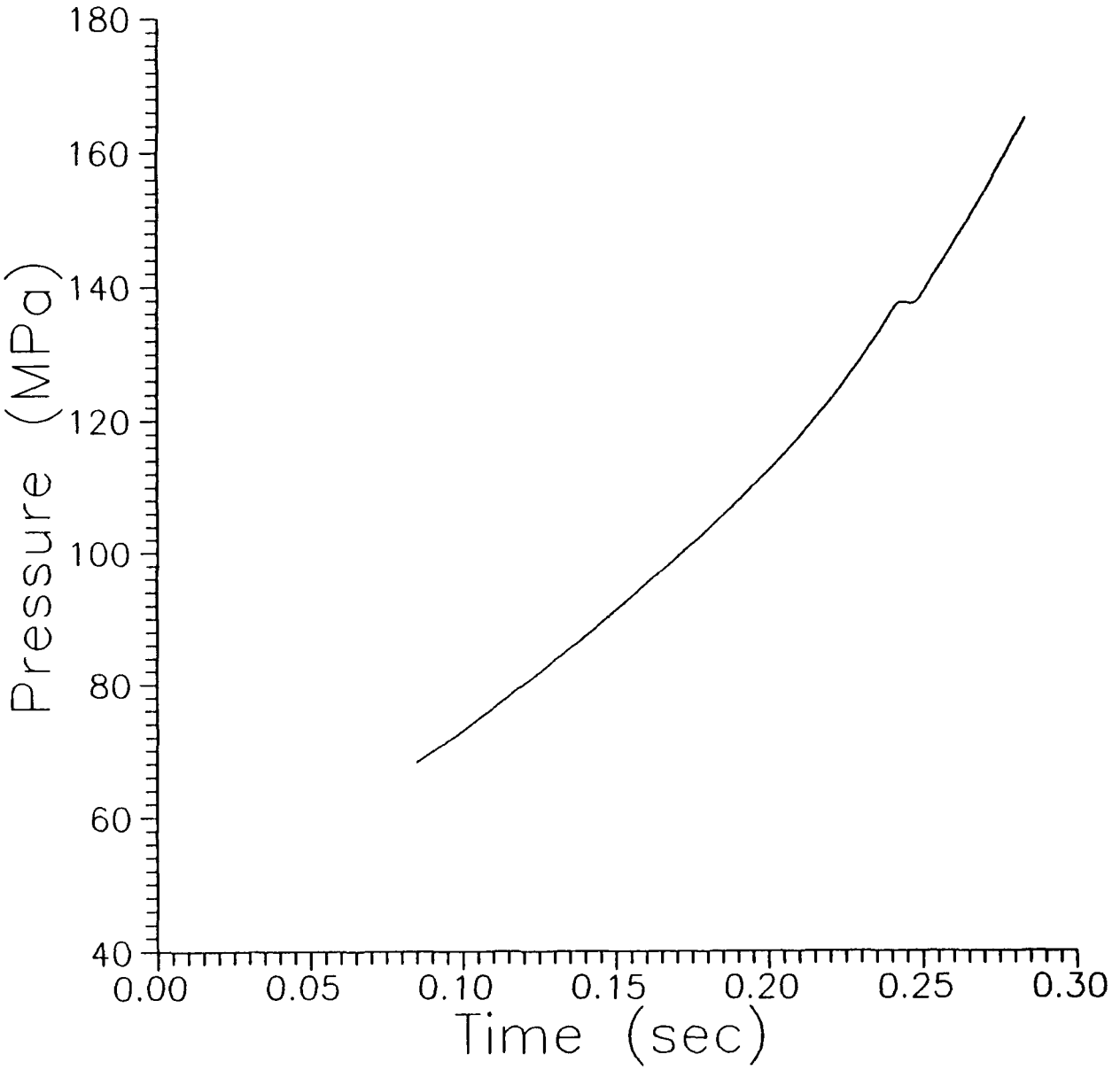

Figure A-20. Pressure vs. Time, Shot 20.

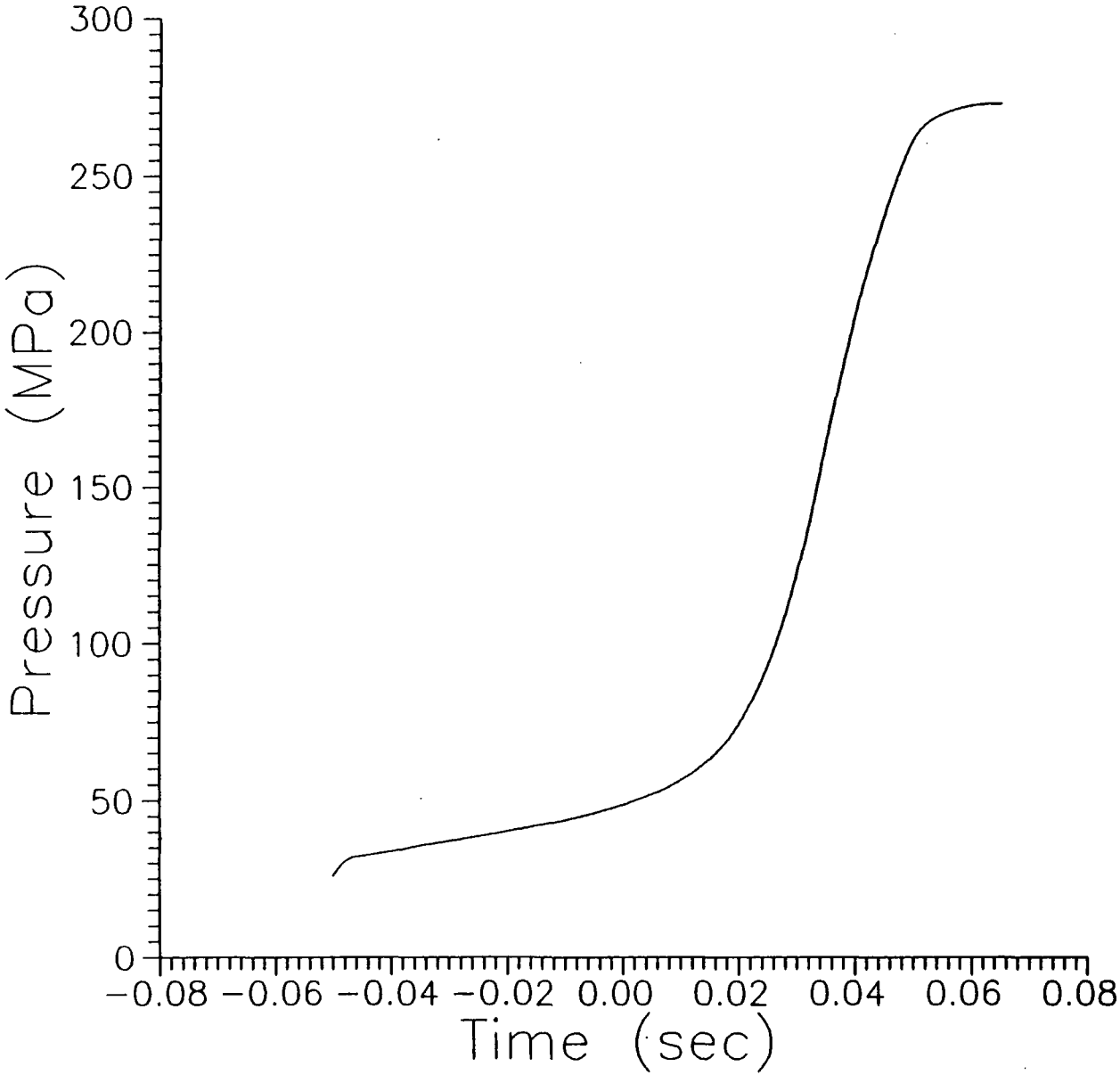

Figure A-21. Pressure vs. Time, Shot 21.

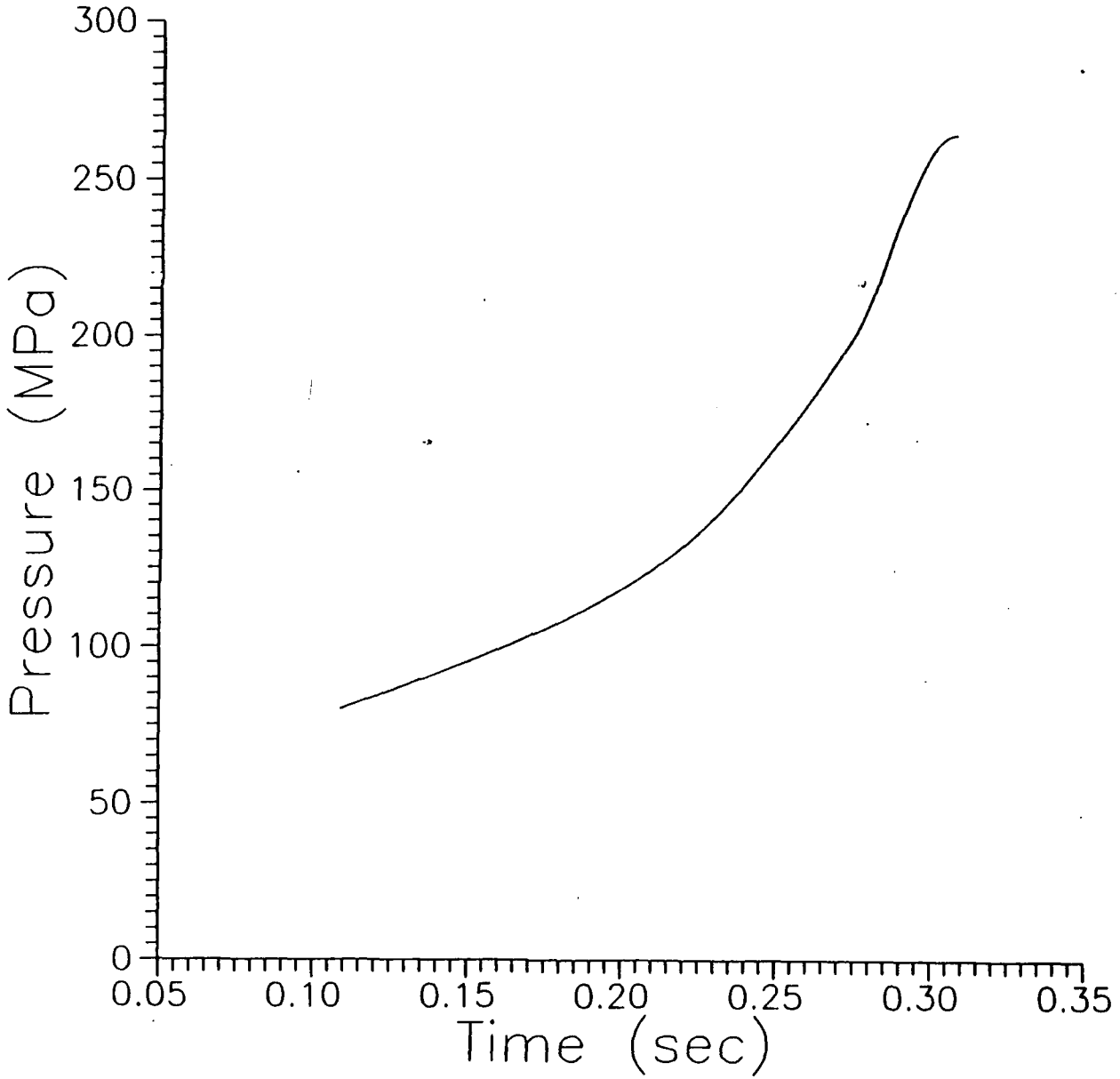

Figure A-22. Pressure vs. Time, Shot 22.

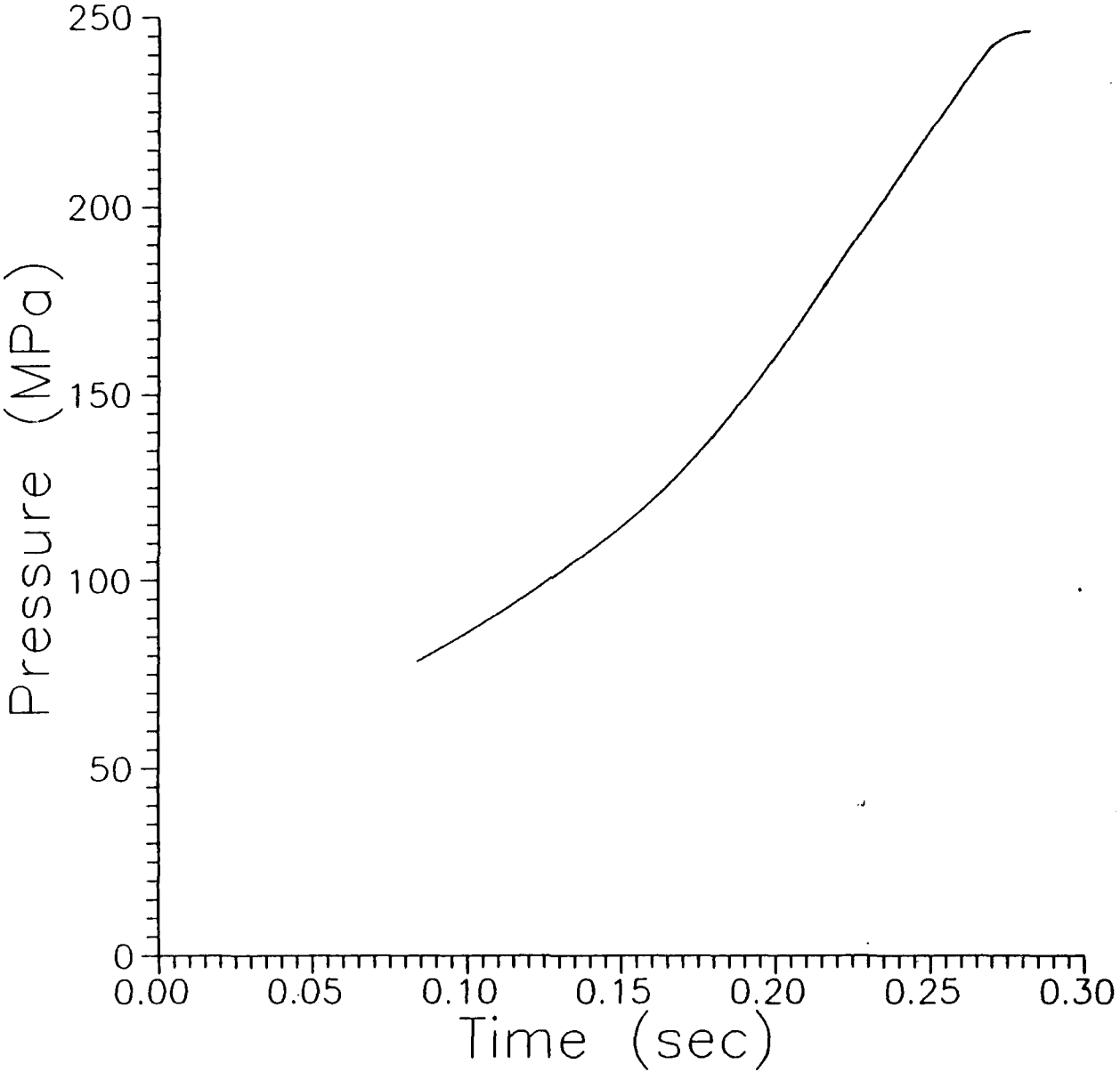

Figure A-23. Pressure vs. Time, Shot 23.

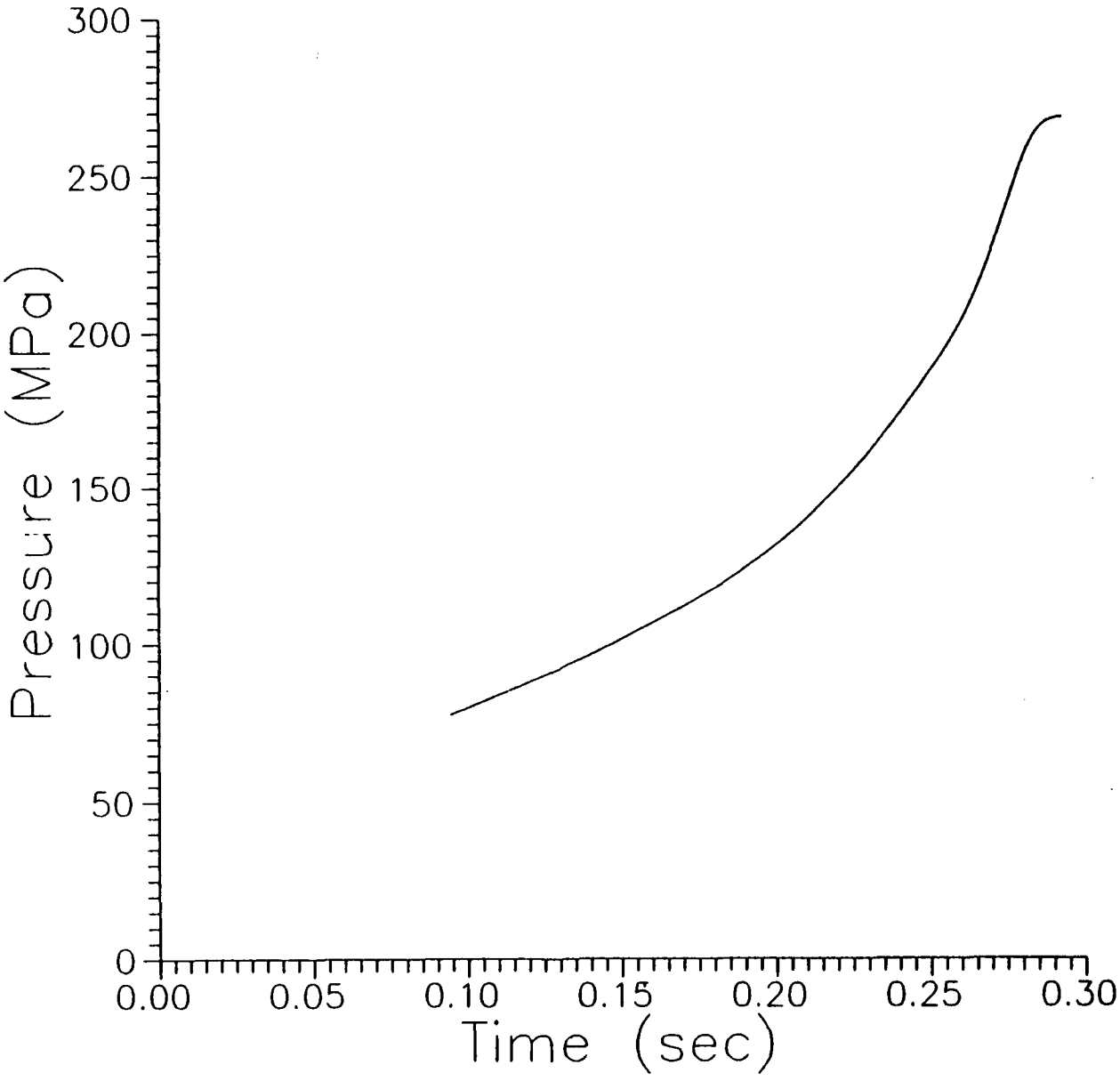

Figure A-24. Pressure vs. Time, Shot 24.

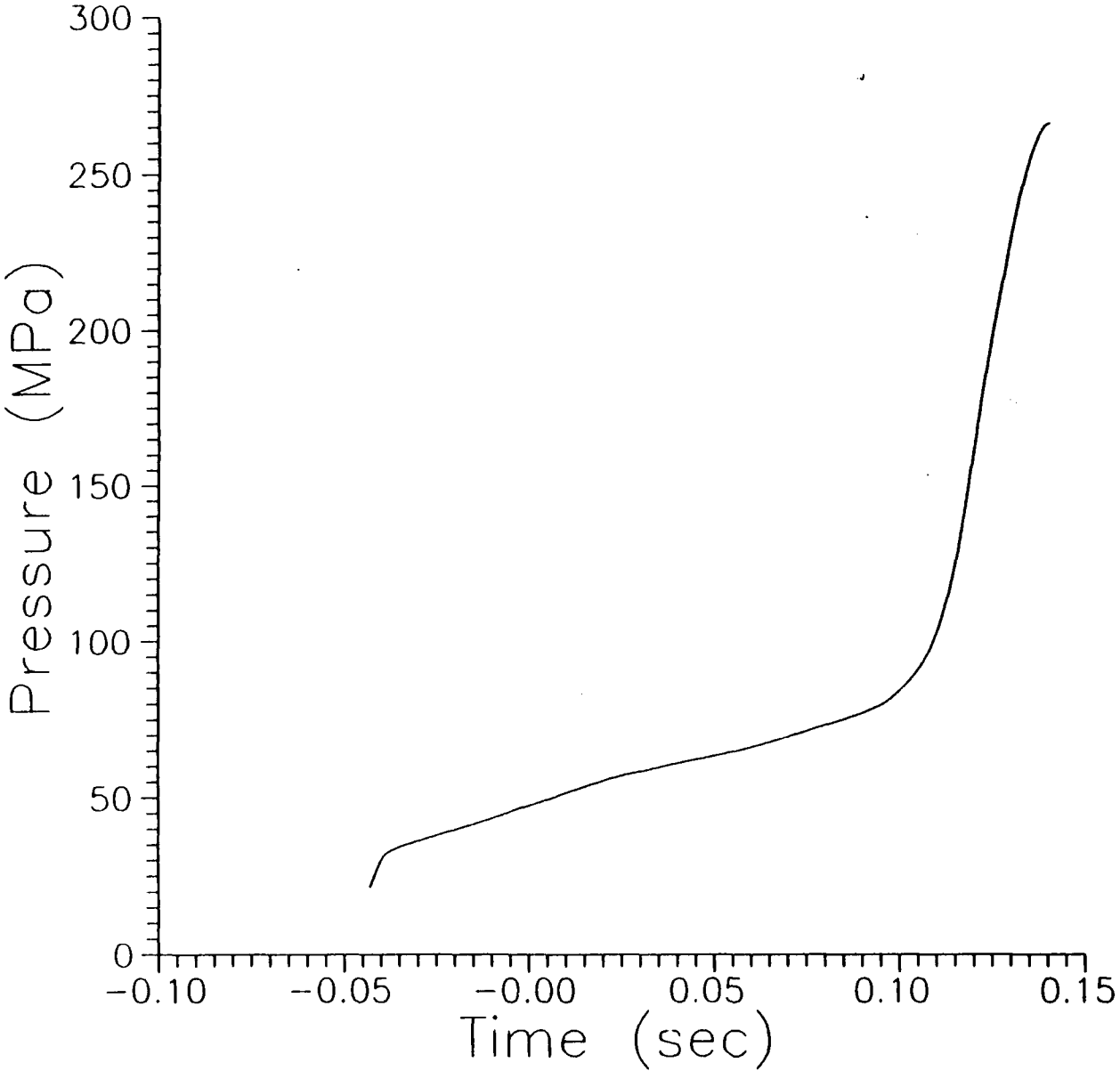

Figure A-25. Pressure vs. Time, Shot 25.

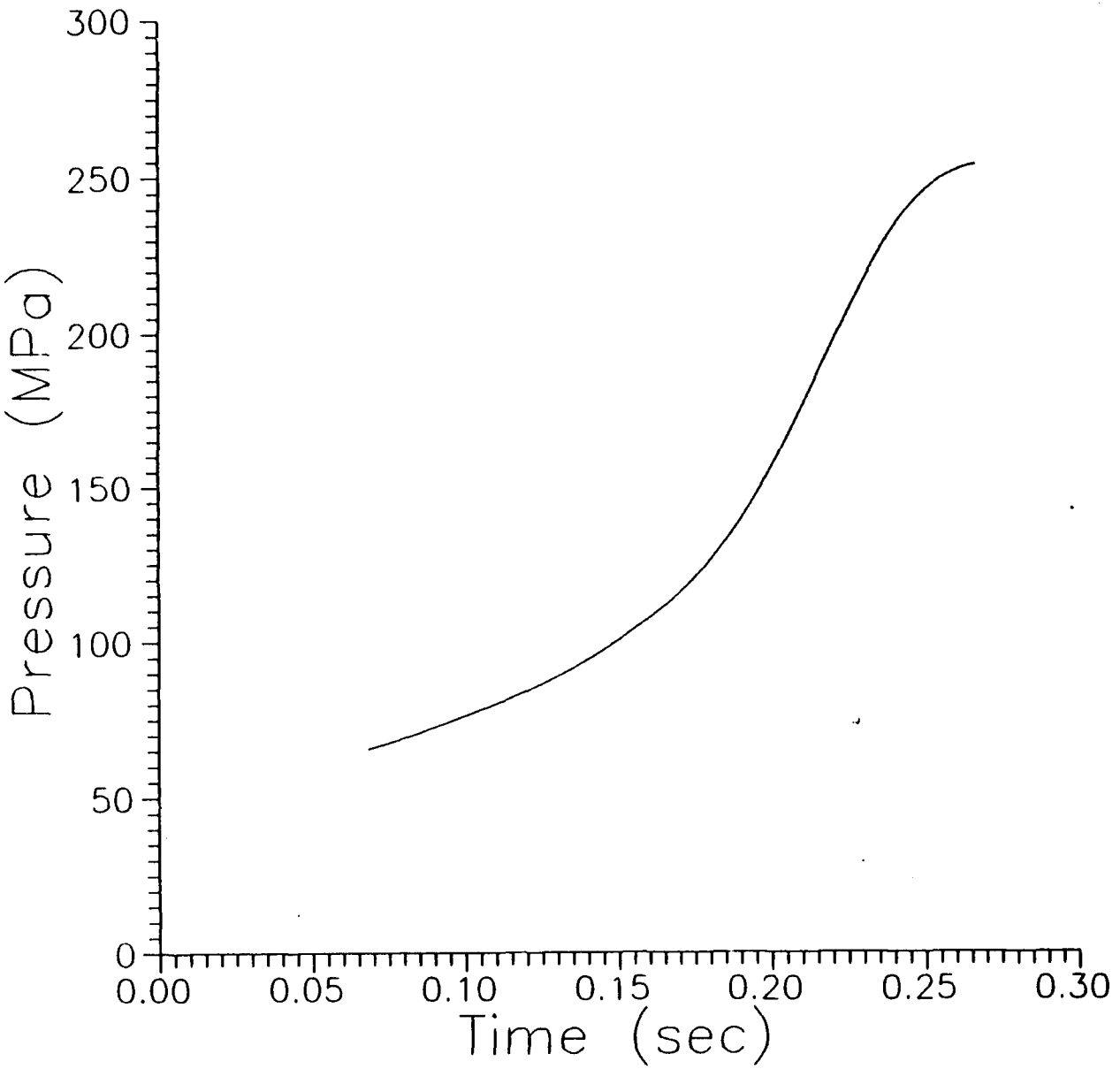

Figure A-26. Pressure vs. Time, Shot 26.

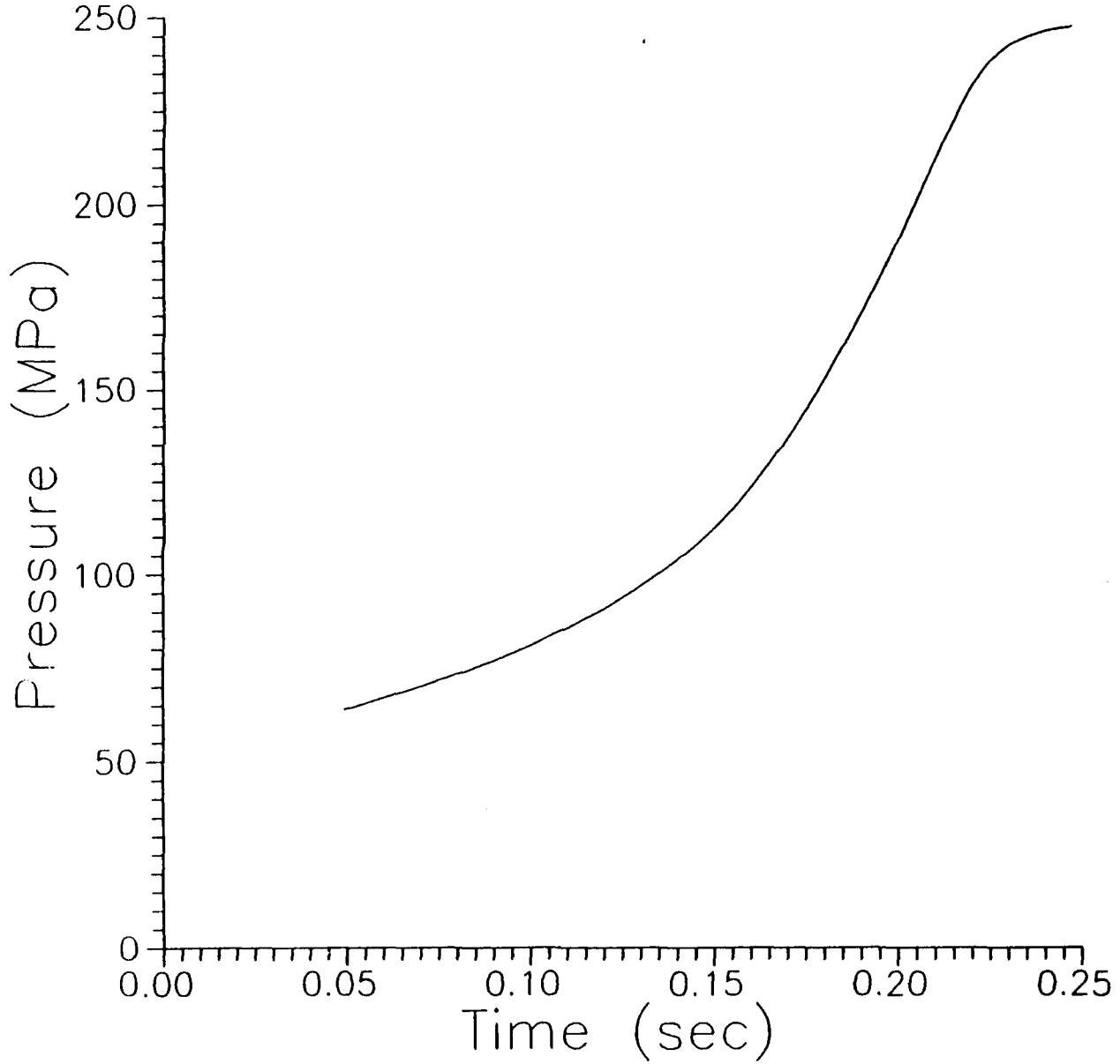

Figure A-27. Pressure vs. Time, Shot 27.

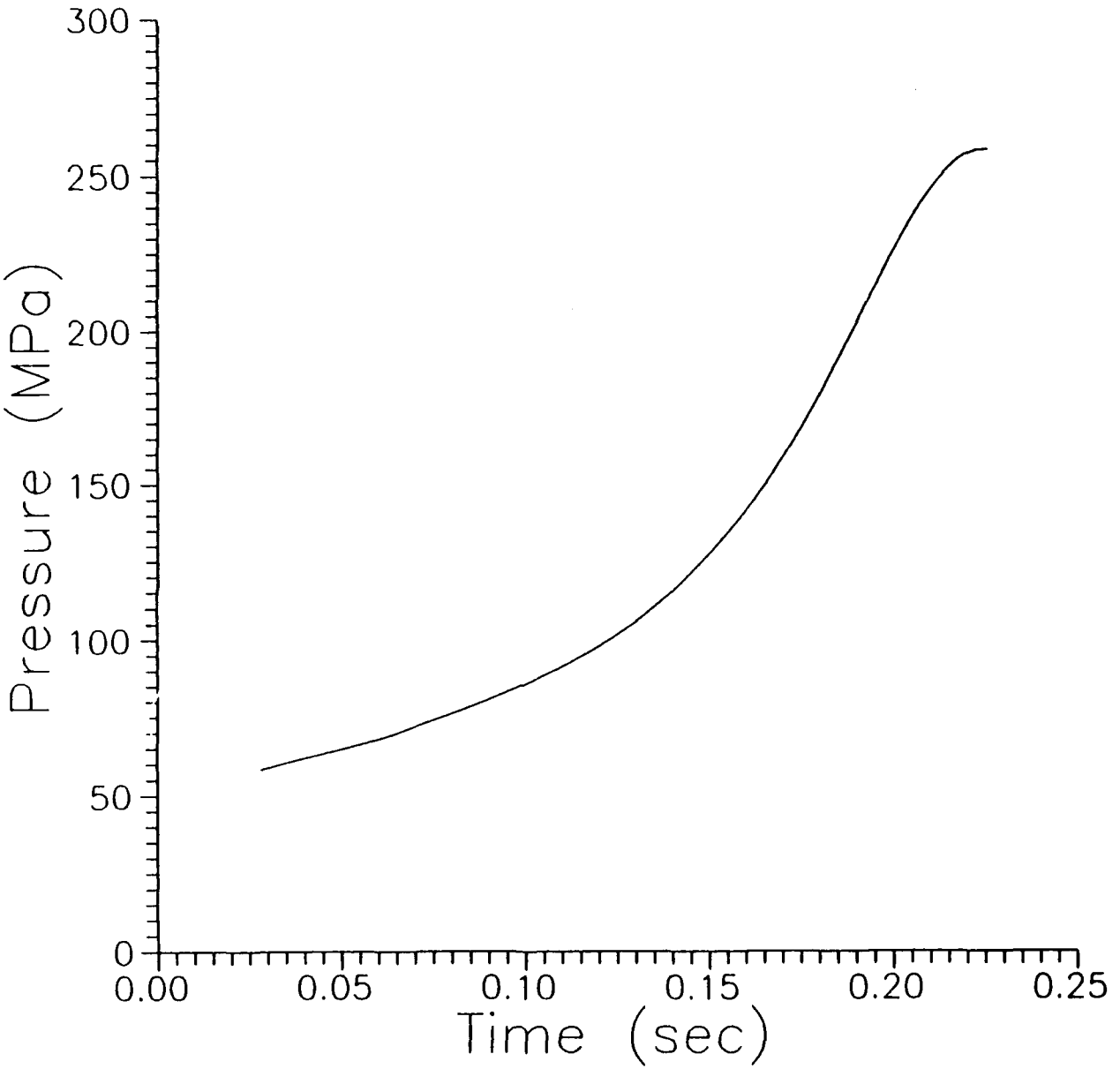

Figure A-28. Pressure vs. Time, Shot 28.

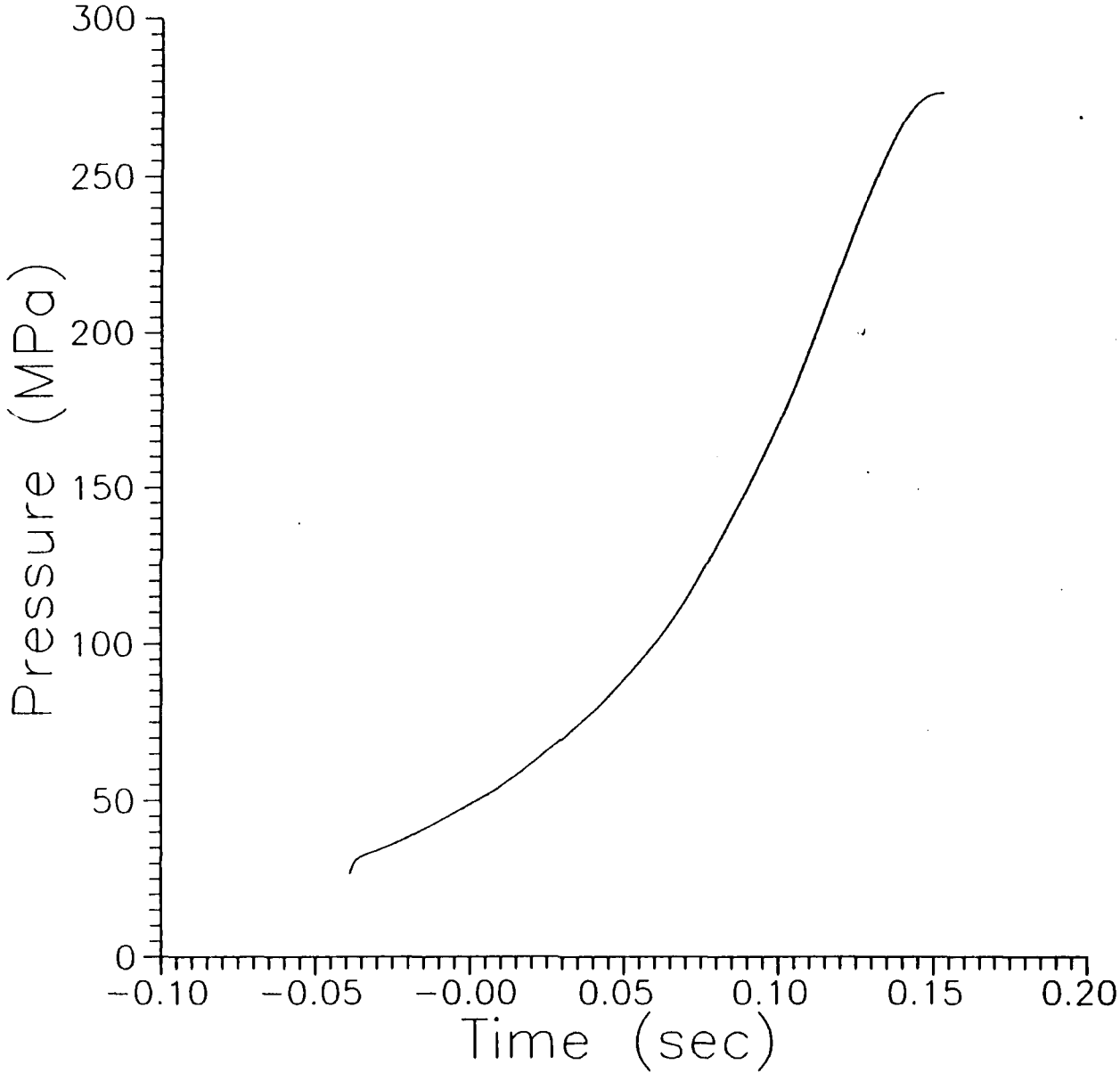

Figure A-29. Pressure vs. Time, Shot 29.

INTENTIONALLY LEFT BLANK.

APPENDIX B:

BURN RATE-vs.-PRESSURE PLOTS

INTENTIONALLY LEFT BLANK.

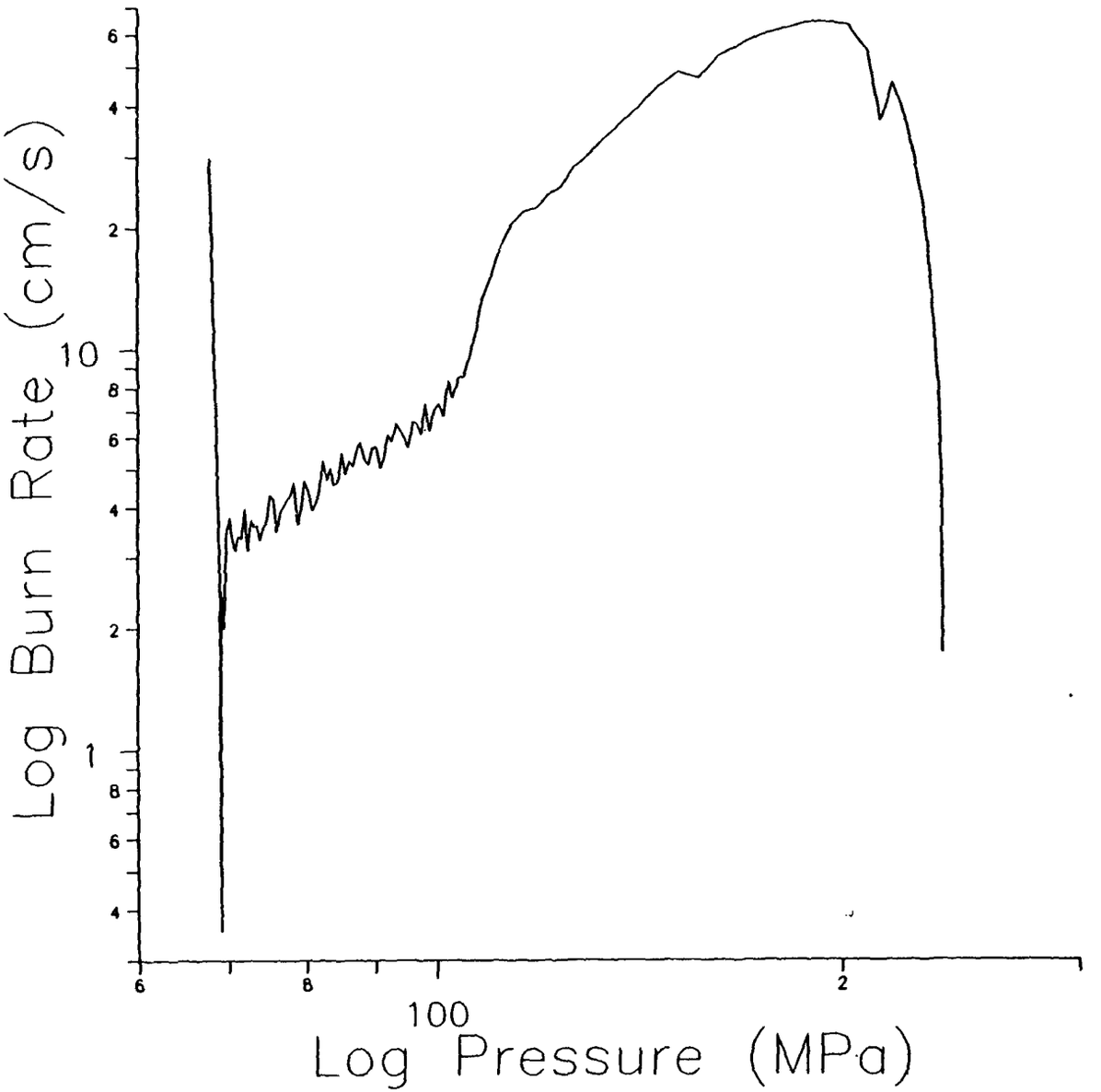

Figure B-1. Log Burn Rate vs. Log Pressure, Shot 1.

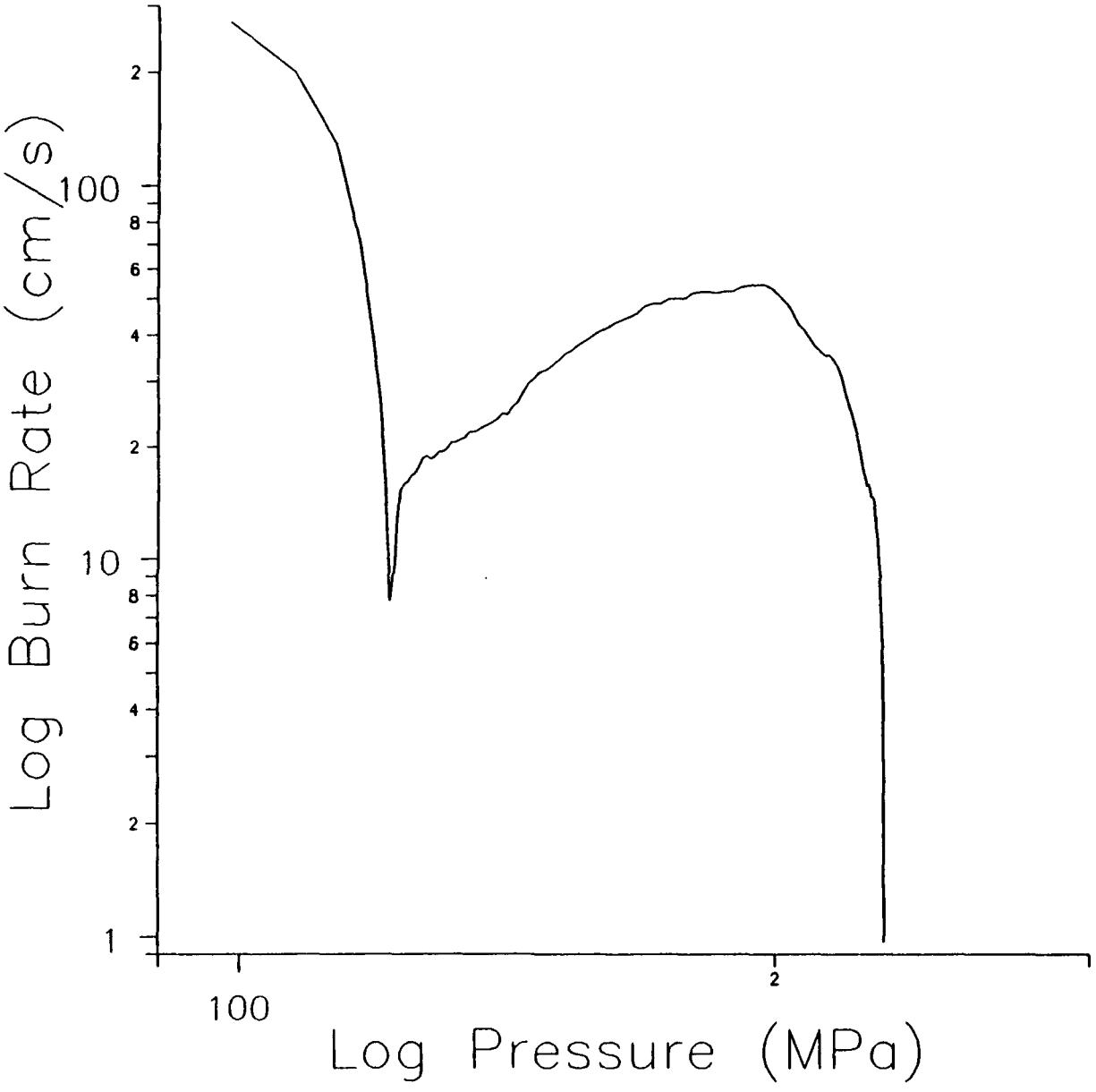

Figure B-2. Log Burn Rate vs. Log Pressure, Shot 2.

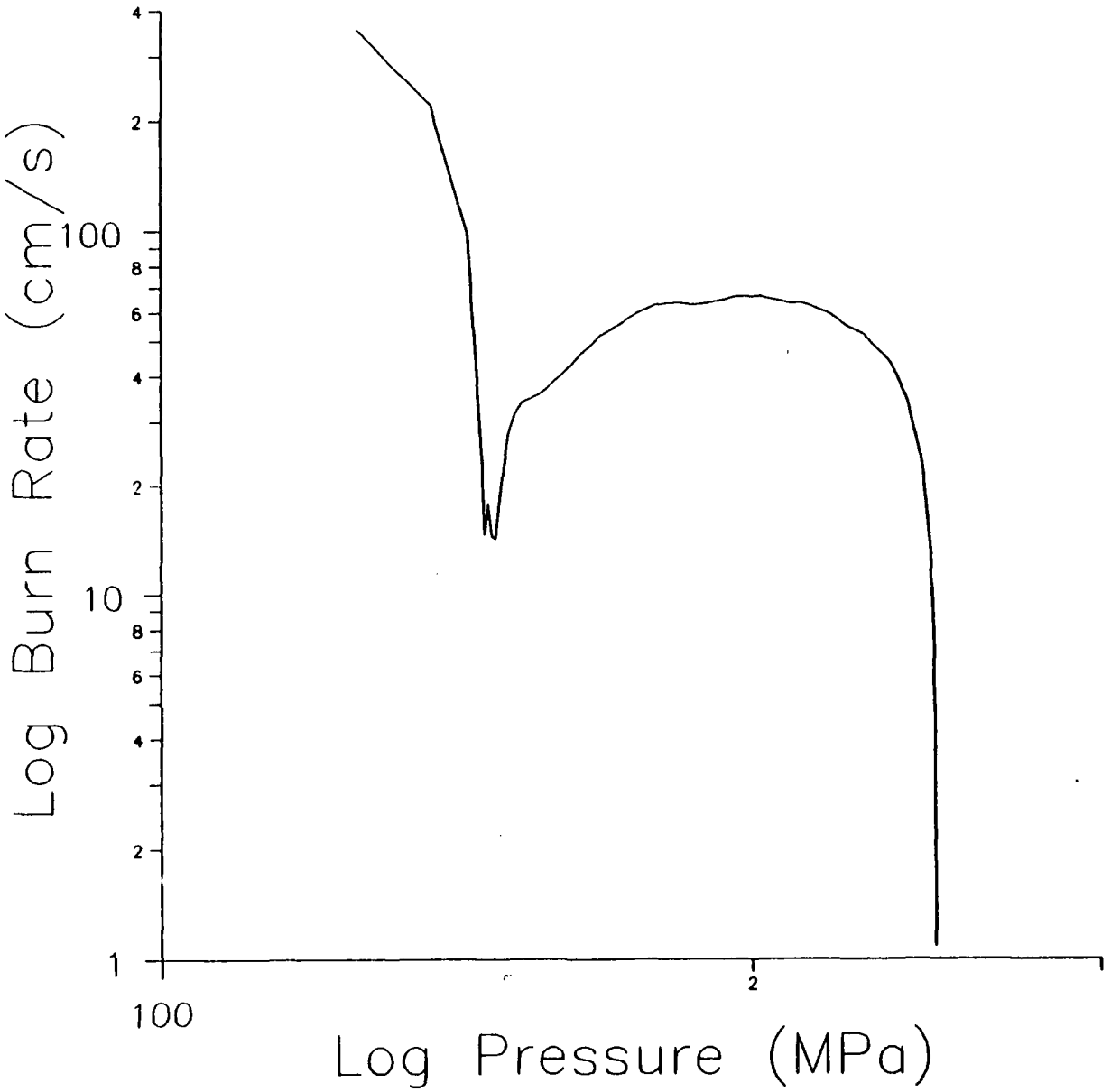

Figure B-3. Log Burn Rate vs. Log Pressure, Shot 3.

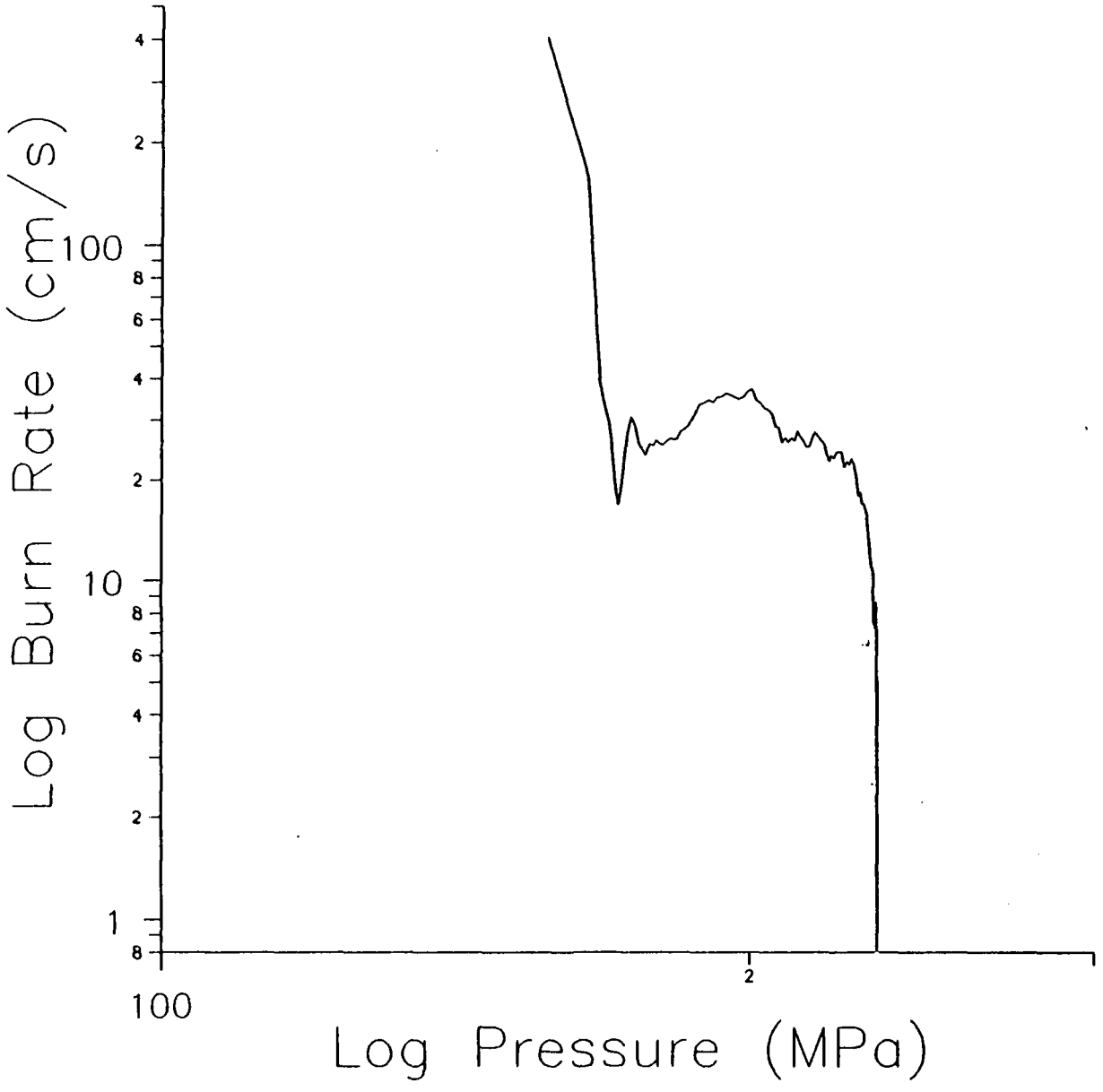

Figure B-4. Log Burn Rate vs. Log Pressure, Shot 4.

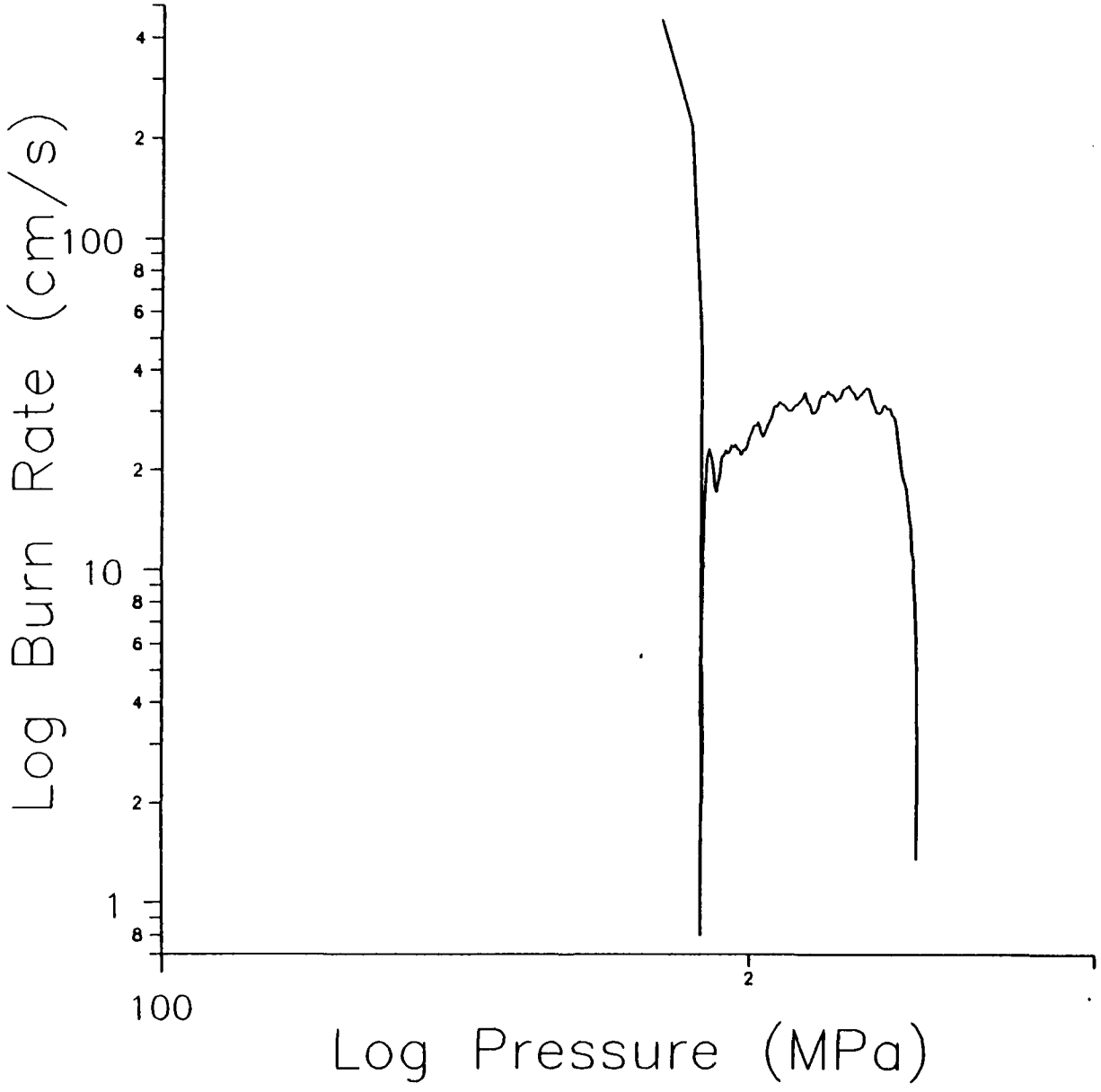

Figure B-5. Log Burn Rate vs. Log Pressure, Shot 5.

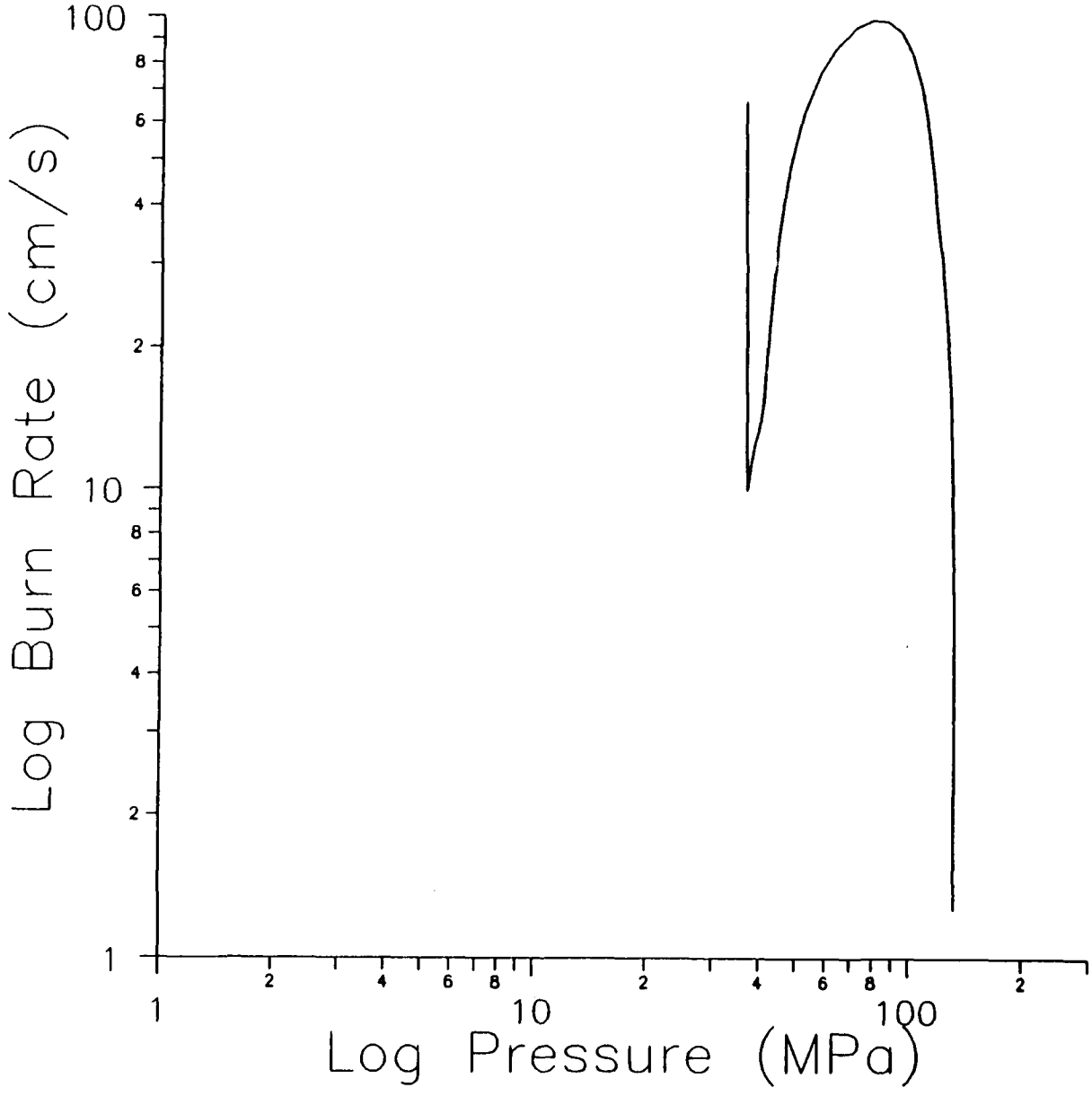

Figure B-6. Log Burn Rate vs. Log Pressure, Shot 6.

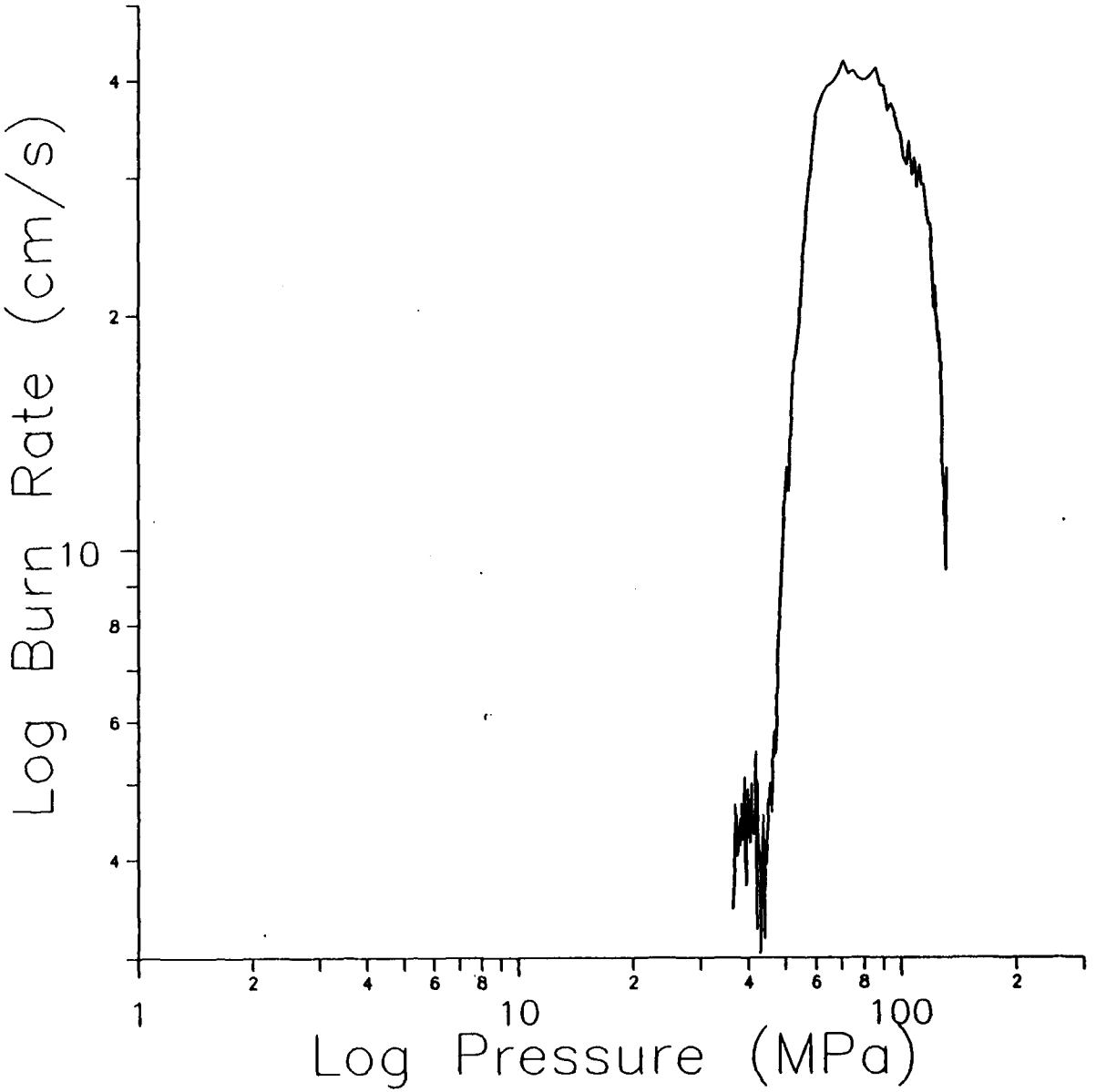

Figure B-7. Log Burn Rate vs. Log Pressure, Shot 7.

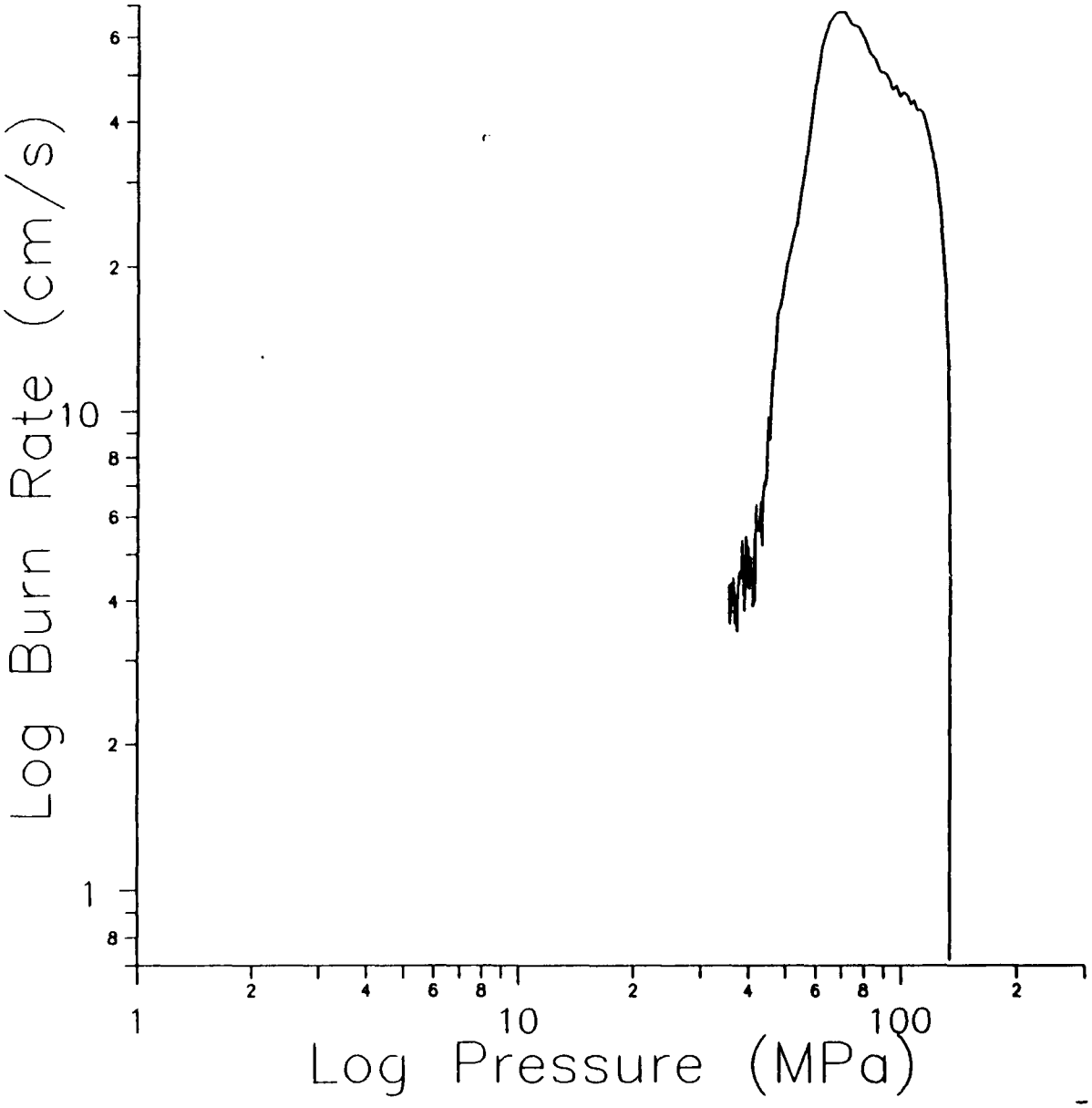

Figure B-8. Log Burn Rate vs. Log Pressure, Shot 8.

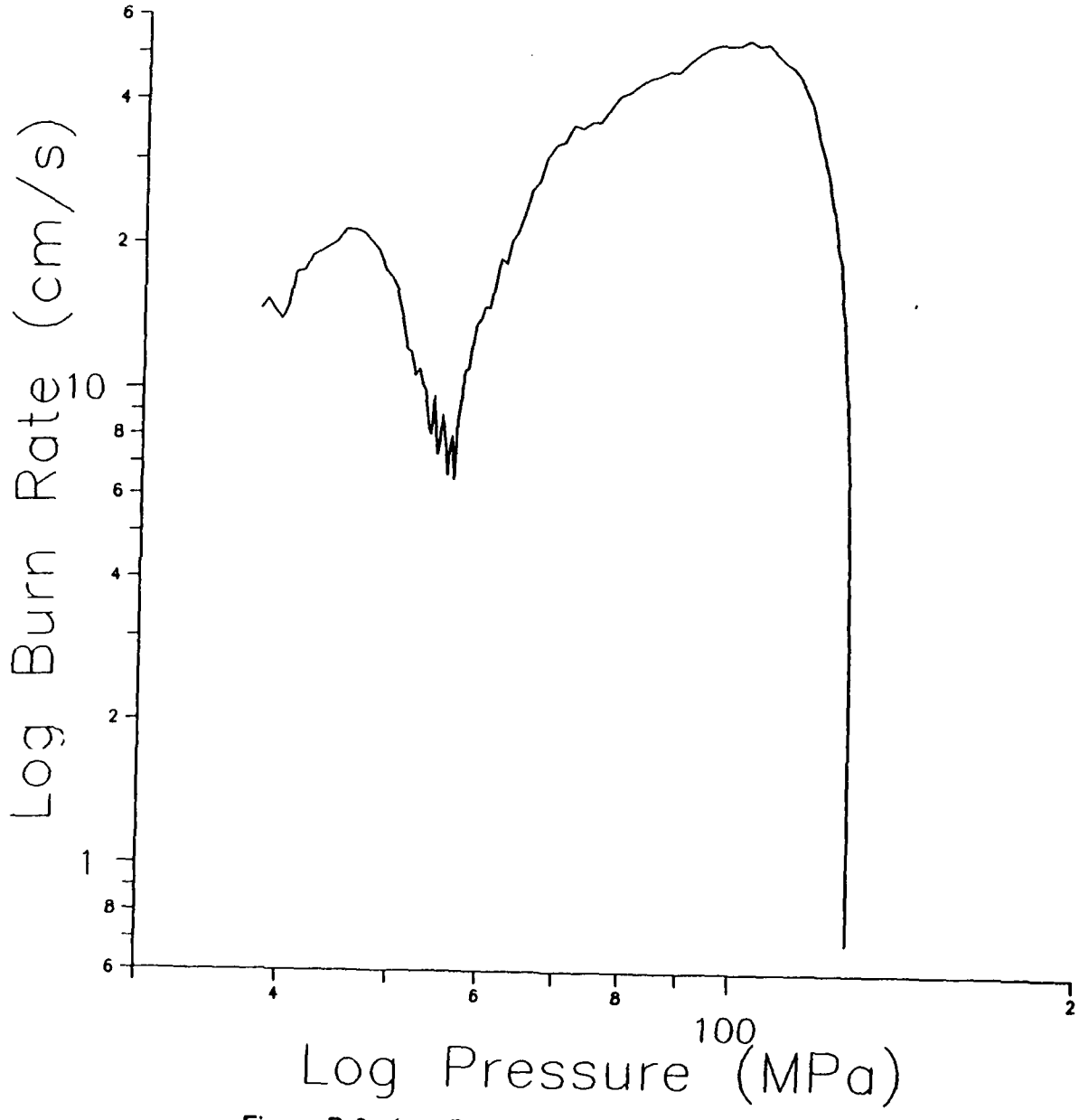

Figure B-9. Log Burn Rate vs. Log Pressure, Shot 9.

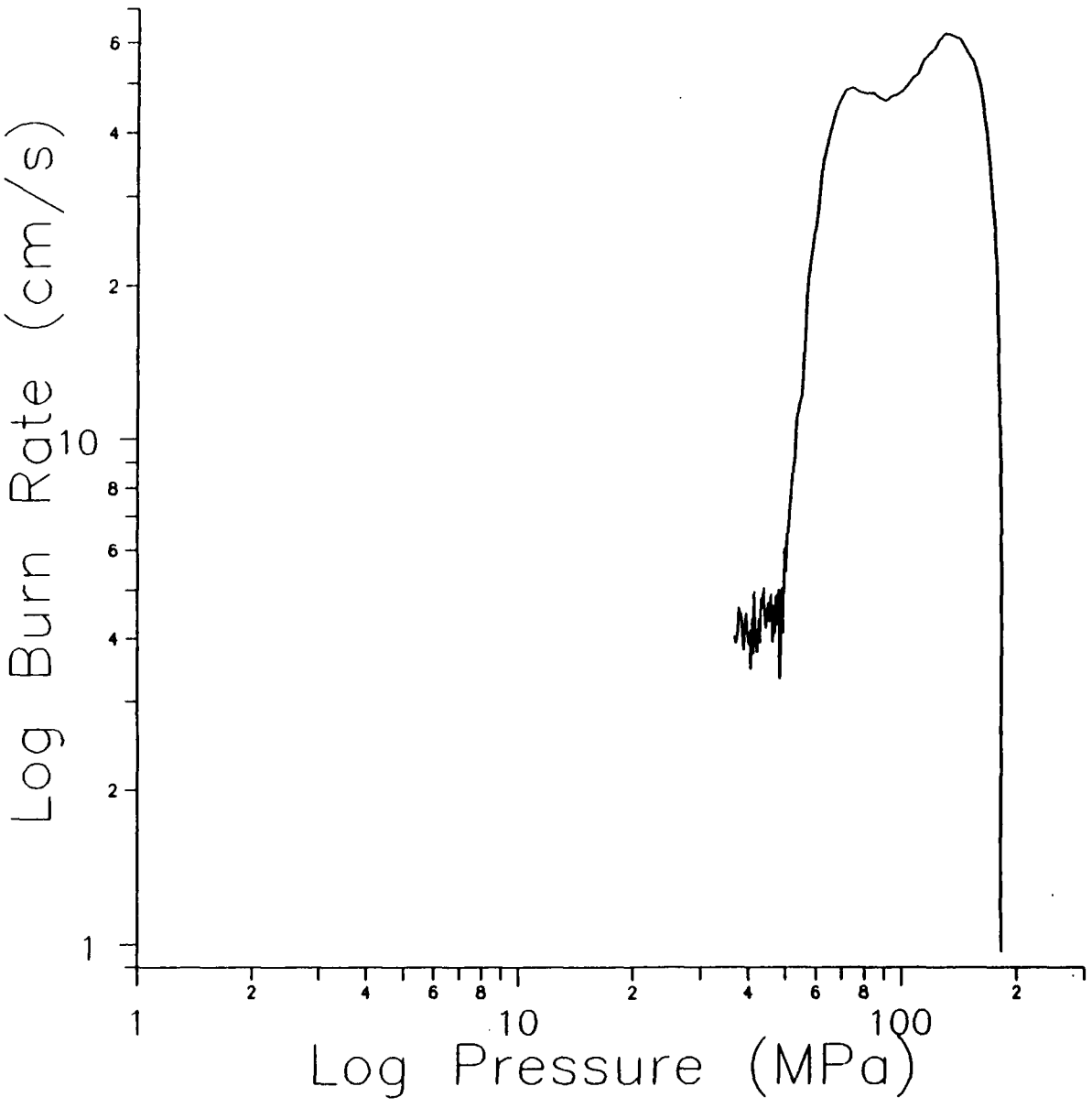

Figure B-10. Log Burn Rate vs. Log Pressure, Shot 10.

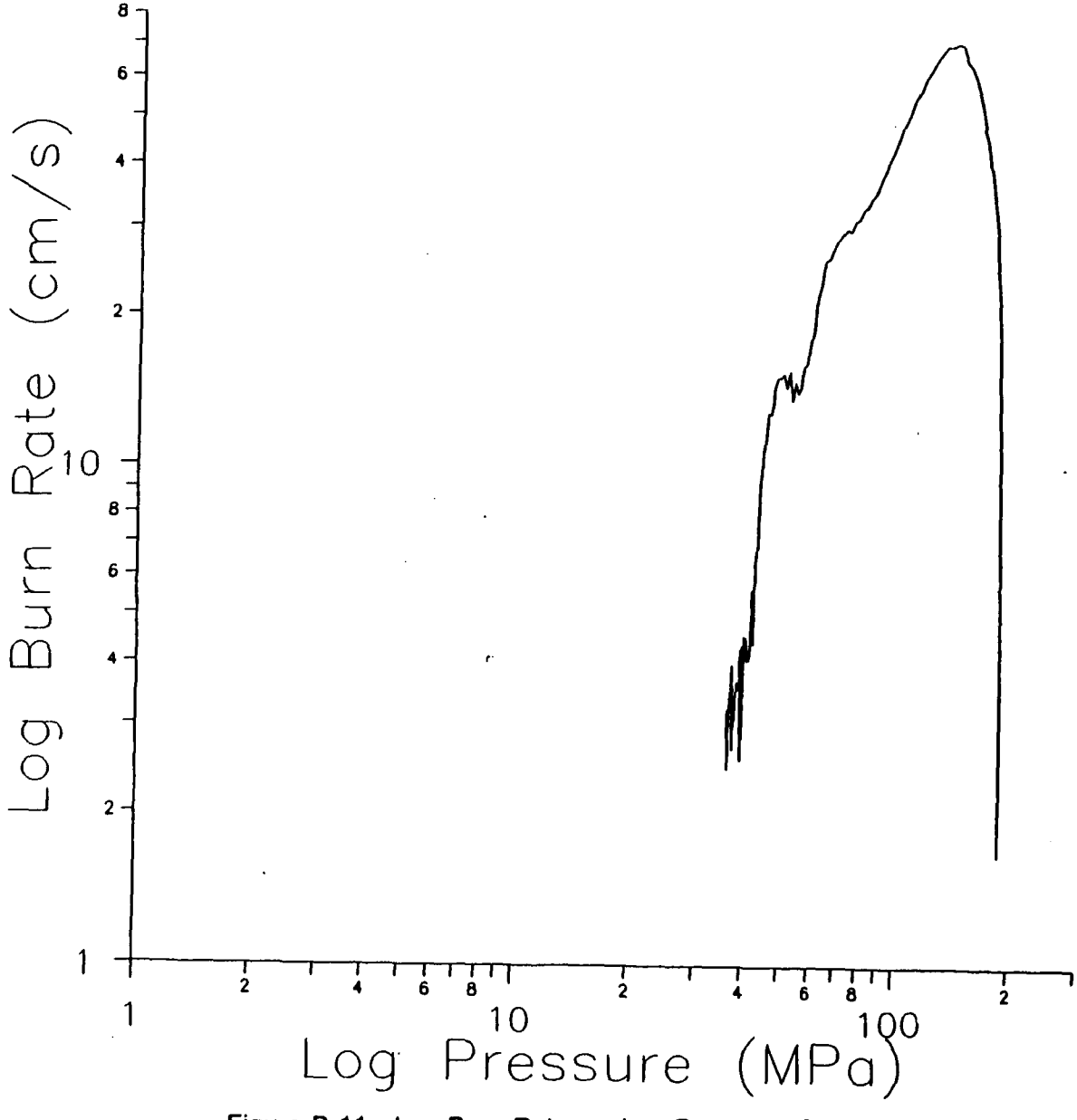

Figure B-11. Log Burn Rate vs. Log Pressure, Shot 11.

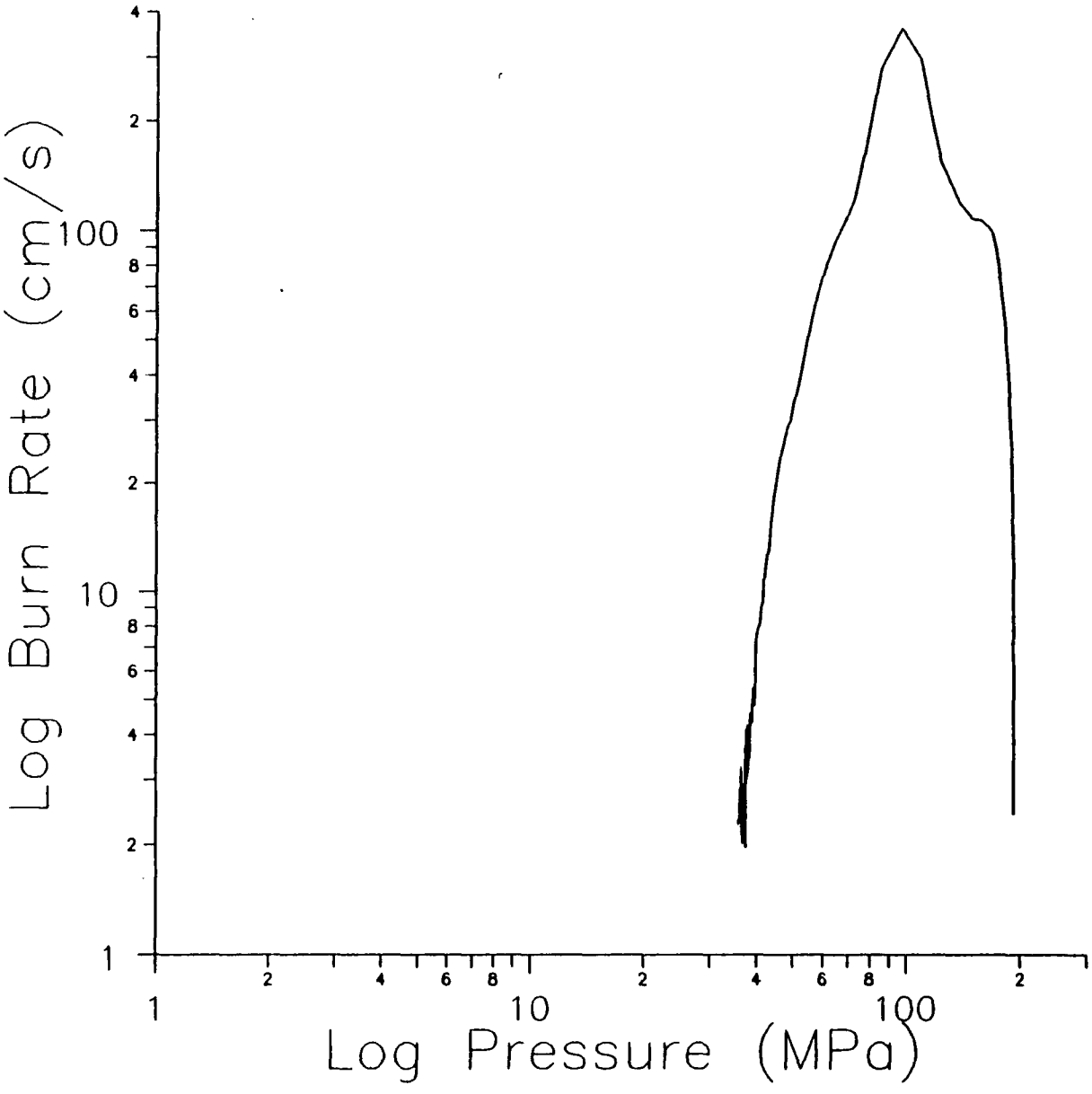

Figure B-12. Log Burn Rate vs. Log Pressure, Shot 12.

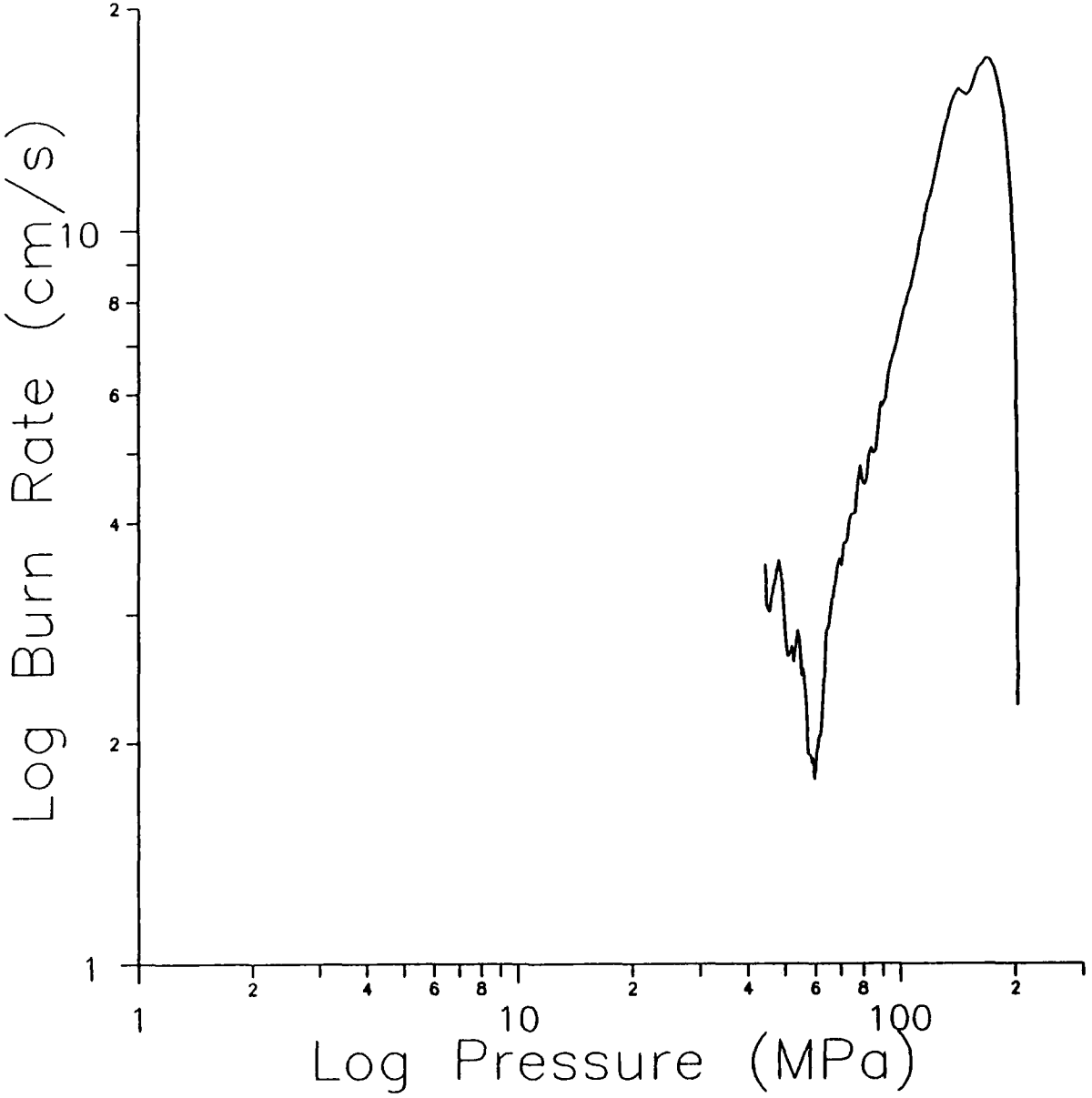

Figure B-13. Log Burn Rate vs. Log Pressure, Shot 13.

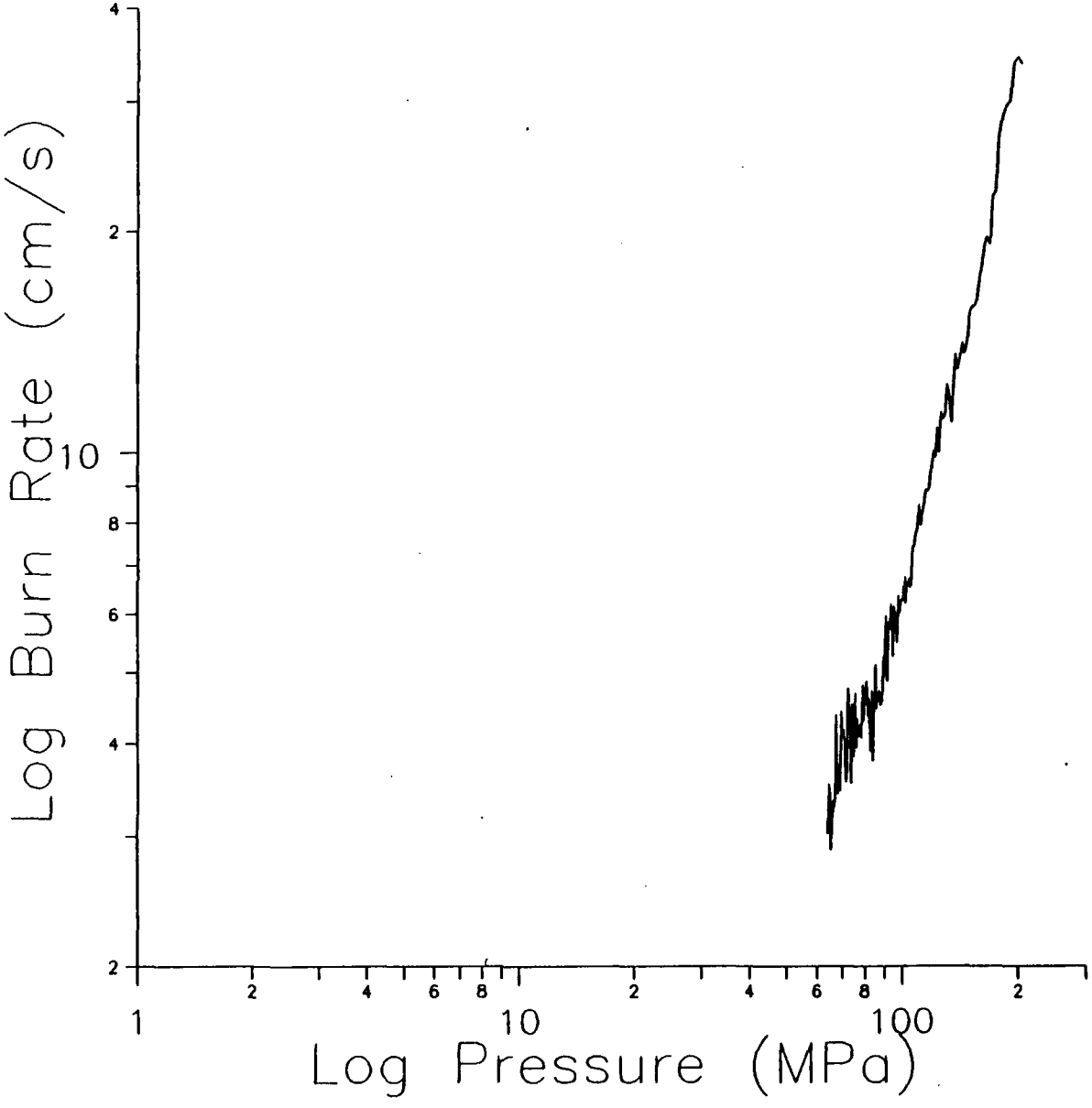

Figure B-14. Log Burn Rate vs. Log Pressure, Shot 14.

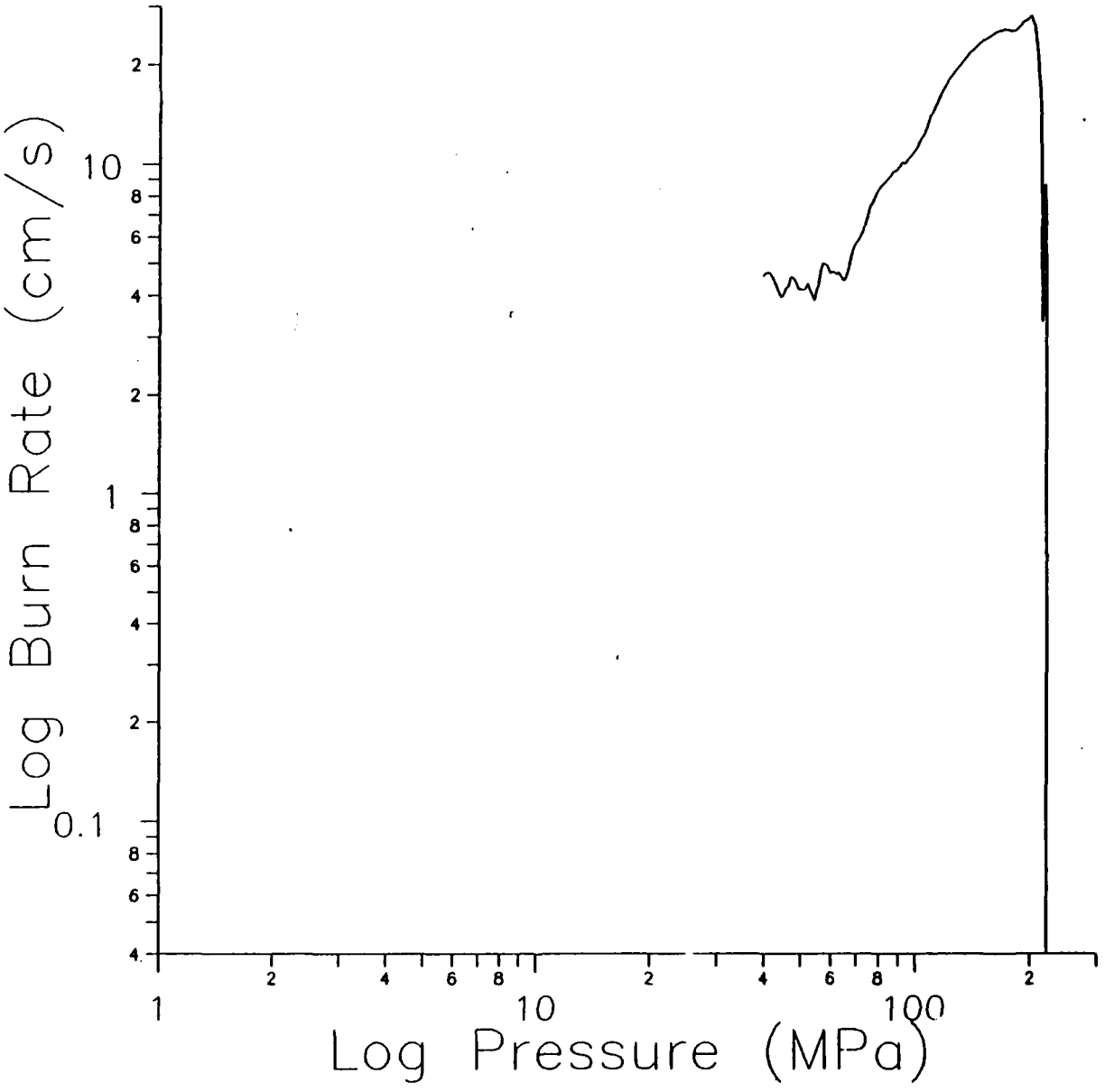

Figure B-15. Log Burn Rate vs. Log Pressure, Shot 15.

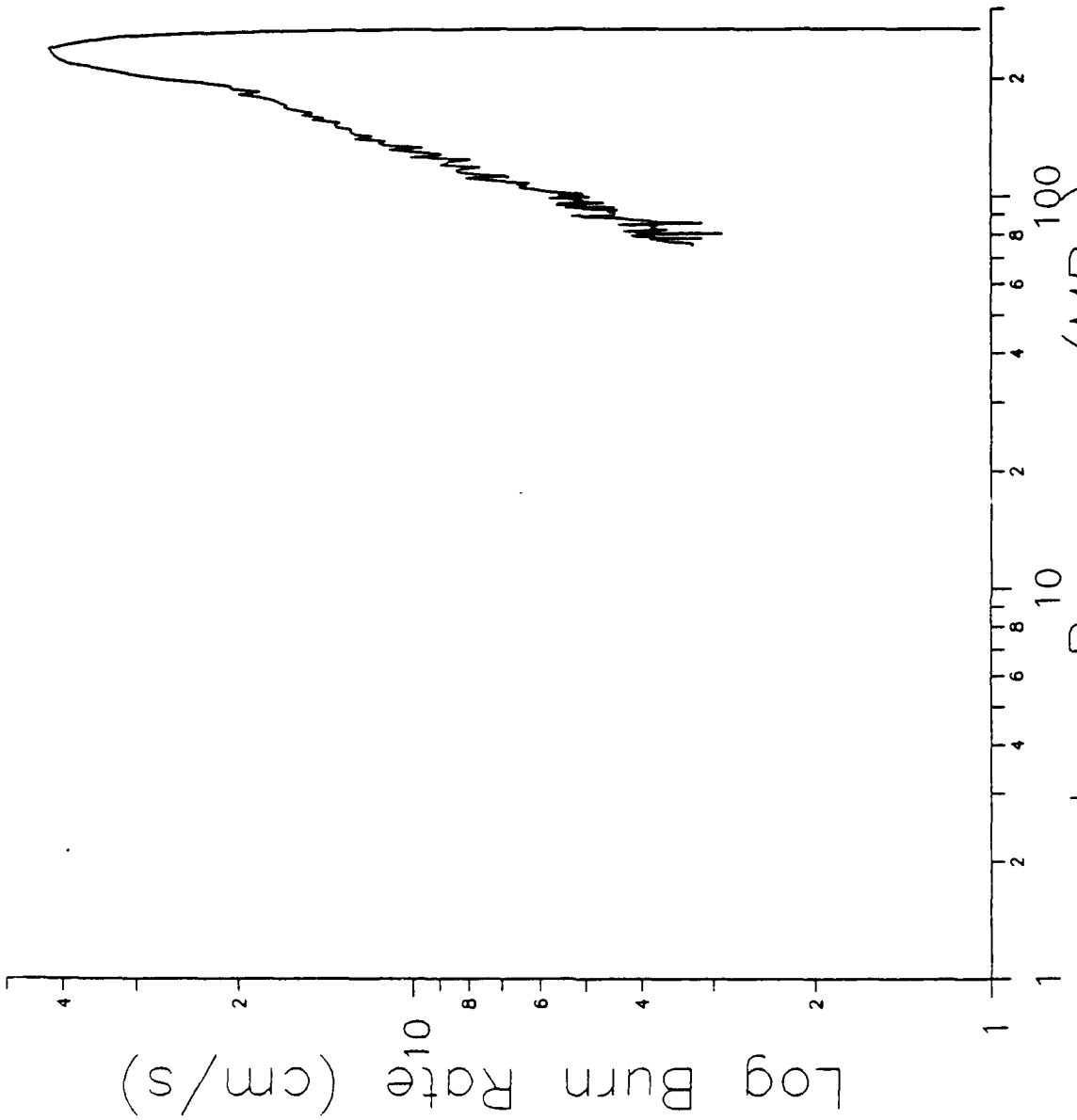

Figure B-16. Log Burn Rate vs. Log Pressure, Shot 16.

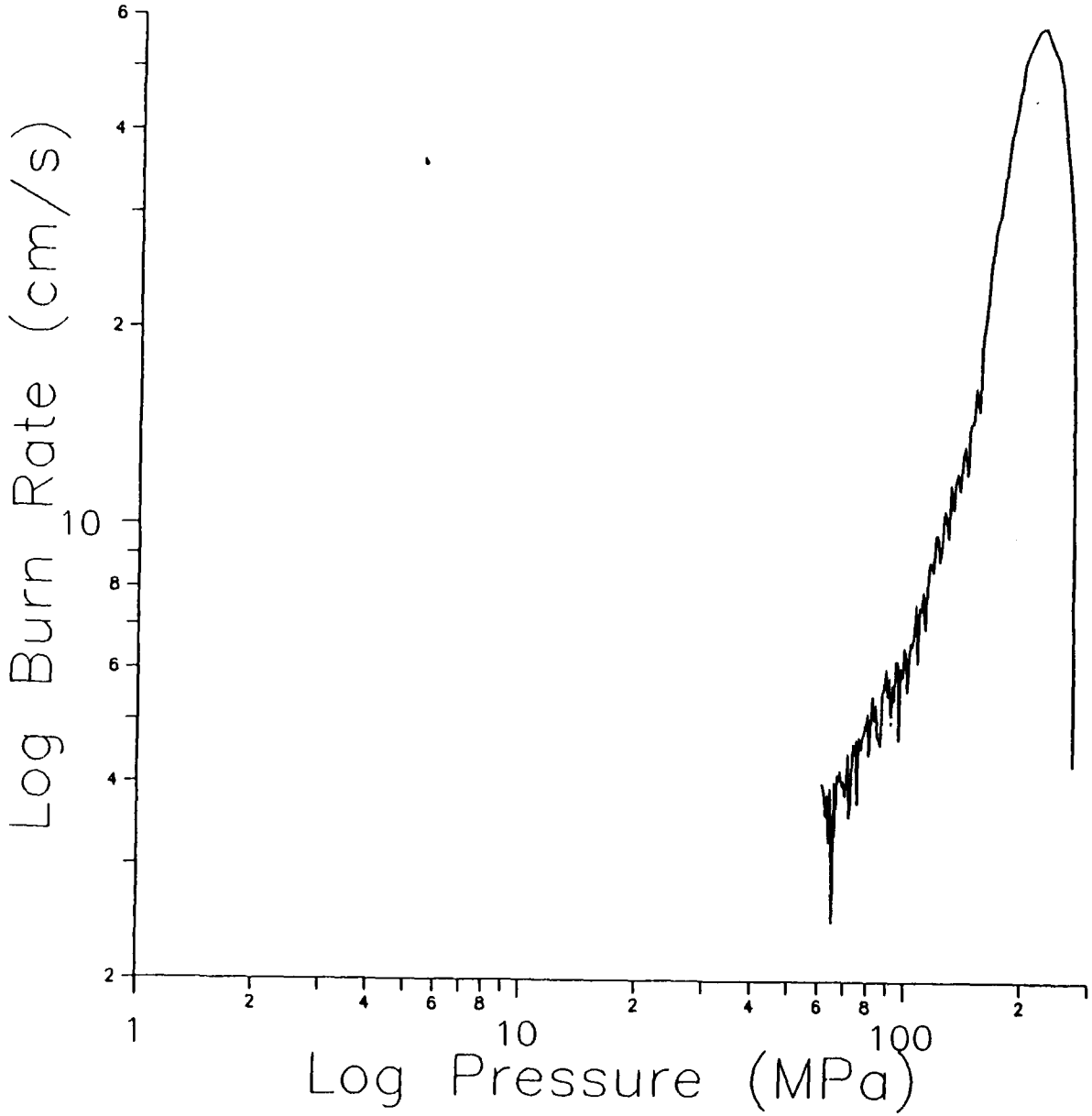

Figure B-17. Log Burn Rate vs. Log Pressure, Shot 17.

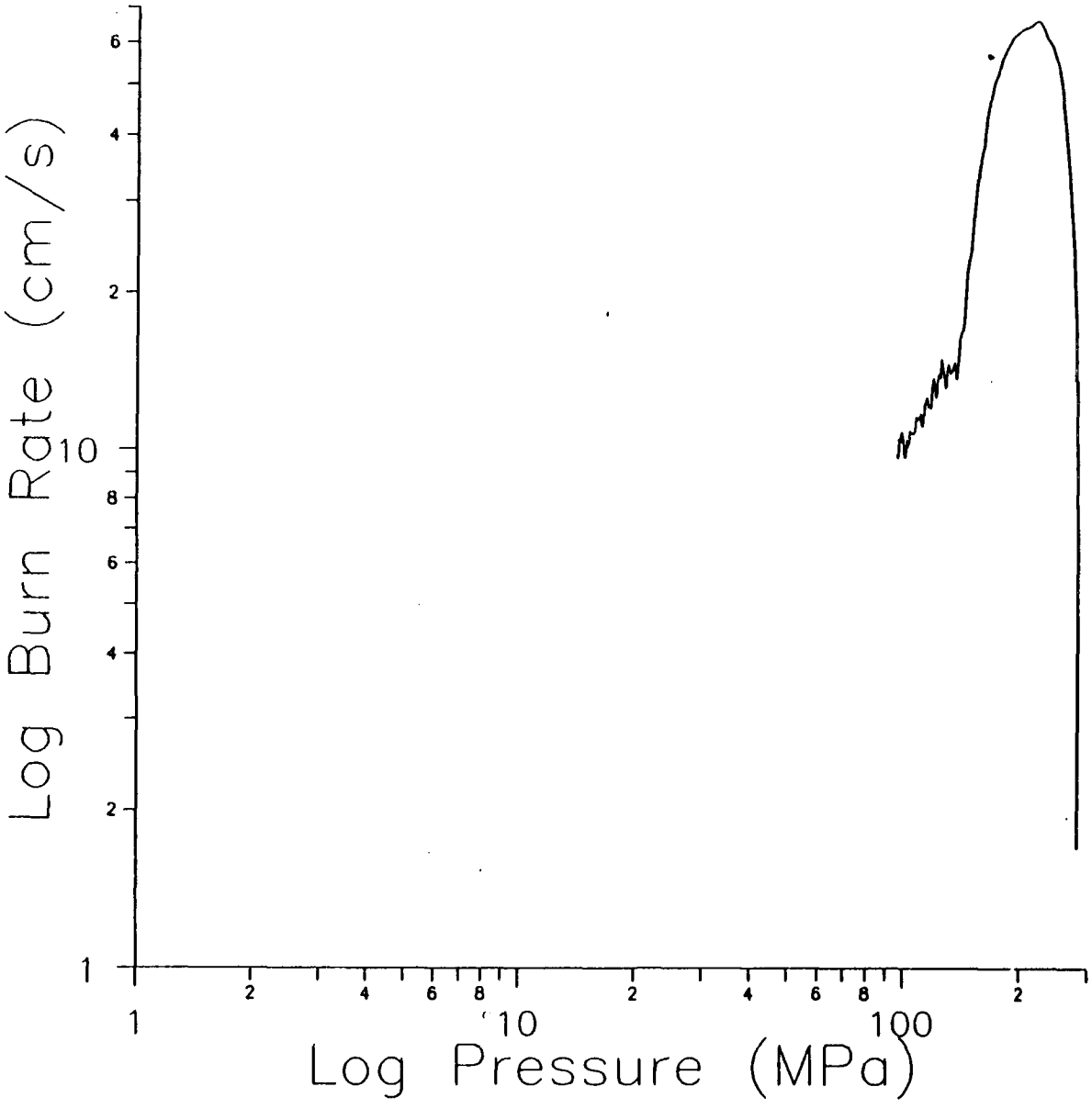

Figure B-18. Log Burn Rate vs. Log Pressure, Shot 18.

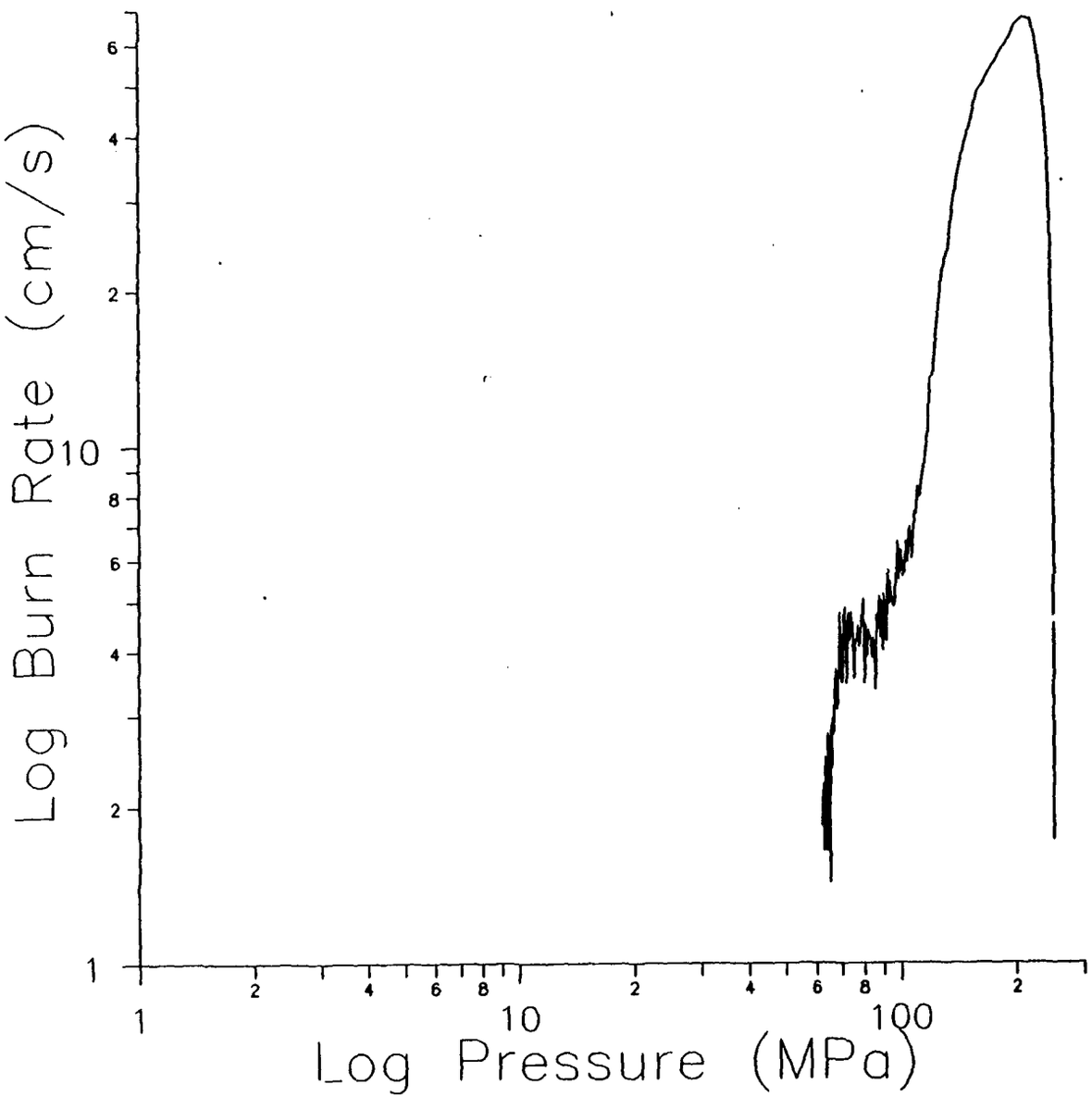

Figure B-19. Log Burn Rate vs. Log Pressure, Shot 19.

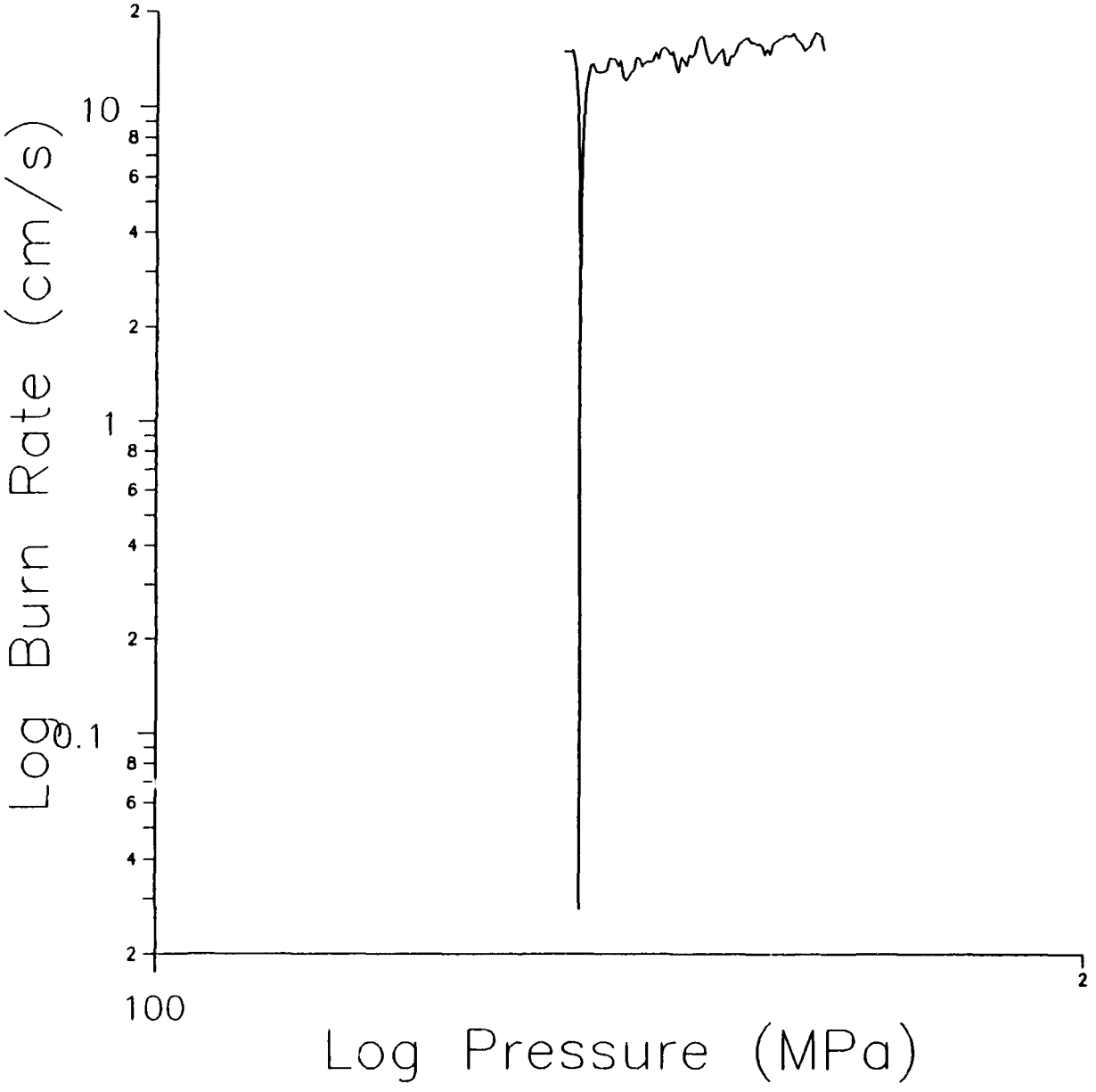

Figure B-20. Log Burn Rate vs. Log Pressure, Shot 20.

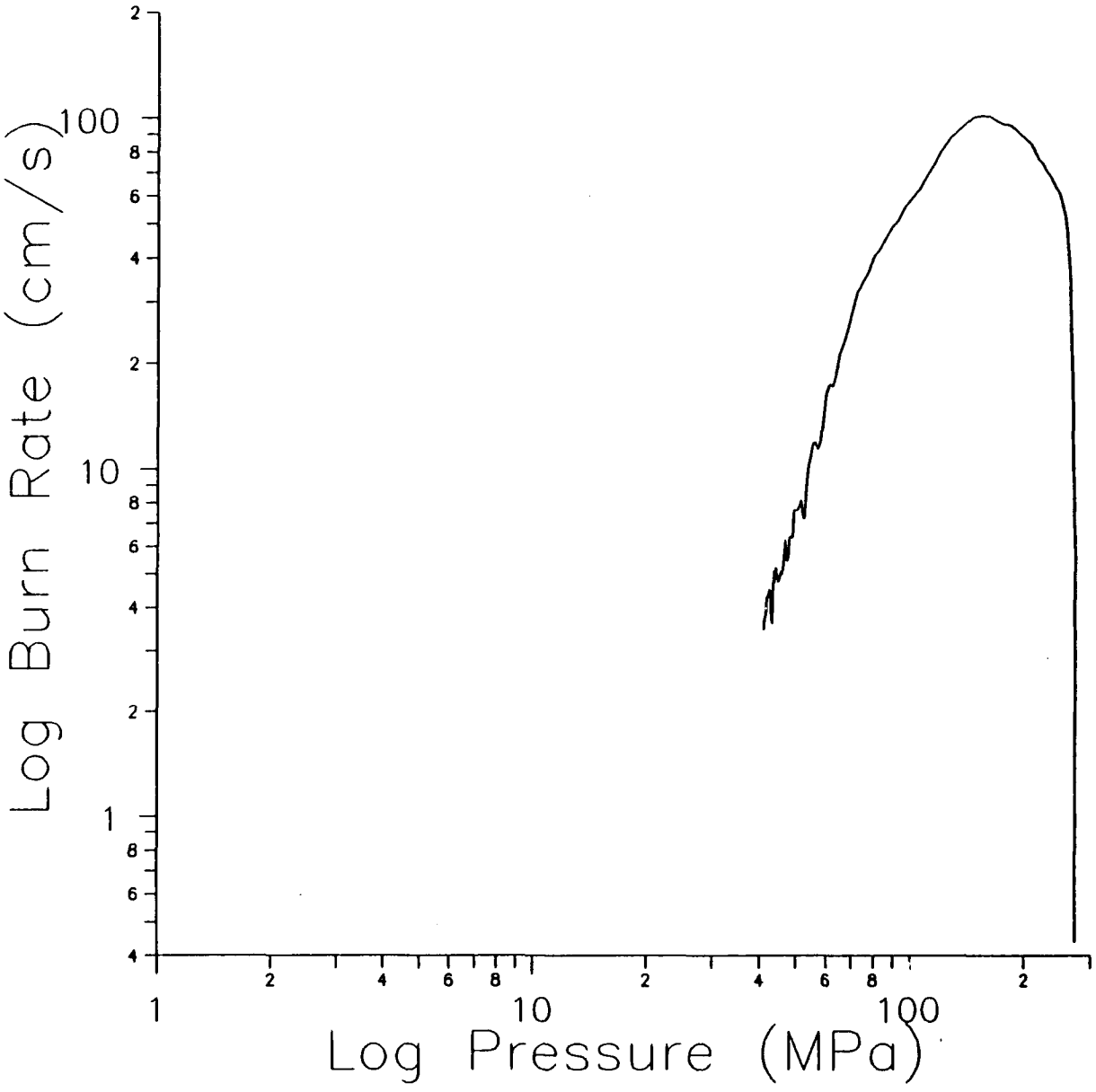

Figure B-21. Log Burn Rate vs. Log Pressure, Shot 21.

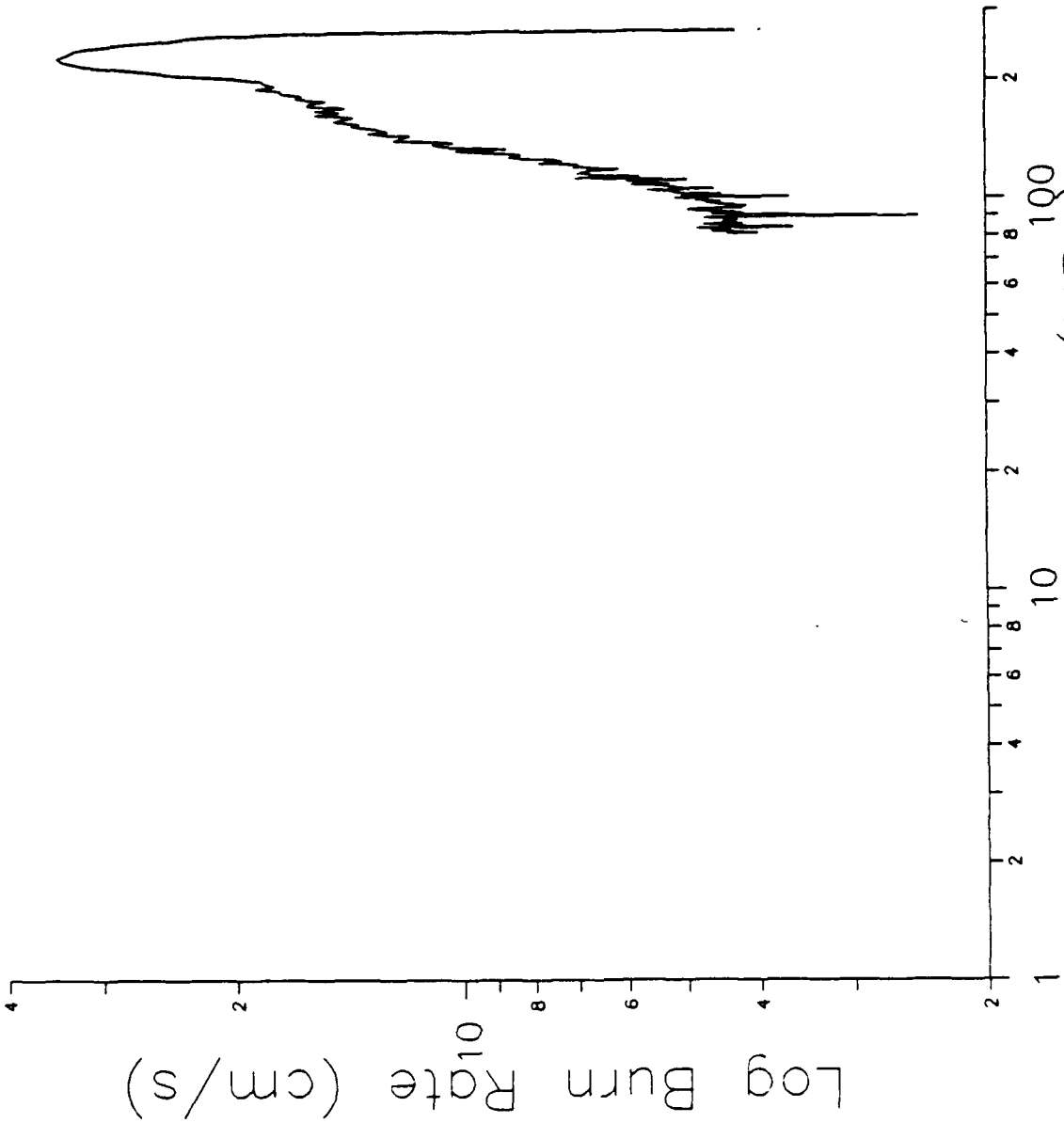

Figure B-22. Log Burn Rate vs. Log Pressure, Shot 22.

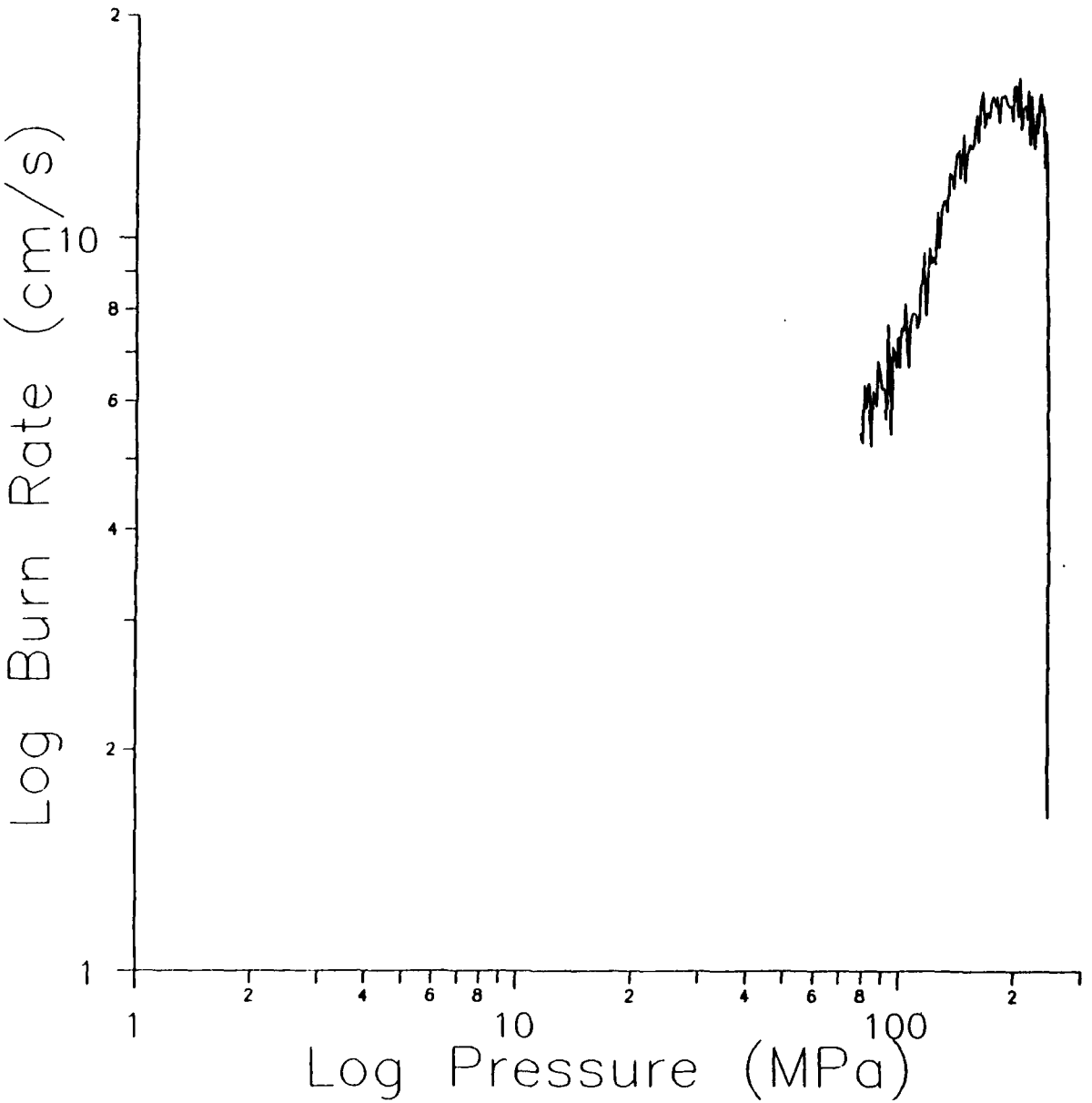

Figure B-23. Log Burn Rate vs. Log Pressure, Shot 23.

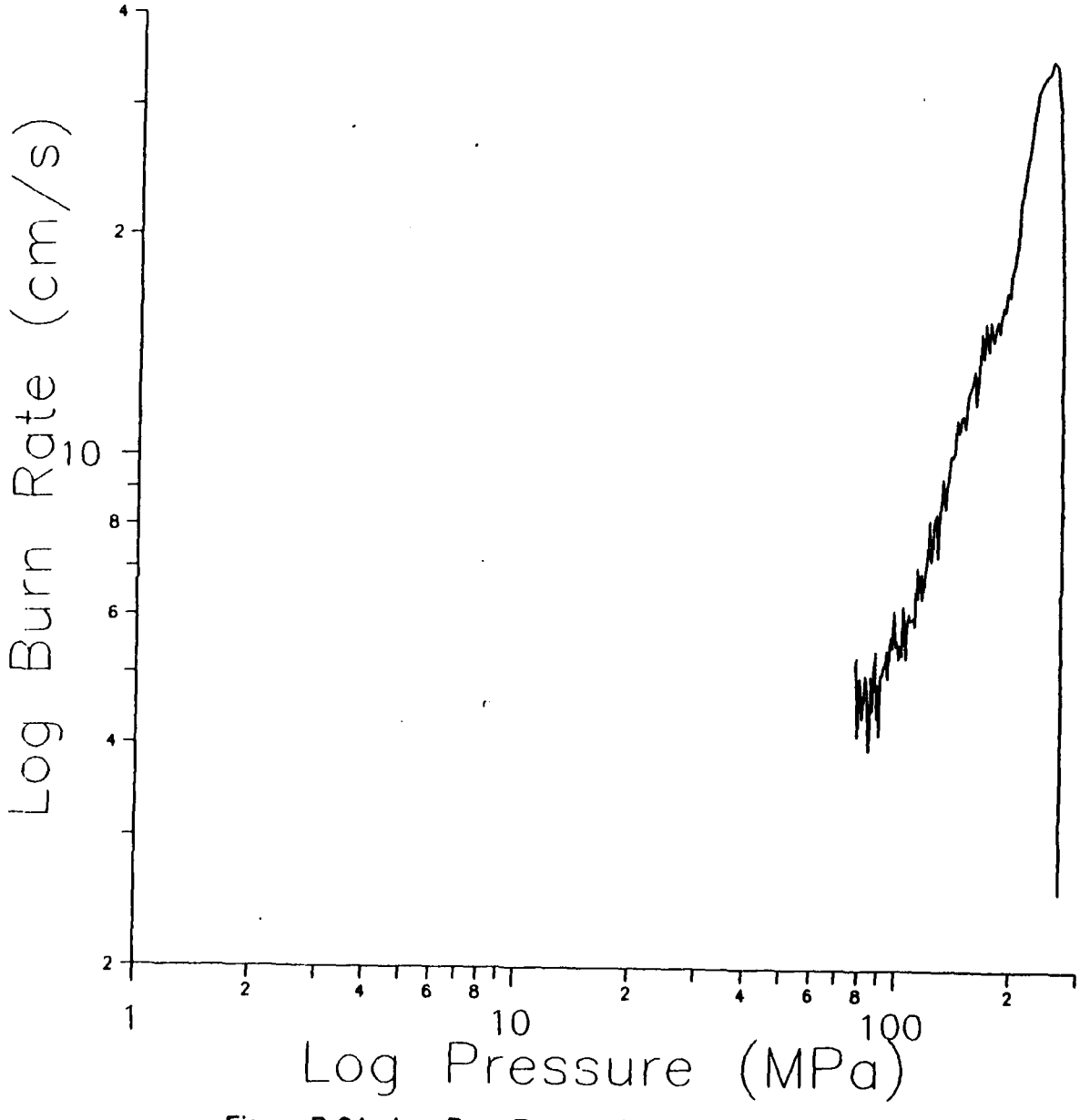

Figure B-24. Log Burn Rate vs. Log Pressure, Shot 24.

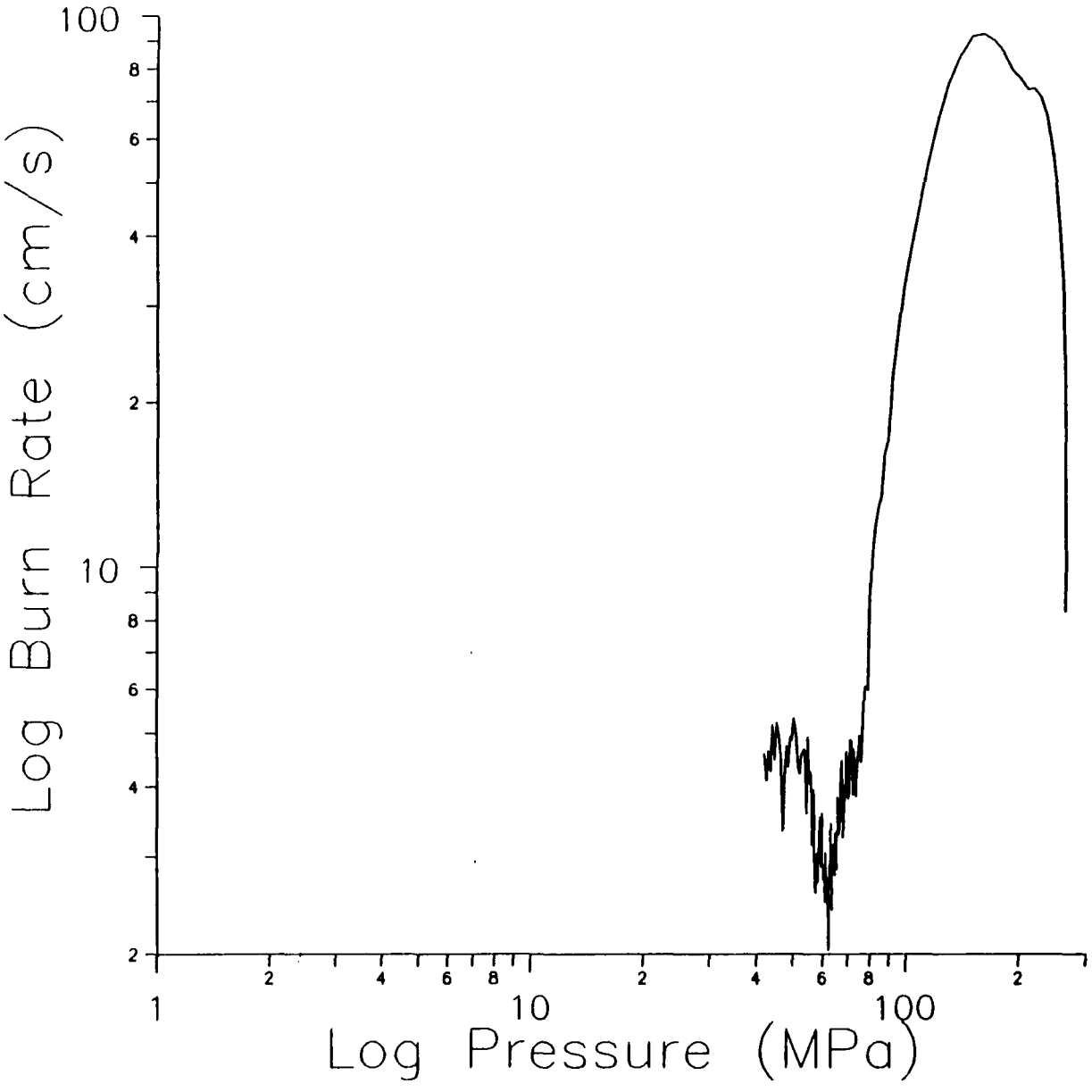

Figure B-25. Log Burn Rate vs. Log Pressure, Shot 25.

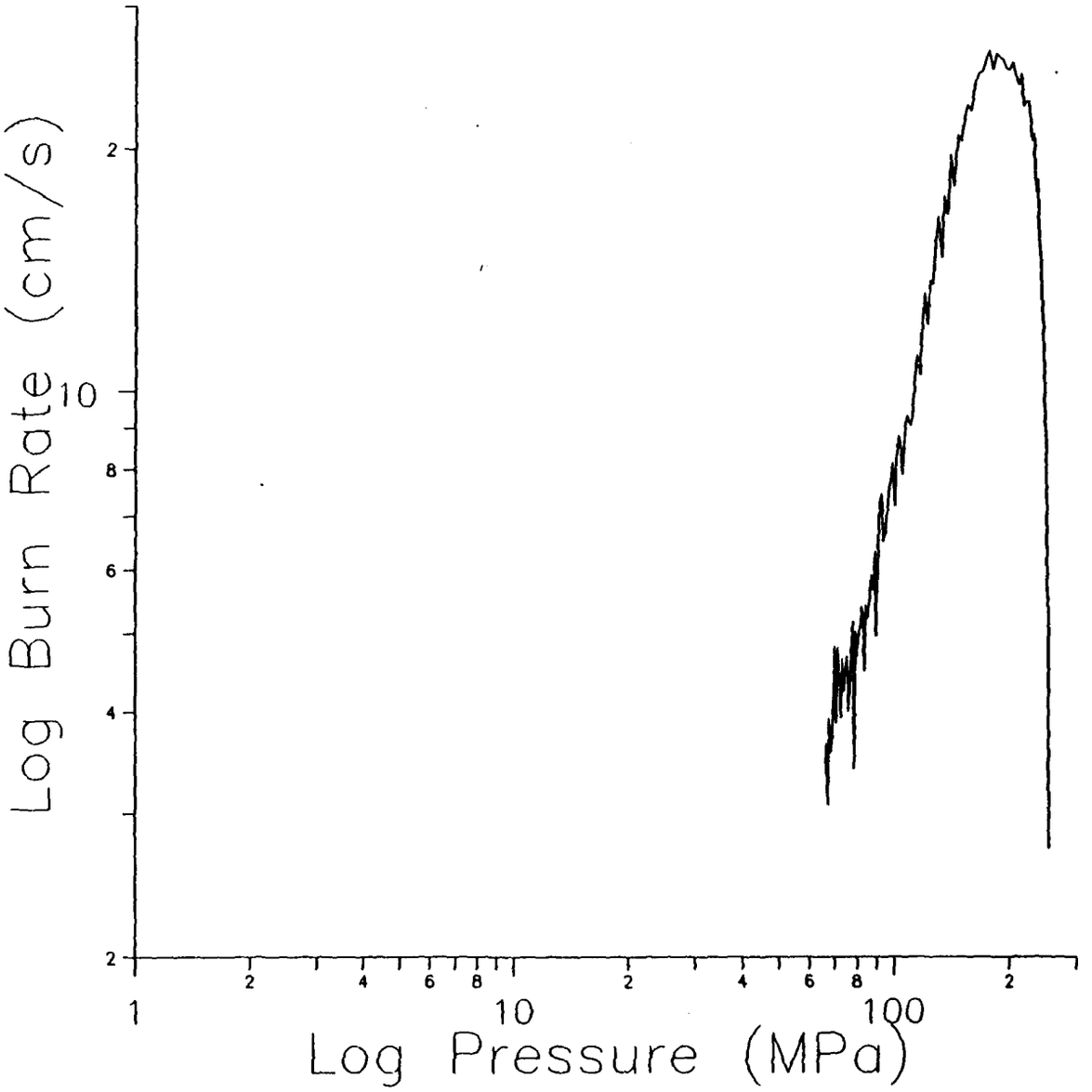

Figure B-26. Log Burn Rate vs. Log Pressure, Shot 26.

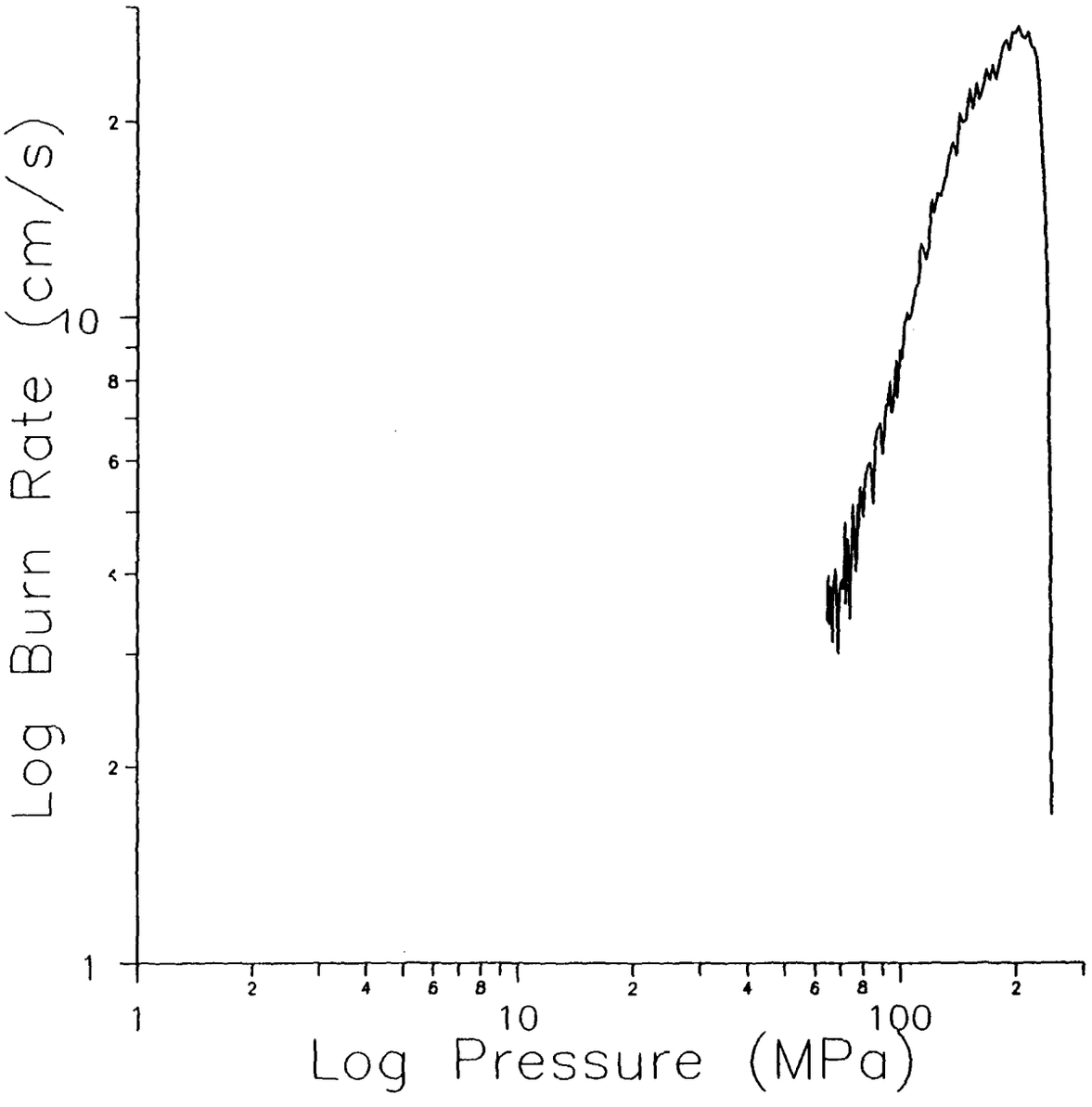

Figure B-27. Log Burn Rate vs. Log Pressure, Shot 27.

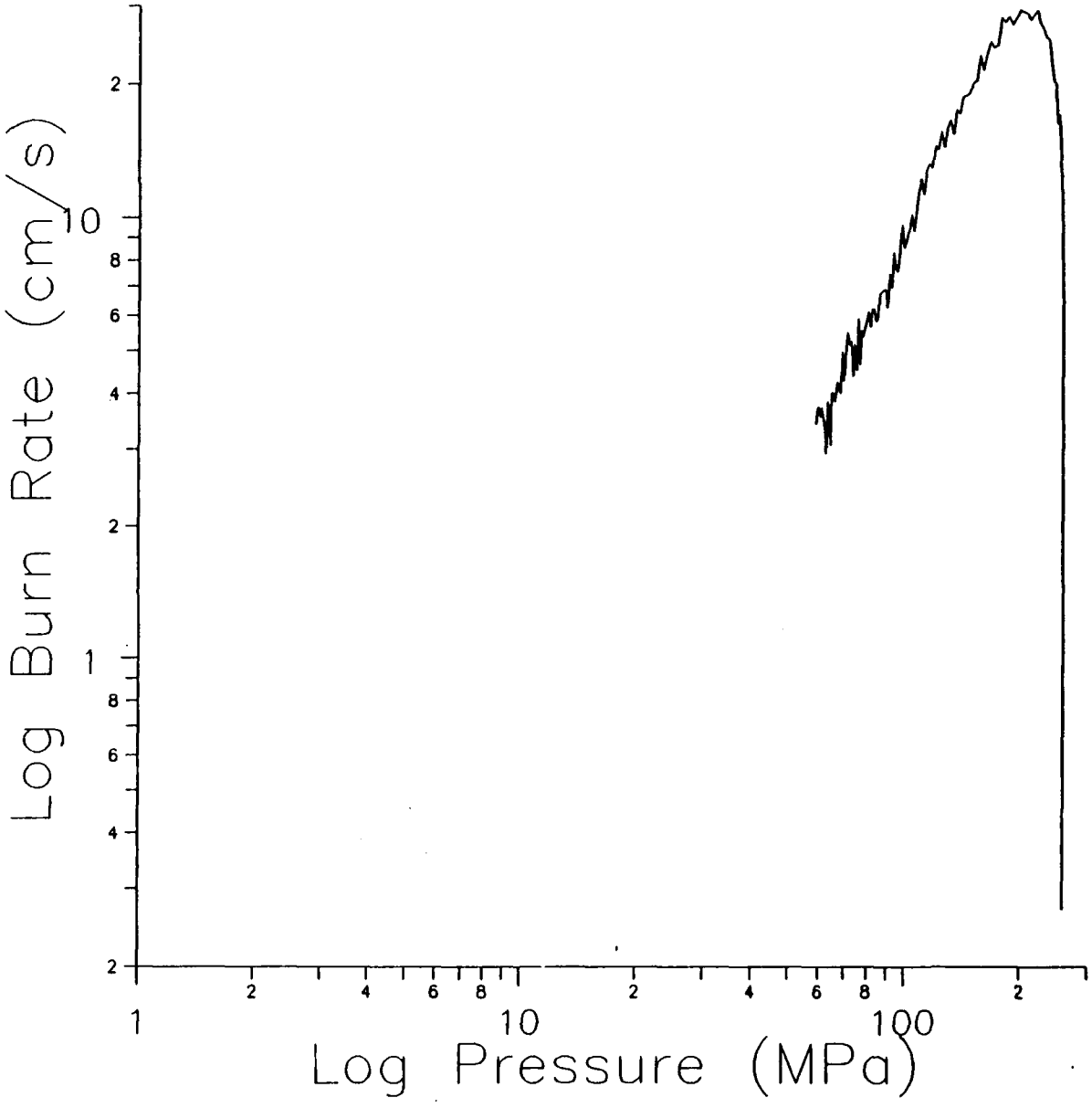

Figure B-28. Log Burn Rate vs. Log Pressure, Shot 28.

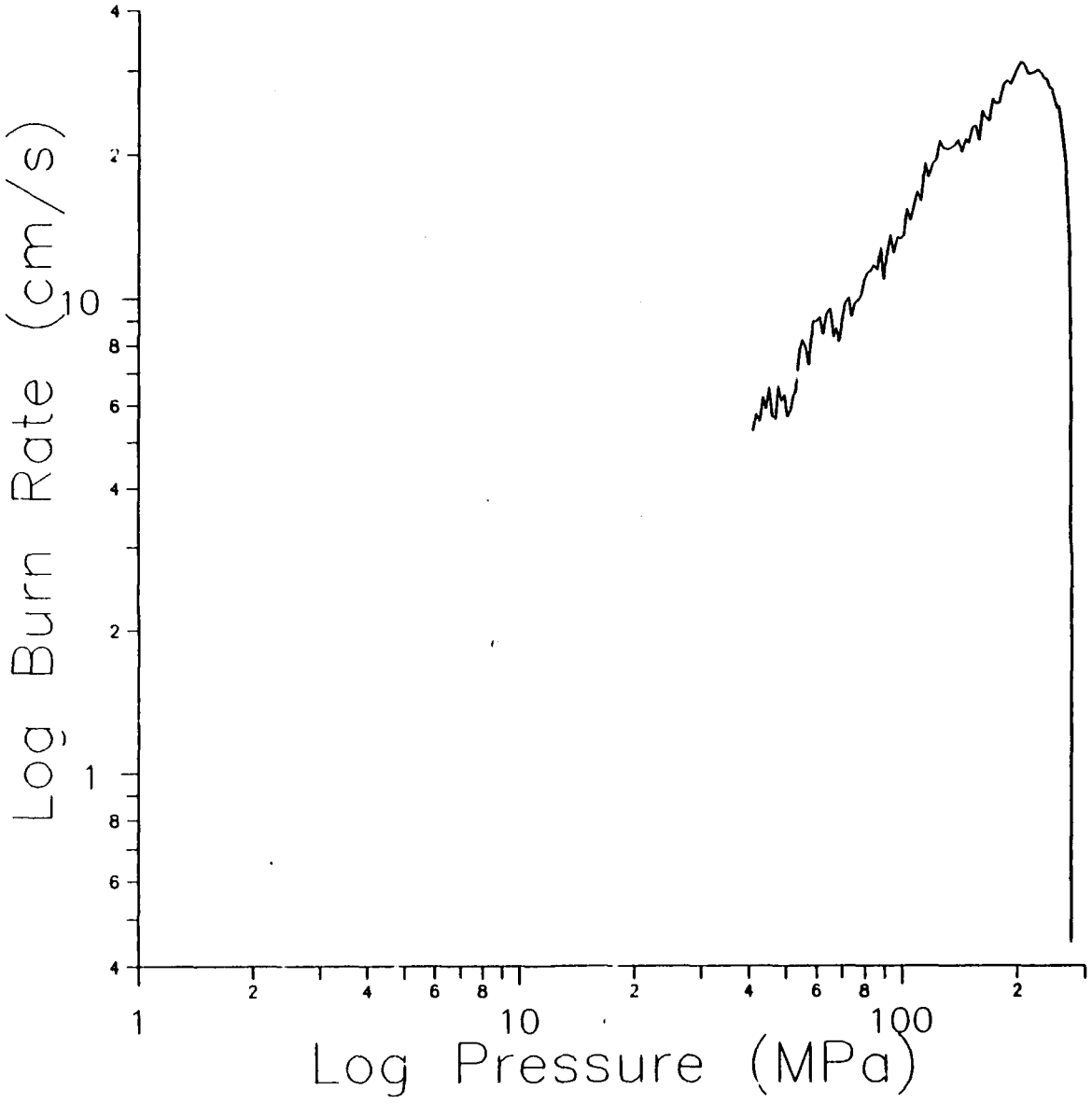

Figure B-29. Log Burn Rate vs. Log Pressure, Shot 29.

INTENTIONALLY LEFT BLANK.

APPENDIX C:

TABULAR BURN RATES

INTENTIONALLY LEFT BLANK.

BURNING RATE ANALYSIS
BRLCB V1.0
ADVANCED BALLISTIC CONCEPTS BRANCH - BRL

Project: Liquid Propellant
Data File: e:lp25.INF
Fired on:
Reduced on:

Requested by: William Oberle
Created From .MAS File: lpcold.MAS
By:
By:

Igniter Information

The Igniter Used Is: IMR 4350 Lot: Unknown
The Source or the Igniter Is: LP Team

Igniter Thermochemical Properties

Impetus (J/g)	: 994.1	Molecular Weight	: 23.78800
Flame Temperature (K)	: 2844.0	Covolume (cm^3/g)	: 1.03685
Density (g/cm^3)	: .94500	Gamma	: 1.24560

Propellant Information

The Propellant Used Is: LP1846 Lot: 1846-05
The Source for the Propellant Is: LP Team

Propellant Thermochemical Properties

Impetus (J/g)	: 900.2	Molecular Weight	: 22.84900
Flame Temperature (K)	: 2578.0	Covolume (cm^3/g)	: .66700
Density (g/cm^3)	: 1.45200	Gamma	: 1.22210

Propellant Grain Geometry

Grain Type: Cigarette

Length	(cm):	2.742211
Outer Diam.	(cm):	2.700020
Perf Diam.	(cm):	.000000
Inner Web	(cm):	.000000
Outer Web	(cm):	.000000

Bomb Information
Bomb Type: Closed Chamber
Bomb Vol. (cm^3): 73.0

Gage Information
Gage I.D.: C11281
Input Voltage: 4.5850
Constants for Fit: $A+Bx+C^2$
A: .30451E+00
B: .53151E-01
C: -.10918E-06

Temperature and Charge Mass Information

Propellant Mass (g): 22.8008
Initial Temp. Prop. (K): 294
Initial Bomb Temperature (K): 294

Igniter Mass (g): 2.8118
Initial Temp. Igniter (K): 294

Table C-1. Burn Rate (cm/s) vs. Pressure (MPa) for Shot 16, Ambient Temperature

Pressure	Rate	Pressure	Rate	Pressure	Rate
76.000	3.665	140.000	12.586	204.000	29.983
80.000	3.373	144.000	12.700	208.000	32.750
84.000	4.042	148.000	12.395	212.000	35.016
88.000	4.491	152.000	13.287	216.000	38.338
92.000	4.514	156.000	14.383	220.000	41.238
96.000	5.109	160.000	15.627	224.000	41.074
100.000	5.213	164.000	15.754	228.000	41.761
104.000	6.011	168.000	16.039	232.000	40.879
108.000	6.138	172.000	17.344	236.000	42.440
112.000	6.588	176.000	18.426	240.000	40.539
116.000	8.206	180.000	18.391	244.000	38.900
120.000	8.337	184.000	18.355	248.000	35.107
124.000	8.884	188.000	20.524	252.000	32.444
128.000	8.975	192.000	23.137	256.000	27.466
132.000	9.752	196.000	25.089	260.000	19.411
136.000	11.246	200.000	27.818	264.000	11.155

BURNING RATE ANALYSIS
BRLCB V1.0
ADVANCED BALLISTIC CONCEPTS BRANCH - BRL

Project: Liquid Propellant
Data File: e:lp32.INF
Fired on: 23 May 90
Reduced on: 9 June 90
Reduction Remarks:
Conditioned to 244 K for 60 min.

Requested by: William Oberle
Created From .MAS File: lpcold.MAS
By: Newberry & Aungst
By: William Oberle

Igniter Information

The Igniter Used Is: IMR 4350 Lot: Unknown
The Source for the Igniter Is: LP Team

Igniter Thermochemical Properties

Impetus (J/g)	: 994.1	Molecular Weight	: 23.78800
Flame Temperature (K)	: 2844.0	Covolume (cm^3/g)	: 1.03685
Density (g/cm^3)	: .94500	Gamma	: 1.24560

Propellant Information

The Propellant Used Is: LP1846 Lot: 1846-05
The Source for the Propellant Is: LP Team

Propellant Thermochemical Properties

Impetus (J/g)	: 900.2	Molecular Weight	: 22.84900
Flame Temperature (K)	: 2578.0	Covolume (cm^3/g)	: .66700
Density (g/cm^3)	: 1.45200	Gamma	: 1.22210

Propellant Grain Geometry

Grain Type: Cigarette

Length	(cm):	2.742211
Outer Diam.	(cm):	2.700020
Perf Diam.	(cm):	.000000
Inner Web	(cm):	.000000
Outer Web	(cm):	.000000

Bomb Information
Bomb Type: Closed Chamber
Bomb Vol. (cm^3): 73.0

Gage Information
Gage I.D.: C11632
Input Voltage: 4.8530
Constants for Fit: $A+Bx+C^2$
A: .12701E+01
B: .52094E-01
C: -.16385E-06

Temperature and Charge Mass Information

Propellant Mass (g): 22.8008
Initial Temp. Prop. (K): 244
Initial Bomb Temperature (K): 294

Igniter Mass (g): 2.8123
Initial Temp. Igniter (K): 294

Table C-2. Burn Rate (cm/s) vs. Pressure (MPa) for Shot 23, Conditioned Cold

Pressure	Rate	Pressure	Rate	Pressure	Rate
80.000	5.300	136.000	11.665	192.000	15.574
84.000	6.239	140.000	13.061	196.000	14.069
88.000	6.076	144.000	13.400	200.000	15.735
92.000	7.043	148.000	12.147	204.000	16.478
96.000	6.984	152.000	14.174	208.000	14.860
100.000	7.481	156.000	14.675	212.000	14.053
104.000	7.797	160.000	13.605	216.000	14.670
108.000	7.968	164.000	14.401	220.000	14.607
112.000	7.461	168.000	15.101	224.000	14.462
116.000	8.726	172.000	15.589	228.000	14.575
120.000	10.230	176.000	16.065	232.000	14.692
124.000	9.899	180.000	14.448	236.000	14.734
128.000	10.822	184.000	15.789	240.000	13.385
132.000	11.034	188.000	15.507	244.000	5.434

BURNING RATE ANALYSIS
BRLCB V1.0
ADVANCED BALLISTIC CONCEPTS BRANCH - BRL

Project: Liquid Propellant
Data File: e:lp35.INF
Fired on: 30 May 90
Reduced on: 8 June 90
Reduction Remarks:
Conditioned to 140° F for 120 min.

Requested by: William Oberle
Created From .MAS File: lphot.MAS
By: Newberry & Aungst
By: William Oberle

Igniter Information

The Igniter Used Is: IMR 4350 Lot: Unknown
The Source for the Igniter Is: LP Team

Igniter Thermochemical Properties

Impetus (J/g)	994.1	Molecular Weight	23.78800
Flame Temperature (K)	2844.0	Covolume (cm^3/g)	1.03685
Density (g/cm^3)	.94500	Gamma	1.24560

Propellant Information

The Propellant Used Is: LP1846 Lot: 1846-05
The Source for the Propellant Is: LP Team

Propellant Thermochemical Properties

Impetus (J/g)	900.2	Molecular Weight	22.84900
Flame Temperature (K)	2578.0	Covolume (cm^3/g)	.66700
Density (g/cm^3)	1.45200	Gamma	1.22210

Propellant Grain Geometry

Grain Type: Cigarette

Length	(cm):	2.742211
Outer Diam.	(cm):	2.700020
Perf Diam.	(cm):	.000000
Inner Web	(cm):	.000000
Outer Web	(cm):	.000000

Bomb Information
Bomb Type: Closed Chamber
Bomb Vol. (cm^3): 73.0

Gage Information
Gage I.D.: C11632
Input Voltage: 4.8530
Constants for Fit: $A+Bx+C^2$
A: .12701E+01
B: .52094E-01
C: -.16385E-06

Temperature and Charge Mass Information

Propellant Mass (g): 22.8008
Initial Temp. Prop. (K): 333
Initial Bomb Temperature (K): 294

Igniter Mass (g): 2.8129
Initial Temp. Igniter (K): 294

Table C-3. Burn Rate (cm/s) vs. Pressure (MPa) for Shot 26, Conditioned Hot

Pressure	Rate	Pressure	Rate	Pressure	Rate
68.000	3.980	132.000	15.046	196.000	24.991
72.000	4.774	136.000	17.443	200.000	24.734
76.000	3.711	140.000	19.583	204.000	25.160
80.000	5.060	144.000	19.963	208.000	25.326
84.000	5.125	148.000	20.032	212.000	23.535
88.000	6.328	152.000	21.719	216.000	22.703
92.000	7.349	156.000	22.645	220.000	23.532
96.000	7.558	160.000	23.549	224.000	22.995
100.000	7.241	164.000	23.823	228.000	20.229
104.000	8.638	168.000	25.126	232.000	18.232
108.000	9.007	172.000	25.579	236.000	17.738
112.000	10.097	176.000	25.632	240.000	14.586
116.000	10.879	180.000	24.619	244.000	11.791
120.000	12.957	184.000	26.176	248.000	8.411
124.000	14.004	188.000	25.779	252.000	5.383
128.000	15.537	192.000	26.077		

No. of Copies	Organization
2	Administrator Defense Technical Info Center ATTN: DTIC-DDA Cameron Station Alexandria, VA 22304-6145
1	Commander U.S. Army Materiel Command ATTN: AMCDRA-ST 5001 Eisenhower Avenue Alexandria, VA 22333-0001
1	Commander U.S. Army Laboratory Command ATTN: AMSLC-DL 2800 Powder Mill Road Adelphi, MD 20783-1145
2	Commander U.S. Army Armament Research, Development, and Engineering Center ATTN: SMCAR-IMI-I Picatinny Arsenal, NJ 07806-5000
2	Commander U.S. Army Armament Research, Development, and Engineering Center ATTN: SMCAR-TDC Picatinny Arsenal, NJ 07806-5000
1	Director Benet Weapons Laboratory U.S. Army Armament Research, Development, and Engineering Center ATTN: SMCAR-CCB-TL Watervliet, NY 12189-4050
nclass. only)1	Commander U.S. Army Armament, Munitions and Chemical Command ATTN: AMSMC-IMF-L Rock Island, IL 61299-5000
1	Director U.S. Army Aviation Research and Technology Activity ATTN: SAVRT-R (Library) M/S 219-3 Ames Research Center Moffett Field, CA 94035-1000

No. of Copies	Organization
1	Commander U.S. Army Missile Command ATTN: AMSMI-RD-CS-R (DOC) Redstone Arsenal, AL 35898-5010
1	Commander U.S. Army Tank-Automotive Command ATTN: ASQNC-TAC-DIT (Technical Information Center) Warren, MI 48397-5000
1	Director U.S. Army TRADOC Analysis Command ATTN: ATRC-WSR White Sands Missile Range, NM 88002-5502
1	Commandant U.S. Army Field Artillery School ATTN: ATSF-CSI Ft. Sill, OK 73503-5000
(Class. only)1	Commandant U.S. Army Infantry School ATTN: ATSH-CD (Security Mgr.) Fort Benning, GA 31905-5660
(Unclass. only)1	Commandant U.S. Army Infantry School ATTN: ATSH-CD-CSO-OR Fort Benning, GA 31905-5660
1	Air Force Armament Laboratory ATTN: WL/MNOI Eglin AFB, FL 32542-5000
	Aberdeen Proving Ground
2	Dir, USAMSAA ATTN: AMXSY-D AMXSY-MP, H. Cohen
1	Cdr, USATECOM ATTN: AMSTE-TC
3	Cdr, CRDEC, AMCCOM ATTN: SMCCR-RSP-A SMCCR-MU SMCCR-MSI
1	Dir, VLAMO ATTN: AMSLC-VL-D
10	Dir, BRL ATTN: SLCBR-DD-T

No. of Copies Organization

1 Commander
U.S. Army Belvoir R&D Center
ATTN: STRBE-WC
Tech Library (Vault) B-315
Fort Belvoir, VA 22060-5606

1 Commander
U.S. Army Research Office
ATTN: Tech Library
P.O. Box 12211
Research Triangle Park, NC 27709-2211

1 Director
U.S. Army Armament Research, Development, and Engineering Center
AMCCOM
Benet Weapons Laboratory
ATTN: SMCAR-CCB-RA, Julius Frankel
Watervliet, NY 12189-4050

1 Commander
U.S. Army Armament Research, Development, and Engineering Center
ATTN: SMCAR-CCS-C, T. Hung
Picatinny Arsenal, NJ 07806-5000

2 Commandant
U.S. Army Field Artillery School
ATTN: ATSF-CMW
ATSF-TSM-CN, J. Spicer
Ft Sill, OK 73503

1 Commandant
U.S. Army Armor Center
ATTN: ATSB-CD-MLD
Ft Knox, KY 40121

3 Commander
U.S. Army Armament Research, Development, and Engineering Center
ATTN: SMCAR-FSS-DA, Bldg 94
J. Feneck
R. Kopmann
J. Irizarry
Picatinny Arsenal, NJ 07806-5000

No. of Copies Organization

11 Comander
U.S. Army Armament Research, Development, and Engineering Center
ATTN: SMCAR-TSS
SMCAR-AEE-BR, B. Brodman
SMCAR-AEE-B, D. Downs
SMCAR-AEE-BR,
W. Seals
A. Beardell
SMCAR-AEE-W, N. Slagg
SMCAR-AEE,
A. Bracuti
D. Chieu,
J. Salo
SMCAR-FSS-D, L. Frauen
SMCAR-FSA-S, H. Liberman
Picatinny Arsenal, NJ 07806-5000

1 Commander
Naval Surface Warfare Center
ATTN: D. A. Wilson, Code G31
Dahlgren, VA 22448-5000

1 Commander
Naval Surface Warfare Center
ATTN: Code G33, J. East
Dahlgren, VA 22448-5000

2 Commander
Naval Surface Warfare Center
ATTN: O. Dengel
K. Thorsted
Silver Spring, MD 20902-5000

1 Commander
Naval Weapons Center
China Lake, CA 93555-6001

1 Superintendent
Naval Postgraduate School
Dept. of Mechanical Engineering
ATTN: Code 1424, Library
Monterey, CA 93943

1 OSD/SDIO/IST
ATTN: Dr. Len Caveny
Pentagon
Washington, DC 20301-7100

No. of Copies	Organization
1	Commandant USAFAS ATTN: ATSF-TSM-CN Ft Sill, OK 73503-5600
1	Director Jet Propulsion Laboratory ATTN: Tech Library 4800 Oak Grove Drive Pasadena, CA 91109
2	Director National Aeronautics and Space Administration ATTN: MS-603, Tech Lib MS-86, Dr. Povinelli 21000 Brookpark Road Lewis Research Center Cleveland, OH 44135
1	Director National Aeronautics and Space Administration Manned Spacecraft Center Houston, TX 77058
1	Director Sandia National Laboratories ATTN: Dr. Ray Rychnovsky, Div. 8152 P.O. Box 969 Livermore, CA 94551-0969
1	Director Sandia National Laboratories ATTN: Dr. Stuart Griffiths, Div. 8244 P.O. Box 969 Livermore, CA 94551-0969
1	Director Applied Physics Laboratory The Johns Hopkins University Johns Hopkins Road Laurel, MD 20707
1	U. of Illinois at Chicago ATTN: Professor Sohail Murad Dept. of Chemical Engineering Box 4348 Chicago, IL 6068066

No. of Copies	Organization
1	U. of MD at College Park ATTN: Professor Franz Kasler Department of Chemistry College Park, MD 20742
1	U. of Missouri at Columbia ATTN: Professor R. Thompson Department of Chemistry Columbia, MO 65211
1	U. of Michigan ATTN: Prof. Gerard M. Faeth Dept of Aerospace Engr Ann Arbor, MI 48109-3796
1	U. of Missouri at Columbia ATTN: Professor F. K. Ross Research Reactor Columbia, MO 65211
1	U. of Missouri at Kansas City Department of Physics ATTN: Prof. R. D. Murphy 1110 East 48th Street Kansas City, MO 64110-2499
1	Pennsylvania State University Dept. of Mechanical Engineering ATTN: Prof. K. Kuo University Park, PA 16802
2	Princeton Combustion Research Laboratories, Inc. ATTN: N. A. Messina M. Summerfield 4275 U.S. Highway One North Monmouth Junction, NJ 08852
1	U. of Arkansas Dept. of Chemical Engineering ATTN: J. Havens 227 Engineering Building Fayetteville, AR 72701
3	U. of Delaware Department of Chemistry ATTN: Mr. James Cronin Professor Thomas Brill Newark, DE 19711

No. of Copies	Organization
1	U. of Texas at Austin Bureau of Engineering Research ATTN: BRC EME133, Room 1.100 H. Fair 10100 Burnet Road Austin, TX 78758
1	California State University, Sacramento School of Engineering & Computer Science ATTN: Dr. Frederick Reardon 6000 J Street Sacramento, CA 95819-2694
1	University of Colorado at Boulder Department of Mechanical Engineering ATTN: Dr. John Daily Engineering Center ME 1-13 Campus Box 427 Boulder, CO 80309-0427
1	Calspan Corporation ATTN: Tech Library P.O. Box 400 Buffalo, NY 14225
7	General Electric Ord Sys Div ATTN: J. Mandzy, OP43-220 R. E. Mayer W. Pasko R. Pate I. Magoon Lou Ann Walter J. McCaleb 100 Plastics Avenue Pittsfield, MA 01201-3698
1	IITRI ATTN: Library 10 W. 35th Street Chicago, IL 60616
1	Paul Gough Associates ATTN: Paul Gough 1048 South Street Portsmouth, NH 03801-5423

No. of Copies	Organization
1	Science Applications Int'l Corporation ATTN: Norman Banks 4900 Waters Edge Drive Suite 255 Raleigh, NC 27606
1	Sundstrand Aviation Operations ATTN: Mr. Owen Briles P.O. Box 7202 Rockford, IL 61125
1	Veritay Technology, Inc. ATTN: E. B. Fisher 4845 Millersport Highway P.O. Box 305 East Amherst, NY 14051-0305
1	Conway Enterprises ATTN: Professor Alistair MacPherson 499 Pine Top Trial Bethlehem, PA 18017-1828

No. of
Copies Organization

1 RARDE
GS2 Division
Building R31
ATTN: Dr. Clive Woodley
Ft. Halstead
Sevenoaks, Kent TN14 7BT
England

1 Imperial College of Science and Medicine
ATTN: Prof. J. H. Whitelaw
Exhibition Road, London SW7 2BX
England

INTENTIONALLY LEFT BLANK.

USER EVALUATION SHEET/CHANGE OF ADDRESS

This laboratory undertakes a continuing effort to improve the quality of the reports it publishes. Your comments/answers below will aid us in our efforts.

1. Does this report satisfy a need? (Comment on purpose, related project, or other area of interest for which the report will be used.) _____

2. How, specifically, is the report being used? (Information source, design data, procedure, source of ideas, etc.) _____

3. Has the information in this report led to any quantitative savings as far as man-hours or dollars saved, operating costs avoided, or efficiencies achieved, etc? If so, please elaborate. _____

4. General Comments. What do you think should be changed to improve future reports? (Indicate changes to organization, technical content, format, etc.) _____

BRL Report Number BRL-TR-3287 Division Symbol _____

Check here if desire to be removed from distribution list. ____

Check here for address change. ____

Current address: Organization _____
Address _____

DEPARTMENT OF THE ARMY
Director
U.S. Army Ballistic Research Laboratory
ATTN: SLCBR-DD-T
Aberdeen Proving Ground, MD 21005-5066

OFFICIAL BUSINESS

BUSINESS REPLY MAIL
FIRST CLASS PERMIT No 0001, APG, MD

Postage will be paid by addressee

Director
U.S. Army Ballistic Research Laboratory
ATTN: SLCBR-DD-T
Aberdeen Proving Ground, MD 21005-5066

NO POSTAGE
NECESSARY
IF MAILED
IN THE
UNITED STATES